The natural killer cell activation compound 815A: solubility, stability, and injectable formulations

Patrícia Alexandra Brandão Morgado

Thesis to obtain the Master of Science Degree in

Pharmaceutical Engineering

Supervisor: Doctor Pedro Boto Pereira Franco Pinheiro

Co-supervisor: Professor Maria Matilde Soares Duarte Marques

Examination Committee

Chairperson: Professor José Monteiro Cardoso de Menezes

Supervisor: Doctor Pedro Boto Pereira Franco Pinheiro

Member of the Committee: Doctor José Gonçalo Deira Duarte de Campos Justino

November 2021

Preface

The work presented in this thesis was performed at Centro de Química Estrutural of Instituto Superior Técnico (Lisbon, Portugal), during the period February-July 2021, under the supervision of Doctor Pedro Franco Pinheiro and Professor M. Matilde Marques.

This work was supported by Fundação para a Ciência e a Tecnologia (RECI/QEQ-MED/0330/2012; SAICTPAC/0019/2015; PTDC/QUI-QAN/32242/2017; SFRH/BD/110945/2015; UID/QUI/00100/2013; UID/QUI/00100/2019; UIDB/00100/2020) and Liga Portuguesa Contra o Cancro (LPCC/NRS – Terry Fox 2015-17 grant).

Acknowledgements

O ano que passou pode ser caracterizado como um ano repleto de desafios, constantes imprevistos e níveis de cortisol por vezes preocupantes. Foi um ano em que por vezes me encontrei perdida e sem saber se valia a pena o esforço. Agora, tendo completado este que foi o meu maior projeto até hoje, olho para trás e vejo que consegui, que superei tudo o que lentamente me prendia e empurrava para o fundo. Se o fiz, muito devo aqueles que me ajudaram e me deram apoio para que o conseguisse.

Em primeiro lugar, quero agradecer a ambos os meus orientadores, à Professora Matilde Marques e ao Doutor Pedro Pinheiro, pela oportunidade e voto de confiança que me deram. Muito obrigada por toda a ajuda e conhecimento que partilharam comigo, foram uma constante fonte de motivação e apoio.

Numa nota mais pessoal ao Doutor Pedro, foi ele quem experienciou na primeira fila o filme "A Patrícia torna-se Mestre". Desde a receção de braços abertos aos momentos mais difíceis esteve sempre presente para me mostrar que para além do óbvio mau resultado, existe sempre um outro lado a partir do qual algo de bom há a reter e que desistir não é opção. Um obrigado é pouco para expressar toda a gratidão e admiração que sinto, especialmente por me ter feito sentir ouvida e por valorizar as minhas opiniões e ideias. Obrigada por acreditares em mim e aturares os meus (pequenos grandes) momentos.

Quero ainda dar um especial agradecimento também às Doutoras Sofia Duarte e Joana Feliciano, pois sem a ajuda delas grande parte do trabalho não poderia ter sido feita.

Aos meus parceiros de laboratório, Cátia Marques e Pedro Rosado, um obrigado não chega. Durante muito tempo fomos só nós os três e foram vocês que, por muitas vezes, me guiaram e evitaram que esta pobre alma causasse pequenos grandes desastres laboratoriais. Um especial agradecimento ainda pelas fofocas, pelas vossas preciosíssimas dádivas, pelas quartas-feiras de frangos e sextas-feiras de doidos.

Ao meu fiel companheiro da Linha de Sintra, um grande obrigada por todos os pequenos momentos em que do nada lá estava eu a tentar lembrar-me que devia parar de rir e começar a respirar, bem como por toda a partilha dos pequenos grandes tesouros musicais e culturais que por aí existem. Maria Callas, Natália Andrade e Cebola Mol marcaram claramente este último ano. Obrigada!

Aos meus pais, devo-vos tudo aquilo que sou e tenho hoje. Sem vocês nada disto seria possível. Obrigada por todo o apoio, amor e compreensão nestes últimos anos, e acima de tudo por aturarem e acreditarem em mim. São vocês que me inspiram a lutar todos os dias por aquilo que ambiciono e é de vocês que eu arranjo força para tal. Ao meu maninho, (sim, a Ilustre não se esqueceu de ti) de nada por te continuar a mostrar como é que realmente se faz, mas muito obrigada por todo o apoio, força e por me mostrares que os Morgados conseguem tudo. Obrigada

ainda por me teres dado uma irmã, a Miss Sóráia, que me dá sempre força e ânimo para continuar. Finalmente, um obrigado muito especial a vocês por me terem dado o picolhito que me alegra o dia sempre que me dá um abracinho e me derrete toda quando chama pela “Tiii”.

Ao Henrique, um obrigado do fundo do coração por toda a boa disposição, carinho e apoio que traz à minha vida. Acreditas mais tu em mim que eu própria e mostras-me que consigo tudo aquilo a que me proponho. Obrigada por me ouvires horas e horas a falar dos meus dilemas, muitas vezes não os percebes, mas acabas sempre por minimizá-los e dar-me força para continuar.

À minha bélhota Joana, a senhora sempre na Lua, obrigada por todos os novelos e por todas as tardes que se fizeram noites na luta para mostrar que afinal os bioquímicos até percebem alguma coisa disto enquanto camisolas e sapatinhos de lã eram cosidos. Ao Alex, o meu parsa de todas as horas, obrigada por todas as chamadas, cafés, palavras de força e preocupação. Estes dois últimos anos não teriam sido a mesma coisa se não vos tivesse a vocês para me aturarem, fazerem rir até mais não e ouvirem os meus dramas e lamúrias a toda a hora. A quarentena teria sido muito pior se não vos tivesse a um ecrã de distância!

Um obrigado muito especial à minha Rissol, quem esteve sempre lá para me relembrar que o difícil é um tipo de chocolate que se come facilmente e que mais festejou por cada pequena vitória que tive. Para sempre recheio de amor com topping de porrada. Um obrigado enorme ainda para a minha Bá, Bia Mariz, Bia Matos e à minha Catty Cat. O melhor de BQ foram vocês, e são vocês que trago no coração para sempre. Obrigada por todas as mensagens de apoio, carinho e ajuda ao longo destes últimos anos. Não foram Pêra Doce, mas estiveram sempre lá à espera com uma garrafinha de Gin para festejar ou chorar comigo.

Finalmente, mas não menos importante, um obrigado enorme aos Melhores do Mundo. Foram, sem dúvida alguma, anos atípicos, mas a amizade, apoio e companheirismo permaneceram. As dificuldades vão e vêm, mas os putos do kuduro e as velhas à janela estão lá sempre.

Muito obrigada a todos, do fundo do coração!

Abstract

Cancer highly impacts the society, being one of the leading causes of death. Immunotherapies have already shown great results in a large number of patients and in different types of cancer. However, these encompass high investments per treatment due to therapeutic individuality, not being readily available as first-line treatment.

Natural killer (NK) cells have been gathering attention considering their essential role in cancer immunosurveillance, by rapidly inducing tumor cell death without prior sensitization. In previous works from the research group, a small organic molecule (**815A**) capable of triggering the cytolytic response of NK cells by engaging an activating receptor of these cells, was developed. Its efficacy has been demonstrated. However, solubility and stability issues hamper more comprehensive studies of its effect.

In this work, a water soluble injectable formulation of compound **815A** was developed. This stable formulation was produced by combining the test compound with mannitol, enabling further studying of compound **815A**. This allowed the determination of the *logP* value of the molecule, its plasma proteins binding profile, plasma stability and the development of a suitable quantification method.

In addition, a controlled-release system was developed to control the activation of NK cells by **815A**. The prolonged NK cell activation effect was achieved with polymeric nanoparticles with biocompatible and biodegradable characteristics that released the test compound at a steady rate, preventing the over-activation and subsequent repression of NK cell response.

Key words: NK cells; Small organic molecule; Immune response triggering; Formulation; Drug delivery system

Resumo

O cancro tem um grande impacto na sociedade, sendo uma das principais causas de morte. Imunoterapias têm vindo a demonstrar ótimos resultados num grande número de doentes e em diferentes tipos de cancro. Contudo, por tratamento, esta acarreta grandes investimentos devido à sua individualidade terapêutica, não sendo, desta forma, a primeira opção terapêutica.

As células *Natural Killer* (NK) têm sido alvo de grande atenção dado o seu importantíssimo papel na imunovigilância do cancro, induzindo rapidamente morte de células tumorais sem necessitarem de sensibilização prévia. Em trabalhos anteriores do grupo de investigação, foi desenvolvida uma pequena molécula orgânica (**815A**) capaz de induzir as respostas citolíticas das células NK através da sua ligação a recetores ativadores destas. Apesar da sua eficácia já ter sido demonstrada, problemas de solubilidade e estabilidade dificultam a realização de mais estudos.

Neste trabalho, uma formulação injetável do composto **815A** solúvel em água foi desenvolvida. Esta foi produzida através da combinação do composto teste com manitol, permitindo desta forma o estudo do composto **815A**. Estes estudos permitiram a determinação do *logP* da molécula, o seu perfil de ligação a proteínas plasmáticas, a sua estabilidade em plasma e ainda o desenvolvimento de um método de quantificação.

Adicionalmente, foi desenvolvido um sistema de libertação controlada para controlar a ativação de células NK pelo **815A**. O efeito prolongado da ativação das células NK foi conseguido com nanopartículas poliméricas com características biocompatíveis e biodegradáveis que libertavam o composto teste a uma taxa controlada, prevenindo a sobre estimulação e consequente inibição da resposta das células NK.

Palavras chave: Células NK; Pequenas moléculas orgânicas; Estimulação de uma resposta imune; Formulação; Sistema de distribuição de fármacos

Index

Figure index

Table index

Abbreviation list

%CV	Coefficient of variability
µL-pickup	Microliter-pickup
ACT	Adoptive cell transfer
ADME	Adsorption, distribution, metabolism, and excretion
API	Active Pharmaceutical Ingredient
BAT3	Human leukocyte antigen-B-associated transcript 3
BiTE	Bispecific T cell engager
BSA	Bovine serum albumin
CAM	Cell adhesion molecule
CAR-T	Chimeric antigen receptor modified T cell
Cl	Clearance
CN	Cyano
CR	Clearance ratio
DAD	Diode-array detector
DMSO	Dimethyl sulfoxide
DruMAP	Drug Metabolism and pharmacokinetics Analysis Platform
ELISA	Enzyme-linked immunosorbent assays
Eq.	Equation
ε	Extinction coefficient
FDA	Food and Drug Administration
$f_{u,p}$	Fraction of drug unbound in plasma
GFR	Glomerular filtration rate
HILIC	Hydrophilic Interaction Liquid Chromatography
HPLC	High Performance Liquid Chromatography
ICI	Immune checkpoint inhibitor
IFN-α	Interpheron-alpha
IFN-γ	Interferon-gamma
IL-10	Interleukin 10
IL-2	Interleukin 2
IS	Internal standard
ITAM	Immunoreceptor tyrosine-based activating motif
IV	Intravenous
LC-MS	Liquid chromatography – mass spectrometry

LOD	Limit of detection
logP	Octanol/water partition coefficient
LOQ	Limit of quantification
mAb	Monoclonal antibody
MHC	Major Histocompatibility Complex
MW	Molecular weight
NCR	Natural cytotoxicity receptor
NCR3	Natural cytotoxicity receptor 3
NDE	New drug entity
NK	Natural killer
NKp30	Natural killer cell receptor 3
NKp44	Natural killer cell receptor 2
NKp46	Natural killer cell receptor 1
NMR	Nuclear magnetic resonance
NP	Nanoparticle
O/W	Oil-in-water emulsion
PAMPA	Parallel Artificial Membrane Permeability Assay
PBMC	Peripheral blood mononuclear cells
PBS	Phosphate-buffered saline
PdI	Polydispersity index
pI	Isoelectric point
PLGA	Poly-lactic-co-glycolic acid
PPB	Plasma protein binding
R^2	Correlation coefficient
RES	Reticuloendothelial system
Rt	Retention time
SD	Standard deviation
SDS	Sodium dodecyl sulfate
TAA	Tumor-associated antigen
TIL	Tumor-infiltrating lymphocytes
TNFR	Tumor Necrosis Factor Receptor
TNF-α	Tumor Necrosis Factor alpha
UV-Vis	Ultraviolet-visible
VD	Volume of distribution
W/O/W	Water-in-oil-in-water emulsion

WHO	World Health Organization

I. INTRODUCTION

1.1. Cancer's impact

According to the European Commission's database, in 2020 approximately 2.7 million new cases of cancer were reported, along with 1.3 million deaths associated to oncologic conditions, in the member countries of the European Union.[1] Around 2.1% and 2.4 % of those represent, respectively, the incidence and mortality of cancer in Portugal. This country's national statistic center (Instituto Nacional de Estatística) stated that, in 2017, cancer was the second cause of death accounting for 25% of all deaths.[2] This is observed worldwide, where, according to the World Health Organization (WHO), cancer is one of the leading causes of death of under 70 years old in 112 of 183 countries, being ranked the third or fourth death cause in all the others.[3]

Increases in cancer incidence have been reported through the years, being correlated with overall social development, namely due to the growth and aging of the population and to lifestyle-associated risk factors such as alcohol intake, overweight, tobacco smoking, pollution, among others.[3,4] However, along with this increase of cancer incidence, a slower increase pace in the mortality is being observed in Europe.[5] This might be correlated to a combination of factors, including the great advances in prevention, early detection and development of new therapies throughout the years.

In fact, as a consequence of its prominent impact in the society, cancer has been receiving a lot of attention in terms of funding for the discovery of new treatments, ways to minimize the associated side effects and new prevention measurements. According to the American Society of Clinical Oncology, only in the United States, cancer research has been given enhanced funding overtime, with increases of approximately 2.5 billion euros of annual investment observed from 2006 to 2018. During this period, the highest portion of investment was to develop new treatments.[6] All these investments are being translated into a large number of new possible therapeutics at the final stages of a new medicine's clinical phase.[7,8]

1.2. Immunotherapy for cancer

Cancer treatment has been primarily based on surgery, chemotherapy, and radiotherapy up until the moment that immunotherapy started gaining attention due to the 1985's findings of Rosenberg and co-workers, which described the first effective immuno-based therapy. Rosenberg's approach encompassed the administration of recombinant Interleukin 2 (IL-2) and lead to a durable regression of metastatic melanoma and renal cancers in humans.[9] The use of this immunostimulant cytokine to treat cancer is a direct consequence of the evidences found in the early 1960s on how the immune system plays a major role in preventing cancer development.[10,11] In fact, it was the immune surveillance hypothesis that triggered all the investigation surrounding this topic and its possible applications in cancer treatment.

The immune surveillance process consists of the continuous state of monitorization conducted by the several immune effector cells, resulting in the elimination of pathogens and/or cancer cells.[10,12] This process ensures that growing tumors are destroyed accounting on the immune surveillance status. However, this happens only at the early onset of the disease, considering that from the moment that the elimination process starts to fail, the surviving cancer cells replicate and acquire resistance to immune cells. Allowing, in this way, the tumor to grow, in what is called the equilibrium stage. These two phases comprise the immunoediting process, being the cancer clinically undetectable and most patients do not show any symptoms of the disease. After the equilibrium, along with tumor progression, starts the escape phase in which cancer cells become able to escape the immune system attack through different mechanisms, resulting in the progression of the disease with symptom onset and eventual metastization.[12]

Supporting the concept of immune surveillance are several evidences showing that, for instance, patients with melanoma survive longer when have higher numbers of lymphocytes, namely tumor-infiltrating lymphocytes (TILs), than the ones with lower numbers of these cells.[13,14] Also, immunosuppressed patients have higher risks of developing malignancies due to immune surveillance impairment.[15,16] Considering this high immune activity during the early stages of the disease, immunotherapy is applied in order to either complement or stimulate the immune system to prevent the disease spreading.[17]

Immunotherapy can be divided into the active and passive immunotherapy. Passive immunotherapy uses immunological components/effectors to (re-)activate the host's immune system. In contrast, active immunotherapy, such as vaccines, relies on the patient's own immune system, aiming to stimulate it to defend against the disease.[17,18] Another important and relevant difference between these two types is the fact that passive therapy will be completely dependent of several administrations due to its short-lived effects.[17] In Figure 1 are presented the main cancer immunotherapy types available.

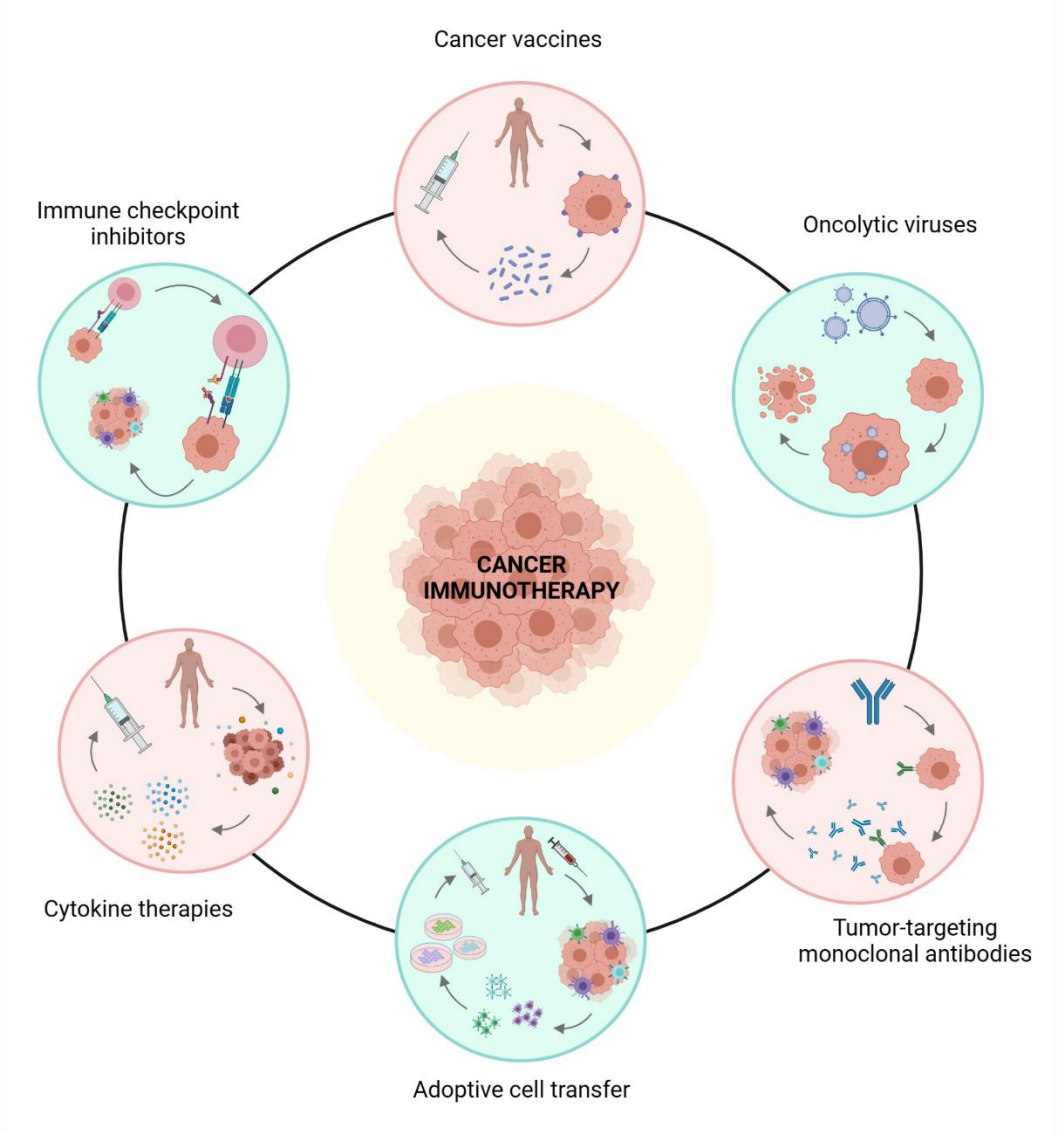

Figure 1: Cancer immunotherapy types.

1.2.1. Active cancer immunotherapy

Falling into the active type of immunotherapy are the vaccines, which can be either used to prevent the development of cancer in patients with genetic predisposition (prophylactic cancer vaccines) or to treat an existing tumor (therapeutic cancer vaccines). Therapeutic vaccines are the ones that gather the most attention being prominently whole cell based. These rely on the use of inactivated tumor cells from the host or a donor (autologous and allogenic, respectively), with a variety of oncogenic antigens on their surface, that will prompt the host's immune system to develop a response. On the other hand, synthetic protein antigen vaccines contain synthetically produced specific tumoral antigens that are administrated to trigger an immune response.[18] It has been described that the concurrent administration of these vaccines with cytokines can enhance the vaccine effect due to the enhancement of immunological response through the recruitment of immune cells and the direct activation of T cells and

natural killer (NK) cells.[17,19] Among those cytokines, IL-2 and Interferon-alpha (IFN-α) have already been approved to treat malignant diseases based on the observed clinical effects.[20]

Oncolytic virus and immune checkpoint inhibitor therapies are also considered active ways of immunotherapy. The oncolytic virus therapy relies on the oncolytic nature of some known viruses to target and kill tumoral cells without harming normal cells. Furthermore, these viruses have also an important role in activating the suppressed immune system within the tumor microenvironment.[21] A similar effect is obtained through the use of immune checkpoint inhibitors (ICIs) that act within the surface receptors of immune cells and/or cancer cells. The administration of these inhibitors will induce the upregulation of the immune response against the malignant cells.[22,23]

1.2.2. Passive cancer immunotherapy

Among all the types of passive immunotherapies available, the adoptive cell transfer (ACT) and the administration of tumor-specific monoclonal antibodies (mAbs) are highlighted. ACT therapies rely on autologous immune cells, mainly T cells, and generally encompass their isolation, *ex vivo* expansion, modification and/or activation, and infusion into the patient, normally, with an enriched antitumor reactivity.[22,24] One type of ACT, the chimeric antigen receptor modified T cell (CAR-T) therapy, which consists of the reprogramming of T cells, maintaining their effector functions while providing them with the ability of recognizing any cell surface antigen without being dependent of the major histocompatibility complex (MHC), is one of the successful approaches of cell-based cancer immunotherapy.[25] By transferring T cells engineered to recognize specific tumor antigens other than the MHC-type that have been lost during immunoediting process of cancer cells, the immune system regains the ability to fight the growing tumor.[26,27]

The other branch of passive immunotherapy encompasses the use of mAbs. Tumor-targeting mAbs are the most widely clinically employed and known form of immunotherapy.[28] They can either inhibit signaling pathways, mandatory for the malignant cells' maintenance and spreading, or they can activate death signaling receptors on their surface, such as the tumor necrosis factor receptor (TNFR), which can activate cell death pathways.[29] Moreover, the mAbs can be coupled to toxins or radionuclides, allowing a target-specific treatment, or they can opsonize cancer cells and further lead to cytotoxic and phagocytic activities.[30,31] Finally, there are the called bispecific T cell engagers (BiTEs) which consist of chimeric proteins that besides recognizing a tumor-associated antigen (TAA), also recognize a T cell surface antigen. These two properties enable the BiTEs to direct the host´s T cells towards malignant cells, inducing and activating an immune response against them.[24]

1.2.3. The need for new immunotherapies

Overall, all these therapies have already shown, individually, their effectiveness in a large number of patients and several types of cancer. The most outstanding results actually indicate that it is possible to restore a state of antitumor immunosurveillance in patients with cancer immunotherapies.[32] However,

there is not a single therapy falling into this category that is effective in every patient and in every single cancer type. Therefore, it is necessary to find new biological targets and pathways to work with in order to generate more efficient and potent cancer treatments.[33] Moreover, the variety of tumor mutations found specifically in each patient, prevents the simple development of generalized and broad-specific immunotherapies. Effective treatments would, therefore, possibly require the development of technologies specifically for each person which, in terms of costs, will most likely not be conducted.[32,33] In fact, the economical aspect of these kinds of treatments is a major drawback. For instance, a therapy course with ipilimumab, a checkpoint inhibitor mAb, costs approximately €100 000, and a single CAR-T treatment can go up to €400 000.[34,35] This, obviously, makes immunotherapy inaccessible for the majority of the patients, thus leaving therapies like radio and chemotherapy as well as surgery as first-line cancer treatments. This also compromises the efficacy of immunotherapy as most patients only have access to this after undergoing chemotherapy or at an advanced disease stage, when the immune system is already jeopardized.[32]

For all these reasons, investment in new immunotherapies or immunotherapies-alike are required to ensure that they go from being the last source of hope to be the first form of acting against the disease. On that aspect, natural killer cells have been collecting the researchers' attention due to their ability to detect and kill transformed cells, being proposed as the next major target for cancer fighting.[36,37]

1.3. Natural Killer Cells

Natural killer cells are a subset of white blood cells first categorized as large and granular lymphocytes in 1975 by Kiessling and co-workers.[38] These cells are part of the innate immune system and are known for being able to exert cytotoxic activity without prior sensitization, as well as an immunomodulatory activity through the production and secretion of cytokines.[39]

Natural killer cells play essential roles in immunosurveillance and there are evidences showing that dysfunctional NK cells and/or a deficiency in their numbers leads to poor therapeutic outcomes in cancer patients.[40] By being outnumbered and dysfunctional, these cells lose their ability to attack and suppress the tumor proliferation, allowing its escape as previously described. Accounting on this, a promising immunotherapeutic approach might consist of restoring the normal function of NK cells. There are several strategies being tested in clinical trials surrounding adoptive transfer strategies, as well as the use of mAbs to target these cells. In some, it was already possible to conclude that the combination of immunotherapy targeting NK cells with other treatments targeting T cells can trigger antitumor activities by both the adaptive and innate immune system effectors leading to better and complemented results.[40,41]

1.3.1. Regulation of NK cell activity

NK cell's response is a direct consequence of an integration of both inhibitory and activating signals arising from receptors present on its surface. Most of these receptors are only present in NK cells and

are constitutively expressed, independent on the activity state of the cells. This is what grants NK cells a key role as effectors of innate immunity.[42]

Activating and inhibitory NK cell receptors are crucial for the regulation of the activity and responses of NK cells. One of the mechanisms by which NK cells target and kill other cells rely on the loss of MHC-I molecules, described as the "missing-self hypothesis".[43] In this mechanism, NK cells target cells that are not expressing this molecule but only in an environment where cells presenting MHC-I molecules exist. The activation of a full cytolytic response in NK cells is not possible with only the lack of the MHC-I's inhibitory signal. In fact, the killing function of these cells depends on the sum of inhibitory and activating signals transduced by different sets of receptors. When the activation signals dominate over the inhibition signals, determined by the amount and type of receptors being engaged, the cytolytic activity of NK cells will be triggered.[44] In addition, whenever the target cell presents the same level of ligands for activation and inhibition receptors, a dynamic equilibrium is reached since those signals cancel one another, rendering the NK cells inactive.[45]

1.3.2. Cytotoxic response and killing mechanisms

When the NK cells are in contact with a target cell, an interface, known as immunological synapse, is formed. With this, a recognition process starts in order to check for inhibitory, activating, or both ligands. The immunological synapse is only maintained if activating ligands are encountered. If so, several cell adhesion molecules (CAMs), present in the surface of NK cells, promote the formation of a tight adhesion between the two cells. However, this process plays a bigger role in maintaining and reenforcing the immunological synapse than inducing a response since, as previously described, full activation is reached when there is an interaction of the activating ligands of the target cell with the activation receptors of NK cells, such as NKp30, NKp44, NKp46 or NKG2D.

Upon full activation, the degranulation process begins. This triggers the reorganization of the cytoskeleton and the polarization of the microtubules in order to transport lysosomes towards the synapse point. The lysosomes are then docked and fused with the cell membrane releasing their content.[46] Several lytic enzymes, mostly perforins and granzymes, are released in the immunological synapse. Granzymes belong to the family of serine proteases and induce cell apoptosis within the target cell, being highly dependent of the co-release of perforins due to their pore-forming ability.[47] Along with this mechanism, NK cells also secrete a series of cytokines such as Interferon-γ (IFN-γ) and Tumor Necrosis Factor-α (TNF-α) as depicted in Figure 2. IFN-γ plays a major role in shaping an adaptive immune system response by activating macrophages. Moreover, this cytokine has shown evidence that it can have antiproliferative effects in tumoral cells as well as suppress the tumor's blood flow causing its collapse.[45,48] Also exerting effects in the tumor vasculature is TNF-α, which can additionally trigger tumoral apoptosis and attract immunological cells such as neutrophils and monocytes into the tumor microenvironment.[49]

The combination of an innate ability of differentiating normal cells from stressed cells, with the cytotoxic and apoptosis-inducing mechanisms, and with immunological attraction and activation pathways, has granted NK cells a relevant role as immunotherapy target.

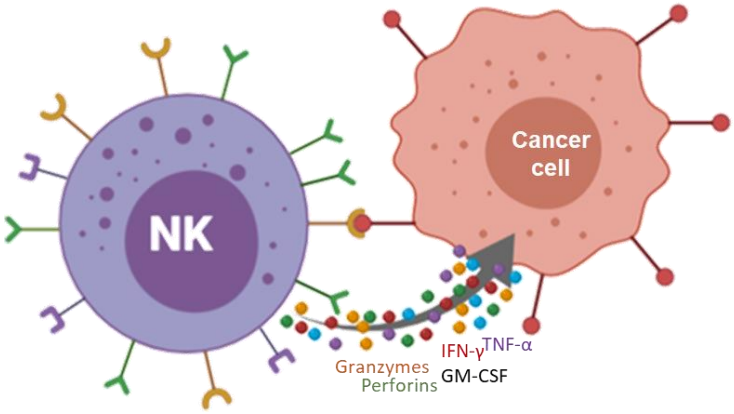

Figure 2: NK cell cytotoxic activity. Upon engagement of an activation receptor, NK cells release the content of the lytic granules (perforins and granzymes) towards the target cell presenting the activation ligands. Cytokines, such as TNF-α, IFN-γ and GM-CSF, are also secreted by NK cells upon activation**.**

1.4. NKp30 Receptor

The Natural Killer protein 30 receptor, also known as natural cytotoxicity receptor 3 (NCR3), is a member of cytotoxicity receptors (NCRs) family, extremely important for NK cell activation. NCRs were first categorized accounting on their ability to start the cytotoxic and cytokine-secretion functions of NK cells towards tumoral cells.[50,51] Nowadays, the ligands identified for these activating receptors include bacterial-, viral- and parasite-derived proteins, as well as stress or transformed cell markers.[50] From this family, the NKp30 has been presenting evidences that it is actually the dominant activating receptor, being responsible for the cytolytic activity against several tumors types.[52]

The NKp30's first structural description was published in 1999 by Pende and co-workers, being characterized as being a type I transmembrane glycoprotein composed by an immunoglobulin-like extracellular domain shortly connected to a transmembrane and cytoplasmatic domains.[51] The extracellular domain consists in eight β-strands that form two antiparallel β-sheets connected by a disulfide bond between two cysteine residues.[52,53] The cytoplasmatic domain of the receptor is short, lacking signaling motifs for signal transduction. For that, NKp30 associates with intracellular adapter molecules containing immunoreceptor tyrosine-based activating motifs (ITAMs), such as FcεRIγ and CD3ζ, through a positively charged arginine residue within the transmembrane domain.[50,54] Upon binding of a ligand that induces conformation changes in the receptor structure, the arginine residue of NKp30 establishes an interaction with an aspartate residue of the adapter protein.[55] This then becomes phosphorylated inducing the activation pathways that will lead to the responses previously described in Section 1.3.2.

As already mentioned, the NKp30 receptor is able to interact with several ligands from different natures. These include proteins expressed by tumor cells, such as the human leukocyte antigen-B-associated transcript 3 (BAT3) and B7-H6. BAT3 is an intracellular protein that contributes to several cell processes such as apoptosis, protein synthesis, quality control and degradation as well as gene regulation.[50] Strandmann and co-workers have presented evidence showing that this protein is released by tumor cells when these are subjected to stress. In their study they submitted tumor cells to non-lethal heat shocks and BAT3, which is predominantly expressed in the nucleus, was found in the plasmatic membrane and afterwards within the extracellular environment. Moreover, they also described that upon tumor cell-NK cell contact, this same protein starts to be expressed in the cellular membrane and/or is released by the cell towards the NKp30 receptor, leading to the immune cell activation.[56] B7-H6 belongs to the B7 family and it is selectively expressed in some tumoral cells. This protein mediates the release of cytokines from NK cells and, due to its expression in many types of cancer, its potential use as a biomarker of cancer prognosis has been considered.[53,57]

1.5. Artificial NKp30 ligand

Previous works developed in the laboratories of the Design, synthesis and toxicology of bioactive molecules group of Centro de Química Estrutural pursued the hypothesis of using small organic molecules to trigger the activity of NK cells through binding of the NKp30 receptor.[58]

In this work, computational studies were conducted to examine the structure of the receptor and develop a series of molecules with high affinity towards the binding site. During the development, structural characteristics that could interfere with physicochemical features important for further pharmacological and toxicological studies, namely the molecule's solubility, were considered. This included, among others, the addition of specific chemical moieties, such as a quaternary amine group, to increase aqueous solubility. The fused-ring system, which was found paramount for the interaction of this type of compounds with the receptor, was also optimized to increase the stability of the molecule. After several modifications of the initial hit molecules, compound **815A** (Figure 3) was identified as a good ligand for NKp30. Extensive biological testing demonstrated that this was able to trigger the cytolytic responses of NK cells *in vitro*.

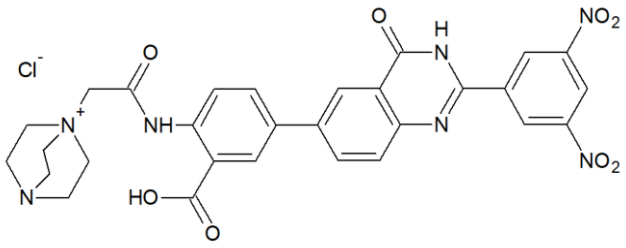

Figure 3: Molecular structure of the NK cell activation molecule 815A.

Degranulation, cytokine secretion and target cell lysis are in fact responses that, depending on its concentration, compound **815A** is able to induce in the NK cells (Figure 4). Previous experiments using primary cultures of NK cells demonstrated that the degranulation process is induced with concentrations as low as 4.8 nM, and the secretion of IFN-γ and TNF-α peaks at 40 nM. As for targeting cell lysis, the optimal responses were observed at concentrations between 0.31 and 2.5 µM.[58]

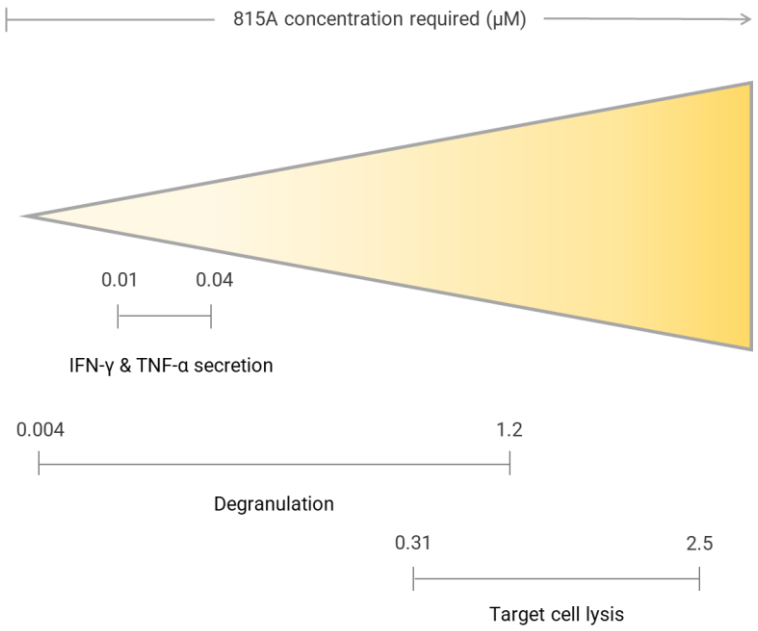

Figure 4: Concentrations of compound 815A required for inducing different NK cell responses. Schematic representation of the amount of **815A** required to induce different NK cell responses, such as cytokine secretion (IFN-γ and TNF-α), degranulation and target cell lysis. Adapted from data retrieved from the original work.[58]

For each response, there is evidence showing that any **815A** concentration above the optimal ranges, depicted in Figure 4, will result in an activity decay. Although this topic is currently being investigated, it is hypothesized that the concomitant stimulation of different NKp30 isoforms may result in a downregulation of the response. In fact, six different isoforms of NKp30 are known, These, resulting from alternative splicing, present differences in the intracellular region that result in the association with different adapter proteins. While isoforms NKp30*a* and *b* associate tightly with ITAM proteins, as mentioned before, the *c* isoform associates poorly with these. Therefore, while engaging the NKp30*a* and NKp30*b* isoforms was found to produce high levels of IFN-γ, NKp30*c* engagement is characterized by low IFN-γ production and the release of high amounts of Interleukin-10 (IL-10), which is known to have immunosuppressing activities.[59] These differences justify the dual immunomodulatory activities of the NKp30 receptor and, in fact, depending on the expression level of each isoform, the immunological outcome will differ. For instance, high expression levels of the *c* isoform are correlated with higher morbidity rates. In contrast, higher expression of the *a* and *b* isoforms is correlated with higher immunostimulatory activities and thus better survival rates.[42] Thus, overstimulating the NK cells with the **815A** probably results in the NKp30*c* isoform activation, inducing, in this way, a counteracting response to the desired.

Because of this pleiotropic activity of compound **815A**, its use as an NK cell trigger requires a thorough study to determine the effective therapeutic window. For that, the pharmacokinetic behavior of this molecule must be understood as several parameters will influence its concentration in circulation.

1.6. Drug-like properties and pharmacokinetic behavior predictions

During the development of new drug entities (NDEs), the pharmacokinetic properties are important characteristics to take into consideration in order to predict how the compound will behave once administrated. The correct pharmacokinetic characterization will enable the prediction of parameters relevant to find whether the molecule will exert any effect at the intended site of action and if it maintains an effective concentration for enough time.

To fully characterize compound **815A**, several parameters regarding its absorption, distribution, metabolism, and excretion (ADME) must be determined. There are a lot of *in silico* methods available to aid the medicinal chemist during the drug discovery process. Usually, these are based on the information extracted from *in vitro* or *in vivo* experimental tests of large compound libraries. Therefore, the information obtained by these methods is not absolute and can only provide some clues on of how the test compound will behave in biological conditions.[60]

As compound **815A** was developed to interact with a receptor expressed in the surface of NK cells, attention was given, during its development, to ensure that it would behave as a water soluble molecule with little capacity to permeate membranes. To do so, a permanent positive charge was included in the structure, as already mentioned. Moreover, a low molecular weight was not considered relevant during the development phase. These two features end up restricting the administration route and may hamper the distribution and elimination profiles of the compound. Because of that, a number of pharmacokinetic-parameters must be determined before further developing the use of **815A** as a therapeutic agent and before developing a pharmaceutical formulation of this compound. Some of the pharmacokinetic parameters have already been predicted based on several models and approaches, that serve as a starting point for the characterization of compound **815A**.

1.6.1. Lipinski's rules

In 1997, Lipinski presented a set of physicochemical descriptors that correlate to the ADME properties. The "rule of 5" encompasses four criteria, namely the number of hydrogen bond donors and acceptors, molecular weight (MW), and octanol/water partition coefficient (*logP*).[61] Contrarily to *logP*, the determination of the other descriptors does not require experimental procedures or computational simulations, only the inspection of the molecular structure. According to Lipinski, a poor absorption or permeation is less likely whenever two or more of the five rules are violated.[61]

A. Molecular weight and partition coefficient

Within the rule of 5, the NDE's molecular weight must not exceed 500 g/mol.[61] Compound **815A** (Figure 3) has a MW of 600.55 g/mol (excluding the counterion), which is well above the limit purposed by Lipinski. Therefore, it is unlikely that the compound will be active when orally administrated due to lower intestinal permeability. Moreover, poor intestinal permeations are also correlated to low *logP* values.[61]

The determination of the *logP* value was predicted using the method described by Moriguchi.[62] This method considers the contribution of several structural features (see appendix Section 6.1) and enables the determination of the partition coefficient value .[62] Using this approach, compound **815A** is expected to have a *logP* value of -2.49, which, according to the Lipinski's rules that state that this value must be lower than five, means that the **815A** might be orally active.[61] However, other descriptors must also be considered to better predict its behavior, especially the high molecular weight, which highly impact the ability to permeate membranes.[63]

B. Hydrogen bond donors and acceptors

The presence of functional groups within a drug's molecular structure capable of forming hydrogen bonds can rapidly increase its solubility and can also be effective in terms of affinity and selectivity to the site if action. However, when in excess, these can also have detrimental effects in the drug's permeation through the plasmatic membrane. The lack of a good hydrophilicity - lipophilicity balance can decrease or block the non-polar interactions between the molecule and a lipidic bilayer, causing, in the case of orally administrated drugs, major consequences in its absorption profile and, therefore, its efficacy.[64] The "rule of 5" considers the number of hydrogen bond donors as well as the number of hydrogen bond acceptors. The first, expressed as the sum of NH and OH groups, must not exceed 5 and the second, which considers the total number of nitrogen and oxygen atoms, has a limit of 10.[61]

In the structure of compound **815A**, (see Figure 3) it is possible to identify three hydrogen bond donor groups, thus not exceeding the limit above mentioned. As for hydrogen bond acceptors, the sum of all nitrogen and oxygen atoms amounts to 15. However, structural limitations reduce this number to 11, considering that nitrogen atoms in both the quaternary ammonium and the nitro moieties cannot accept hydrogen bonds, and that the oxygen atoms in the nitro groups are not able to form strong hydrogen bonds. Nevertheless, by having a total of 11 hydrogen bond acceptors, compound **815A** surpasses the implemented limit of 10 by the Lipinski's rules.

Considering all descriptors studied under the "rule of 5", the compound in study violates two of the four rules by having a high molecular weight and too many hydrogen bond acceptors.[61] Therefore, as previously mentioned, a structure that violates two of the rules is more likely to have a poor pharmacological effect when orally administrated due to its difficulties in being adsorbed in the gastrointestinal tract.

1.6.2. Solubility

Considering the predictions previously made, compound **815A** is not expected to freely permeate lipidic bilayers, which imparts its bioavailability if administered orally. This is a key finding to the development of a correct and effective delivery system. Moreover, considering the early phase of the drug discovery process, an intravenous (IV) administration route is preferred. Therefore, solubility parameters must be taken into consideration not only for the development of an IV formulation but also for the bioavailability of the active pharmaceutical ingredient (API).

A compound's solubility is highly influenced by structural properties and form.[65] In fact, as mentioned in Section 1.5, during its computational design and synthesis, structural properties were considered in order to enhance the aqueous solubility of compound **815A**. The one that has drastically impacted the **815A**'s solubility was the addition of a quaternary amine moiety conferring a formal positive charge to the compound. Moreover, properties like the *logP* value and the MW of the molecule also impact the solubility.[65] The *logP* value indicates the logarithm of ratio between the concentration of the compound in the organic and the aqueous phases, meaning that negative values indicate that the compound is predominantly in the aqueous one. Actually, there has been defined a *logP* cut-off point between 2 and 3, in which values above this limit indicate that the correspondent molecule has poor hydration.[66]

Considering the *logP* value predicted, a good aqueous solubility is expected. However, the compound's high MW and the high number of functional groups, might result in solubility issues. Despite that, considering the predic

tions made based on the compound's structure using an *in silico* tool (Drug Metabolism and pharmacokinetics Analysis Platform (DruMAP))[67], **815A** belongs to the class of compounds with high solubility at physiological pH, with an aqueous solubility due to be higher than 10 mg/L. Hence, no conclusions can be drawn on the compound's solubility due to conflicted predictions.

1.6.3. Plasma protein binding

The plasma protein binding (PPB) is another of the many factors highly influencing bioavailability, distribution, and effect of a drug. It is the free form portion of API, meaning the amount that it is free to be transported through the body, that determines its effectiveness. Once in the systemic circulation, the portion of API in its free form highly depends on its affinity for plasma proteins.[63]

Plasma proteins are mainly albumin and globulins and they correspond to around 10% of plasma constitution, along with ions, nutrients, and other constituents, being water the remaining 90%.[68] Usually, acidic and basic API's tend to be extensively bound to albumin and globulins, respectively.[63] Regarding the amphoteric properties of the molecule in study (see appendix Section 6.1), depending on the pH, its behavior will either be of an acid or a base. At physiological conditions, however, the molecule will probably behave like a zwitterion due to the pK_a values of both carboxylic acid and the DABCO moiety, approximately 4.4. and 3 respectively. When in comparison to acidic and basic drugs, zwitterions are likely to be less bound to plasmatic proteins than acids, but more than bases.[69]

In addition to this, the lipophilicity of the drug and its MW also impacts the extent of PPB. A drug's lipophilicity is directly correlated to PPB and, concerning the MW, drugs between 500 and 700 Dalton are expected to be approximately 98% bound to proteins according to Lalatsa and co-workers.[69] Corroborating this probable high affinity for plasma proteins of **815A**, is the predicted value of the extent of unbound drug in plasma ($f_{u,p}$) of approximately 8%, as estimated using the DruMAP tool.

In conclusion, considering the **815A** structural properties discussed here and the predictions made, it is very likely that this compound, once systemically administered, will become almost completely bound to proteins, affecting its pharmaceutical effectiveness.

1.6.4. Distribution and Elimination

Focusing on an IV administration, upon entering the systemic circulation, the drug is distributed through the body depending on the blood flow, the affinity for plasma proteins and other blood components, and also depending on the drug's ability to permeate cellular membranes. At the same time that the drug is being distributed, elimination organs such as liver, kidneys and intestinal tissues start the drug's metabolization and excretion.[63]

The compound's volume of distribution (V_D) represents the apparent volume in which the amount of drug administrated (dose) is distributed. The bigger the volume of distribution, the bigger will be the compound's concentration in extravascular tissues.[70] Considering the conclusions previously made regarding its PPB, it is very likely that the compound has a low V_D accounting on the expected low $f_{u,p}$, and the probable low membrane permeability.

Overall, for an IV bolus, the total clearance is defined as the sum of the renal and hepatic clearance, being disregarded all the others. This is due to the important and predominant role of the liver within drug's elimination. However, no tools are available to best predict either total or hepatic clearance (Cl), being only possible to have an idea of how this compound will behave after entering the kidneys. Renal excretion can be either conducted by glomerular filtration, tubular reabsorption, or active tubular secretion.[70] The virtual DruMAP tool allowed the categorization of the compound considering the clearance ratio (CR), which is described as the renal extraction ratio and is calculated in accordance to Equation 1.

$$CR = \frac{Cl_{renal}}{(f_{u,p} \times GFR)} \qquad \text{Eq. 1}$$

Besides depending on the renal clearance and the unbound fraction of drug in plasma, the clearance ratio also depends on the glomerular filtration rate (GFR) which describes the volume of plasma containing free drug that is filtrated and enters the tubular lumen per unit time. For the CR's prediction the GFR was assumed as 126 mL/min by considering a 70 kg man (1.8 mL/min/kg).[70,71] As mentioned, the CR allows the categorization of drugs in three different categories determining whether the

compound is reabsorbed (CR < 0.67), secreted (1.5 ≤ CR), or neither of them (0.67 ≤ CR < 1.5).[71] The predictions, based on estimated values of $f_{u,p}$ and GFR, indicate that compound **815A** is due to be part of the secreted type of drugs, with a predicted CR value superior or equal to 1.5, meaning that, upon its entrance in the kidney, most of it will be eliminated through urine.[63,70]

1.7. Key objectives

In the present work, the main goal is to develop an IV formulation of the small organic molecule **815A**. The development of such formulation will require, in first place, the development of a sensitive and robust analytical method to detect and quantify the compound in a variety of complex matrices, bearing low concentrations. The second step it will then involve the development of a formulation susceptible to be intravenously administrated. Compound **815A** presents some parameters that will make its use challenging, especially when considering its predicted high solubility, high plasma protein binding and fast excretion, combined with narrow therapeutic windows and pleiotropic effects depending on its concentration. This might mean that a simple free-form formulation might not be indicated, and, at some point, controlled release forms might have to be considered in order to better control the levels of the compound in circulation. Therefore, after the complete characterization and determination of key pharmacokinetic-influencing parameters of compound **815A**, a modified release system will be developed and tested to verify its adequacy as a method of controlling the circulating amount of the test compound.

II. RESULTS & DISCUSSION

Further development of compound **815A** as an NDE directed at triggering the activity of NK cells against cancer requires que complete characterization of this molecule in terms of its effect, its pharmacokinetic properties, and its overall behavior in biological medium. These steps are crucial and must be performed before moving towards more comprehensive tests such as *in vivo* assays. For this, it is necessary to be able to identify and quantify the test compound among the other molecules present in the system. Therefore, before starting the development of injectable formulations of compound **815A**, this was extensively characterized and specific procedures to allow its extraction, identification and quantification in serum samples were developed.

2.1. Physicochemical characterization of 815A

2.1.1. Solubility and preparation of stock solutions

Previous works conducted in the research group on the solubility of compound **815A** allowed to conclude that this, although being engineered to contain structural moieties intended to increase its aqueous solubility, is not readily soluble in aqueous media. Therefore, stock solutions in an organic solvent had to be prepared. Dimethyl sulfoxide (DMSO) was found able to easily dissolve the compound, whilst other solvents such as acetonitrile or acetone were unable. Ethanol and other alcohols could also be used, but the solubility of **815A** in these was far lower than in DMSO.

Despite being able to dissolve the compound, stock solutions of high concentration in DMSO were difficult to prepare and required heating and sonication to achieve complete solubilization. This approach, however, was abandoned as heating of the compound in DMSO could lead to its degradation and, once cooled, the compound would usually precipitate. It was found that the addition of sodium bicarbonate to the mixture of compound **815A** and DMSO increased its solubility. Therefore, a typical preparation of a stock solution in DMSO comprised the initial suspension of a known amount of **815A** in a volume of DMSO to give a final concentration of 10 mM, followed by the addition of 1.5 molar equivalents of sodium bicarbonate, stirring until complete dissolution of the compound, and filtration of the undissolved bicarbonate. Stock solutions obtained by this method were found to be stable at room temperature, could be stored at -20 ºC and, once thawed, no precipitate was observed.

2.1.2. Melting point

The determination of the melting point of an organic compound is a fast, easy, and common technique used to identify and to verify a substance's purity. According to the European Pharmacopeia, the standard method to determine the melting point of a certain compound is the capillary method. In

this, a thin glass capillary tube containing a sufficient and compacted amount of dry compound is introduced into a heated stand nearby a thermometer. The melting interval is determined, being the melting temperature defined as the temperature at which the last solid particles of the compacted column of substance in the tube pass to a liquid form.[72] The melting interval, defined as the difference between the melting point and the temperature at which the solid starts to fuse, should be smaller than 2 ºC for the compound to be considered pure.[73]

The capillary method was used to determine the melting temperature of compound **815A**. The compound used in the work was obtained with a purity greater than 98%, as determined before by nuclear magnetic resonance (NMR) titration experiments and liquid chromatography – mass spectrometry (LC-MS).[58] Despite using a high-range melting point determination device (see Section 4.1.5), it was not possible to determine the melting temperature of compound **815A**. The system used had a limit of 400 ºC and, even at that temperature, the compound present in the capillary showed no signs of melting. This may be attributed to the size of the molecule, the formation of intramolecular and intermolecular hydrogen bons and other electrostatic interactions, as well as to the fact that the compound is in the form of a salt, due to the presence of a permanent charge in the ammonium moiety with a chloride as counterion.

2.1.3. Ultraviolet-visible Spectroscopy

Ultraviolet-visible (UV-Vis) spectroscopy techniques are commonly used to characterize and quantify molecules containing bonding and non-bonding electrons that can absorb energy in the form of ultraviolet or visible light. Organic compounds with high degree of conjugation, as in the case of compound **815A**, tend to absorb light in the UV and visible regions of the electromagnetic spectrum.[74]

As can be seen in Figure 5, the **815A** UV-Vis spectrum acquired in DMSO presents two clear absorbance maxima at 280 and 330 nm. While the maximum at 280 nm can be attributed to the aromatic ring systems, such as the biphenyl core, the maximum of 330 nm is probably attributed to the dinitrobenzene ring. Functional groups such as the nitro substituents, influence the conjugated systems, causing the absorption peaks to appear at longer wavelengths.

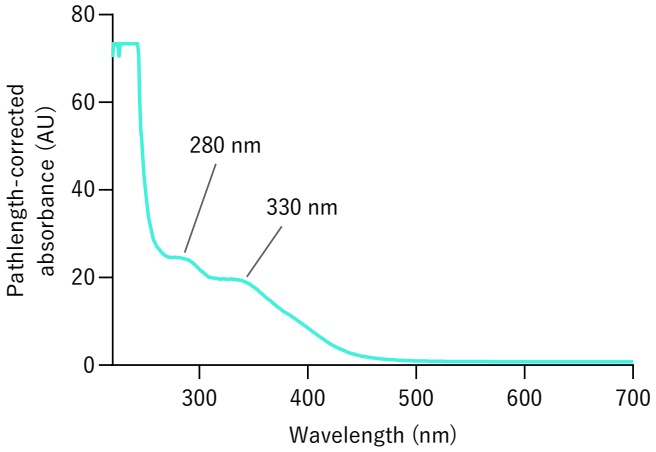

Figure 5: UV-Vis absorption spectrum of 1 mM of compound 815A in DMSO, recorded between 700 and 220 nm. Two characteristic maximum absorbance peaks are observed at 280 and 330 nm.

2.2. Quantification of compound 815A

As mentioned before, the further development of **815A** requires the ability to unequivocally identify and quantify this molecule in several matrices that include biological fluids such as blood plasma. As the test compound was found to have a distinctive UV-Vis absorption profile, techniques based on this property were used, including UV-Vis spectroscopy and high-performance liquid chromatography (HPLC) coupled with spectrophotometric detection systems.

2.2.1. Ultraviolet-visible Spectroscopy

The two absorbance maxima of compound **815A** previously identified were found useful for its unequivocal identification. As such, these same wavelength values were used to plot two calibration curves in DMSO to determine the molar extinction coefficients (Ɛ) of **815A** at both 280 and 330 nm. The two calibration curves were obtained measuring the absorbance values of DMSO solutions containing 0.25, 0.5, 1 and 2 mM of compound **815A**. Measurements were performed using a micro-volume system (see Section 4.1.3), corresponding to a pathlength (l) of 0.5 mm. The pathlength-corrected absorption values were plotted against the concentration as seen in Figure 6 and one calibration curve was extracted for each wavelength. Both of them present a coefficient of determination (R^2) of approximately 0.999 and, considering the Lambert-Beer's law, the correspondent $Ɛ_{280\ nm}$ and $Ɛ_{330\ nm}$ are 24210 and 18100 $M^{-1}.cm^{-1}$ respectively.

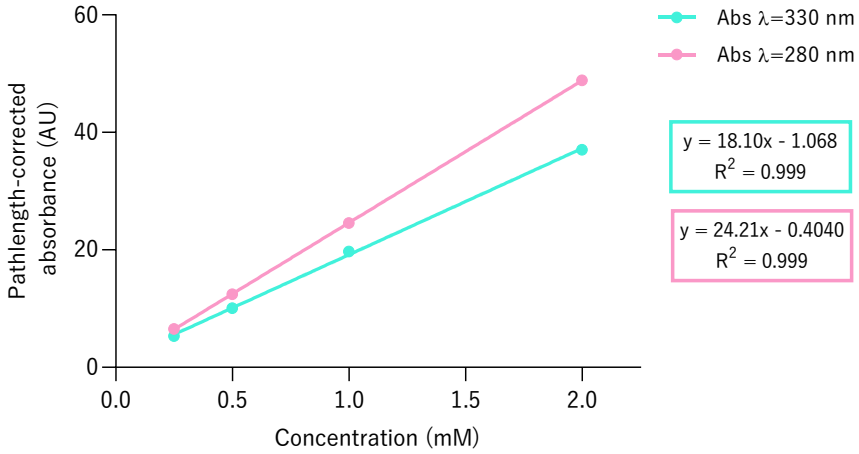

Figure 6: Calibration curves of compound 815A obtained at wavelengths of 280 and 330 nm. The molar absorptivity coefficients were retrieved from the slope of the linear regressions applied to each dataset.

2.2.2. HPLC-UV-Vis

HPLC is the most widely used and versatile type of elution chromatography.[75] In a chromatographic process the separation of compounds is accomplished through their partition between a mobile and a stationary phase. Depending on how much an analyte interacts with the stationary phase, the time required for its passage from the point of injection to the detector, defined as the retention time (Rt), will be greater if the distribution ratio favors the stationary phase.[76]

In an HPLC system, the mobile phase is a liquid, being the stationary phase a solid medium packed in a column. The constitution of these phases highly impacts how the sample will interact with them and, subsequently, how the separation process will evolve. The four major chromatographic separation types are based on size-exclusion, ion exchange, normal- and reverse-phase. In these, the column is, respectively, packed with a porous gel, with a solid support functionalized with anionic or cationic groups, or with silica beads coated with either polar or non-polar molecules.[75,76]

A complete HPLC system encompasses the solvent delivery system, an injection valve, a column, a detector, and a data processing unit. The solvents used must be of HPLC grade in order to mitigate the introduction of contaminants and/or particles that could possibly damage the system's components and interfere with the detection system used. [73] Another important aspect and requirement in HPLC systems is that no air circulates within its components since dissolved gases can lead to irreproducible conditions and poor signal quality. Therefore, the mobile phase must be degassed before entering the system, either manually, using vacuum systems and/or ultrasounds, or in-line through a degasser module included in the solvent delivery system.

To enable the passage of the mobile phase from the solvent reservoir to the column, and further through the detector, the pump creates high pressures and ensures a constant flow rate through the system. Sample injection is performed by an injection valve that allows the introduction of a precise and

defined volume of sample into the mobile phase in high-pressurized flow conditions and without interrupting the flow.[77] In this work, all assays performed encompassed the analysis of small sample volumes (10-20 µL), which is only possible using an analytical system equipped with either a small sample loop or a microliter-pickup (µL-pickup) system, reducing the errors associated with sampling with high volume loops. Once injected, the sample starts interacting with the mobile phase while also being moved through the column, and the several components of the mixture start to separate based on the partitioning between the two phases. It is important to highlight that pre-columns are commonly used between the injector and the analytical column to assure that major particulates and impurities do not enter the stationary phase.[75]

The identification of the sample's components is conducted downstream of the column using a suitable detector. In this work, due to the UV-Vis absorption properties of the test compound, its detection was performed using a diode-array-type detector (DAD). This enables simultaneous acquisition of a wide range of wavelengths in contrast to the more common UV-Vis detectors, which only allow the acquisition of discrete wavelengths per run. The data generated using this system, fully described in Section 2.1.3, enables the linking of each individual chromatogram's peak to an UV-Vis spectrum, allowing for the identification of a molecule based not only on its Rt but also on its UV-Vis absorption profile.[78]

2.2.2.1. Chromatographic separation optimization

In the optimization of the chromatographic conditions, 1 mM samples of compound **815A** in DMSO, prepared as described before, were used. Several approaches were attempted, varying mobile phase constitution, different stationary phases, elution programs and additives, as described in detail below.

A. Reverse-phase chromatography

Initially, a reversed-phase chromatographic approach was conducted using a C18 column due to the presence of hydrophobic moieties, such as aromatic rings, within structure of the test compound. In this, 18 carbon-length chains are bonded to silica beads creating a non-polar surface. When compared to another non-polar stationary phases, such as C8 and C4 (with 8- and 4-carbon chains bonded to silica beads, respectively), a C18 column provides a greater hydrophobic surface area increasing the interaction with the analyte. Therefore, this is a type of stationary phase that allows a more selective and effective separation of non-polar compounds.[79]

Several elution methods were tested with this stationary phase, as summarized in Table 1.

Table 1: Different elution conditions tested using a reverse-phase Phenomenex Luna C18 (2) column (250 mm x Ø4.6 mm). Samples (10 uL) of compound **815A** at the concentration of 1 mM in DMSO were analyzed using the system described in 4.1.2. Chromatograms were monitored at 254 nm.

Elution program	Rt (min)	Peak width (min)	Observations
1 mL/min, 30 min Multistep gradient: A: 0.1% formic acid in water , B: acetonitrile 0-2 min 95% A; 2-21 min 95-0% A; 21 – 27 min 0% A; 27 – 29 min 0 – 95% A; 29 – 30 min 95% A	12.8 - 19.11	0.24 - 1.13	Lack of repeatability; co-elution with vehicle and several peaks detected along the chromatogram
1 mL/min, 20 min Isocratic: 25% of 0.1% formic acid in water, 75% of acetonitrile	2.26	0.26	Co-elution with vehicle
1 mL/min, 30 min Isocratic: 50% of 0.1% formic acid in water, 50% of methanol	7.03-19.9	0.13-1.45	Lack of repeatability; co-elution with vehicle, lack of signal symmetry
1 mL/min, 30 min Isocratic: 70% of 0.1% formic acid in water, 30% of methanol	-	-	No elution
1 mL/min, 30 min Isocratic: 60% of 0.1% formic acid in water, 40% of methanol	21.7-28.0	3.46	Two broad peaks detected. Lack of signal symmetry and lack of repeatability
1 mL/min, 30 min Multistep gradient: A: 0.1% formic acid in water, B: methanol 0-2 min 90% A; 2-12 min 90-50% A; 12 – 22 min 50% A; 22 – 27 min 50 – 90% A; 27 – 30 min 90% A	13.8-19.8	0.29-0.50	Lack of repeatability; several peaks detected along the chromatogram
1 mL/min, 30 min Isocratic: 0.1% formic acid in water, methanol, acetonitrile (1:1:1)	3.13	0.21	Symmetrical signal
1 mL/min, 30 min Isocratic: 0.1% formic acid in water, methanol, acetonitrile (1:2:1)	2.44	0.16	Co-elution with vehicle
1 mL/min, 30 min Isocratic: 0.1% formic acid in water, methanol, acetonitrile (1:1:2)	2.89	0.3	Co-elution with vehicle
1 mL/min, 30 min Isocratic: 0.1% formic acid in water, methanol, acetonitrile (1:2:2)	2.51 – 4.33	0.17 – 0.37	Lack of repeatability; co-elution with vehicle, lack of signal symmetry
1 mL/min, 30 min Isocratic: 0.1% formic acid in water, acetonitrile (1:1)	2.67 - 8.64	0.35 – 0.43	Lack of repeatability; co-elution with vehicle, lack of signal symmetry

All the conducted experiments demonstrated that, despite the presence of hydrophobic moieties in the analyte's structure, in the majority of the assays, the compound was eluted along with the hydrophilic sample's constituents, such as the vehicle (DMSO). Therefore, it was possible to conclude that, despite the presence of less hydrophilic groups, such as the dinitrobenzene, in the structure of **815A**, the presence of formally charged groups, amines, and other polarizable chemical functions was sufficient enough to overcome the interactions between the analyte with the stationary phase, being its distribution ratio favoring the mobile phase. This was in fact predictable when considering that the estimated *logP* value of the compound is -2.49 (Section 1.6.1).

Besides the co-elution with other polar molecules, other peaks at several retention times presenting the same UV-Vis absorption profile of compound **815A** could be observed in the chromatogram. This effect can be possibly explained by different ionization states of this compound caused by differences in eluent composition through time. In fact, using a gradient elution program starting with a mobile phase composed by 95 – 5% of 0.1% aqueous formic acid – acetonitrile, with a steady increase of the acetonitrile fraction during the run causing pH variations along the elution time, could result in different ionization states and, therefore, lead to multiple elution peaks of the compound, as can be seen in Figure 7.

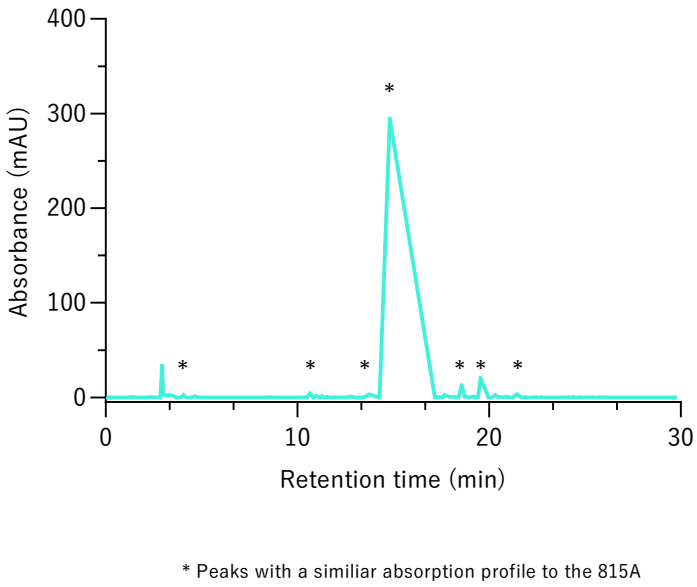

Figure 7: HPLC analysis of 815A with pH variations during the elution process results in multiple peaks in the chromatogram. Result of the injection of 10 µL of a 1 mM **815A** solution in DMSO, with a gradient elution of 95 – 5% of 0.1% aqueous formic acid – acetonitrile at a flow rate of 1 mL/min. Chromatogram monitored at 254 nm.

The fact that none of the tested methodologies employing a C18 column was efficient and selective enough to allow the separation of the test compound, prompted the use of other stationary phases. One of these approaches involved using a cyano (CN) column in which cyanopropyl groups are bonded to the silica beads. The propyl part of the group grants a non-polar functionality whilst the cyano part

confers more polar characteristics to the column. As such, depending on the constitution of mobile phase utilized, a CN column can be either used in reverse- or normal-phase chromatography.[79]

When a CN column is used in a reversed-phase approach, the non-polar interactions are expected to be less strong and fewer than the ones occurring with a C18 column. Therefore, **815A** would be allowed to interact more with the stationary phase through both its polar and non-polar structural components. In fact, good results were obtained with this column using different elution programs (see appendix Section 6.2). The best elution conditions, resulting in symmetrical and single peaks of the compound were obtained using an isocratic elution program with a of 1:1 mixture of 0.1% aqueous formic acid – acetonitrile (Figure 8). These conditions enabled the tracing of a calibration curve comprising concentrations of compound **815A** from 0.004 up to 1 mM with a R^2 of 0.997. Despite being quite sensitive, the method lacked reproducibility as injections of the same solutions often resulted in very different peak area values. In fact, the use of CN columns in quantification procedures is hampered by their low reproducibility.[80,81] Concerns regarding the robustness of the analysis using this column were amplified when the sample's matrix was changed. For instance, when spiked plasma samples were used, the compound's Rt changed drastically from 7-8 minutes to 4-5 minutes. This suggests that CN columns are not suited to quantify the test compound in complex matrices, and thus their use was abandoned at this point.

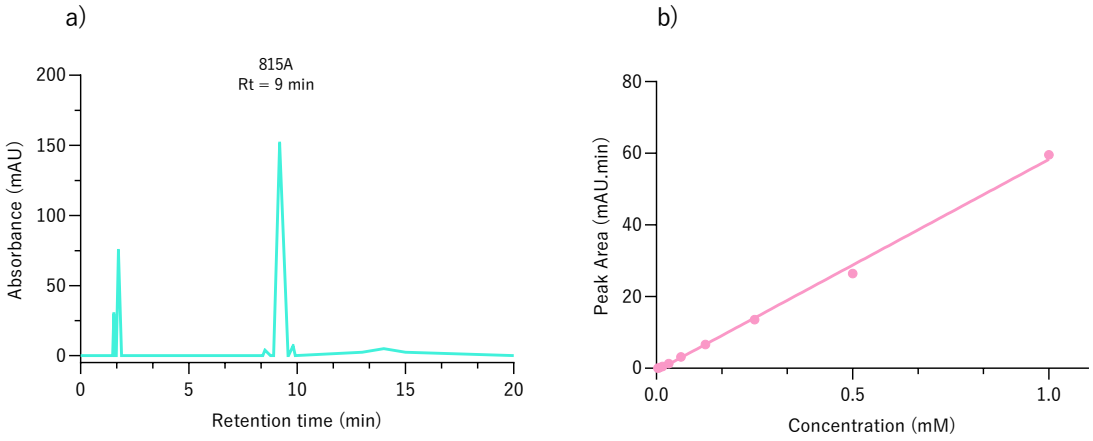

Figure 8: a) Resultant chromatogram of the analysis of 815A in a CN column. Result of the injection of 10 µL of a 1 mM **815A** solution in DMSO, with an isocratic elution with a 1:1 mixture of 0.1% aqueous formic acid – acetonitrile at a flow rate of 1 mL/min. Chromatogram monitored at 254 nm; **b) Calibration curve obtained for compound 815A using the elution program described before and samples of the test compound in DMSO.** A trendline with R^2 of 0.997 could be traced using the experimental data, allowing the quantification of **815A** between 0.004 and 1 mM.

Considering all of this, another approach was attempted resorting to a C8 column to reproduce the same chromatographic conditions used with the CN column. In terms of polarity and retentive ability, the C8 column's capacity of forming non-polar interactions with a sample's constituents is bigger than a CN column, yet smaller than a C18. Therefore, it was expected that this column would produce similar results to the ones observed with the CN column, but with higher reproducibility. However, this was not observed, and it was not possible to conceive any sort of chromatographic conditions enabling the adequate separation of **815A**. At this point, it became obvious that, due to the physicochemical

characteristics of the compound, there was no reversed-phase chromatographic conditions capable of simultaneously separate and quantify the compound of interest.

B. Normal-phase chromatography

Due to the lack of non-polar interactions between the **815A** and a reverse-phase column, normal-phase chromatographic conditions were assessed using an HILIC (Hydrophilic Interaction Liquid Chromatography) column. For these assays, the chosen mobile phases were the ones that already had been tested in other conditions, such as a 1:1 mixture of 0.1% aqueous formic acid – acetonitrile, a gradient elution starting and ending with a mobile phase composed by 95 - 5% of 0.1% aqueous formic acid – acetonitrile, with increase of acetonitrile's proportion during the run, and also the opposite gradient starting and ending with 5 - 95% of 0.1% aqueous formic acid – acetonitrile.

Considering what was observed whilst using hydrophobic stationary phases to separate compound **815A**, namely the small or barely existing interactions between the column's surface and the non-polar moieties of its molecular structure, in here, it was expected that that effect would result in a substantial amount of compound being adsorbed to a polar surface and, therefore, high retention times. However, in all the conducted experiments that did not happen. The test compound was eluted along the sample's vehicle (DMSO). With this, it was conceivable that a distribution ratio favoring a polar stationary phase would not be possible to obtain mostly due to highly hydrophobic groups present in its structure. The same groups that, in the presence of a non-polar stationary phase, are not able to interact enough with it to be adsorbed as a consequence of the compound's hydrophilic groups. Hence, the compound is neither polar enough to enable a normal-phase chromatographic separation nor non-polar enough to allow a reverse-phase approach, becoming clear that a good chromatographic separation might not be liable to be conducted only accounting on polar or non-polar interactions with the column.

C. Ion exchange chromatography

Another approach attempted to separate compound **815A** by HPLC involved the functionalization of a C18 column with an anionic surfactant to allow it to perform as cation exchange stationary phase. In this type of system, elution of compounds is achieved by changing the pH of the eluent, causing changes in the ionization of the adsorbed compounds or of the stationary phase. Therefore, before proceeding with this, it was necessary to confirm that the absorption maxima previously identified for compound **815A** were not significantly affected by changes in the pH. As seen in Figure 9, no significant variations on the absorption maxima are observed for pH values between 2 and 10, allowing for the development of an ion exchange methodology without recharacterization of the test compound

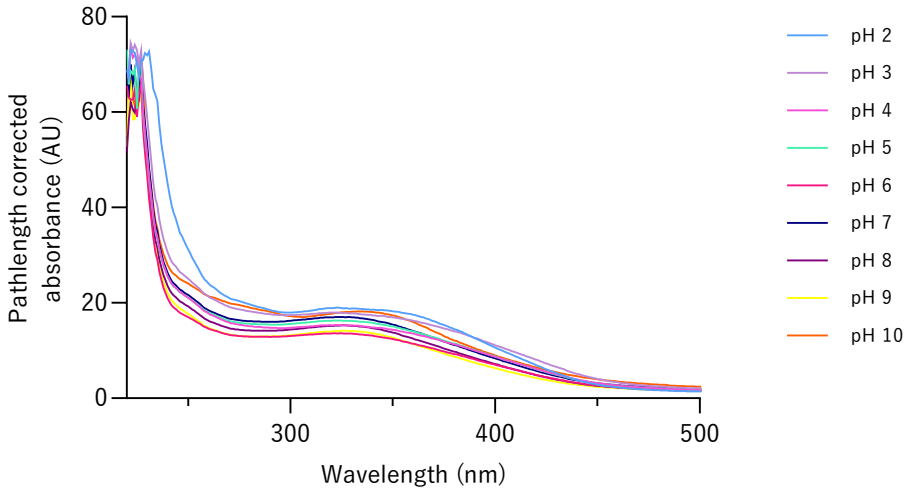

Figure 9: Compound 815A's UV-Vis absorption profile at different pH values. Samples of 2 mM **815A** were prepared in 0.15 mM ammonium acetate buffer solutions with pH values ranging from 2 to 10, and their absorption spectra traced between 220 and 500 nm. The spectra presented are a mean of three different readings.

Since no pre-packed ion exchange columns were available, the use of reverse-phase silica-based columns was attempted. Modified silica-based columns have been receiving attention regarding their use in ion exchange chromatography as surfactant coatings are semi-permanent, meaning that different ion exchange natures and capacities can be achieved with a single column.[82]

In this study, an approach to ion exchange chromatography was conducted using sodium dodecyl sulfate (SDS) and octanoic acid, as seen in Figure 10, as coating modifiers of a C18 column. Both these surfactants allow the transformation of a reverse-phase column into cation exchangers, conferring a negative charge to the stationary phase by getting the lipophilic part embedded in the C18 coating, while maintaining the ionized portion at the surface of the modified beads. The column's coating procedure was conducted according with the Fasciano and co-workers study of 2016, described in detail in Section 4.1.2.[83]

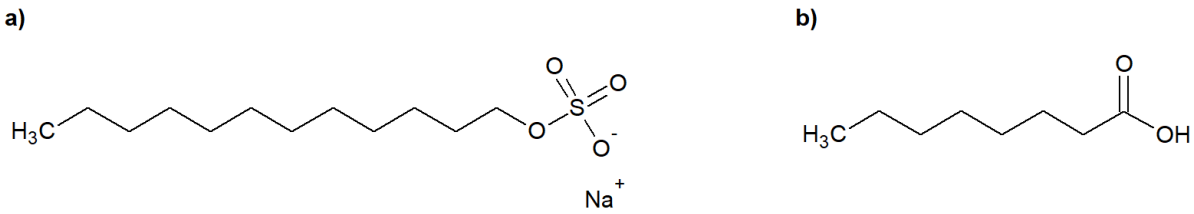

Figure 10: a) Sodium dodecyl sulfate and **b) octanoic acid structures.** It was expected that the cation present within the structure of compound **815A** would interact strongly with the sulfonate or carboxylate group of these surfactants

The first tests were conducted with an SDS-coated column and, initially, an isocratic elution program with 0.1% aqueous formic acid was used. These conditions were found unable to elute compound **815A**

from the column. The same was observed even when the concentration of formic acid was increased to 1% in the mobile phase. The relatively low strength of formic acid was considered as the possible cause for this and, hence, a stronger acid was used. However, a mobile phase containing 1.84 mM of sulfuric acid (H_2SO_4) was also unable to release the test compound from the stationary phase, even when acid concentration was increased to, approximately, 0.1 M.[83] The same type of problems was observed with the octanoic acid functionalization. It was expected that, because carboxylic acids are less strong than sulphonic acids, the interactions between the compound's permanent cation and the carboxylate groups in the column would be less strong. However, the test compound appeared to stay too strongly adsorbed to the column, not being possible to elute it. It is important to point out that it is being assumed that the test compound is becoming strongly adsorbed to the stationary phase considering that the coatings were correctly performed, and that the surfactant was majorly interacting with the C18 chains and not being also eluted within the passage of an aqueous mobile phase. Although, if so, there are other aspects to take into consideration. For instance, there is the possibility that the surfactant molecules are creating interactions between them and/or with the solvent, such as hydrogen bonds, not leaving the acid part of it free enough to interact with the test compound. Moreover, another possibility could be the creation of non-polar interactions between the test compound and the carbonated chains present in both surfactants (a C12 on SDS and a C8 on octanoic acid). However, this might not be case, considering what was already seen with the reverse-phase assays in which only weak interactions were presumably formed. One last possibility encompasses the probable formation of micelles in which the **815A** is trapped within an aggregate of surfactant molecules due to its amphipathic properties, meaning that the compound would most likely not be possible to detect. However, there is no simple way to determine if the coating was well succeeded or if it is stable enough to continue with the tests resulting on a technique extremely difficult to reproduce.[83] Based on this, it was decided to not further explore the use of modified stationary phases in the present study.

2.2.2.2. Optimization's final remarks

All the tests conducted suggest that the use of HPLC techniques is not indicated for the simultaneous separation and quantification of the test compound. Matrix interferences, together with the dual hydrophobic and hydrophilic characteristics of **815A**, hamper the direct use of HPLC, affecting significantly both reproducibility and sensitivity of the method, as summarized in Table 2.

Table 2: Summary of the most observed issues during the HPLC quantification process optimization.

Type of chromatography	Stationary phase	Main problems experienced	Possible cause
Reverse Phase	C18	Multiple peaks of the test compound. Impossible to obtain a single isolated peak	Presence of different ionizable groups in the compound structure
		Elution of the compound along and/or before the vehicle	Lack of non-polar interactions between the compound and the stationary phase
	CN	High matrix interference affecting Rt and signal quality	Low sensitivity and reproducibility common for these type of stationary phase
	C8	Elution of the compound along and/or before the vehicle	Lack of interactions between the compound and the stationary phase
Normal Phase	HILIC		
Ion Exchange	C18 – SDS	Non-elution of the test compound from the column	Too many interactions between the compound and the stationary phase
	C18 – Octanoic acid		

Due to these setbacks, to allow the quantification of **815A** in biological matrices, namely blood plasma samples, an appropriate sample preparation method had to be developed and combined with HPLC analysis. Therefore, a standard HPLC procedure was defined, based on the results obtained in the several attempts, to unequivocally identify the presence of the test compound in the samples and to determine its concentration.

2.2.2.3. Quantification process

As determined before, a well-defined, symmetrical, and sharp peak with a reasonable resolution of the **815A** could only be obtained using a C18 column with an isocratic elution program consisting of a 1:1:1 mixture of 0.1% of aqueous formic acid – acetonitrile with 0.1% formic acid – methanol, at a flow rate of 1 mL/min. The chromatogram obtained with this method is depicted in Figure 11, in which compound **815A** can be identified as a major peak eluting at approximately 3 min. Besides the signal associated with the vehicle (DMSO), one other is observed at 2.4 min. This presents an absorption profile similar to the one of compound **815A**. However, the area of this peak was considered too small relatively to the major peak observed and was disregarded.

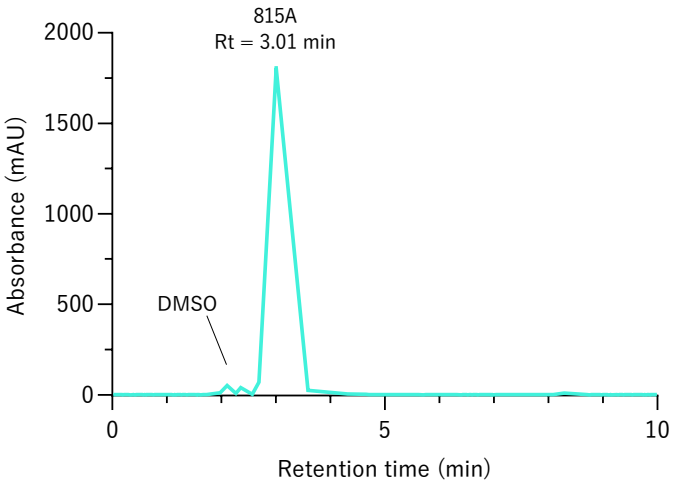

Figure 11: Chromatogram obtained from the analysis of 815A with a Phenomenex Luna C18 (2) column operated at 1 mL/min with a 1:1:1 mixture of 0.1% of aqueous formic acid – acetonitrile with 0.1% formic acid – methanol. A 10 µL sample of a 2.5 mM solution of **815A** in DMSO was used, and the chromatogram was recorded with the detector operating at 254 nm. Unequivocal identification of the test compound was based on the UV-Vis absorption profile extracted for each peak.

With these chromatographic conditions the lowest concentration possible to detect of compound **815A** was approximately of 0.15 mM, which is thirty seven times higher than the smallest concentration detected using the CN column. This might be a direct consequence of the insufficient interactions of the compound with the C18 stationary phase, as already explored in Section 2.2.2.1. Despite the higher sensitivity of the CN column, the lack of reproducibility associated with this column prevented its use in quantification experiments. However, one operation aspect was identified as the probable source of these variations. When attempting to trace a calibration curve with the C18 column, several issues regarding the interday variation were observed, as clearly demonstrated in Figure 12. The standard deviations obtained for each concentration analyzed, shown in Table 3, also sustain how disperse these data are and how poor reproductible this method is.

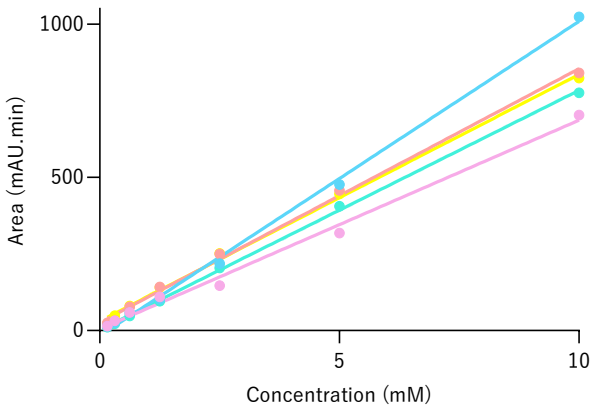

Figure 12: Calibration curves of 815A in DMSO traced in five consecutive days, showing the high inter-day variability. Assessment conducted using a C18 column with a 1 mL/min flow of 1:1:1 0.1% aqueous formic acid – acetonitrile with 0.1% formic acid – methanol, with the absorption values recorded at 254 nm.

Table 3: Mean values and standard deviations of peak areas for each concentration, considering the five calibration curves traced in different days.

815A concentration (mM)	Peak Areas (mAU.min)					Mean	Standard deviation	%CV
	Blue curve	Orange curve	Yellow curve	Green curve	Pink curve			
0.15	13.10	24.7	22.4	11.3	14.1	17.1	5.39	31.4 %
0.31	25.40	32.3	48.8	22.4	32.1	32.2	9.12	28.3 %
0.62	58.20	77.6	79.9	47.7	59.2	64.5	12.2	19.0 %
1.25	101.0	141	140	96.2	110	118	19.3	16.4 %
2.50	218.0	250	251	204	146	214	38.2	17.9 %
5.00	476.0	457	445	405	317	420	56.2	13.4 %
10.0	1024	840	823	775	703	833	106	12.8 %

As it can be seen in Table 3, most of the inter-assay (or inter-day) coefficients of variation (%CV) are above or near the usually acceptable value of 15%, translating into a poor method of quantification of compound **815A**.

These variations were identified as being the result of the injection system. The µL-pickup system, although accurate, introduced a small error depending on several factors that can include the atmospheric pressure and the room temperature, that interfere with the amount of pickup liquid being drawn in each injection. Considering this factor, and since the HPLC system used had a closed architecture comprising a fixed volume loop of 1000 µL that does not allow an easy system adaptation, the use of an internal standard (IS) was adopted to mitigate these errors.[84] Initially, biphenyl was chosen due to its structural similarities to the **815A**, being, therefore, expected to have a similar behavior within the column. However, biphenyl only eluted after almost 20 minutes of run, being this a direct consequence to its highly hydrophobicity. At this point, preference for the maintenance of the chromatographic conditions and short running times was given, thus prompting the selection of another IS.

The use of anthranilic acid, a precursor for the synthesis of **815A**, was considered. The two compounds present similar UV-Vis absorption profiles, absorbing strongly at *ca*. 330 nm. Moreover, this compound is eluted at an Rt of approximately 3.5 min (Figure 13), after **815A** (Rt of 2.9 min). The resolution attained with the C18 column is sufficient to allow the observation of two individualized peaks in a short time run.

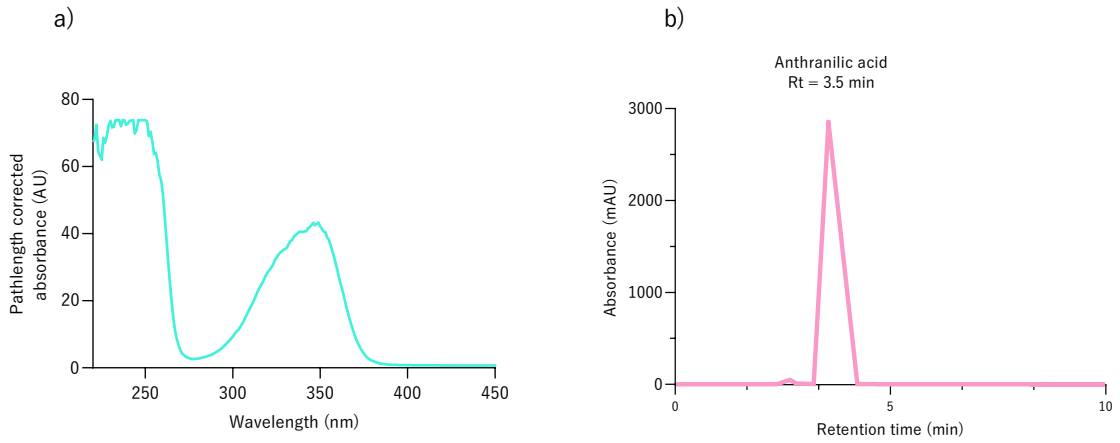

Figure 13: Chromatographic and spectrophotometric characterization of anthranilic acid. a) UV-Vis absorption profile of anthranilic acid extracted from the HPLC-DAD data, showing an absorption maximum at *ca*. 350 nm. b) Chromatogram of an anthranilic acid sample (10 µL, 10 mM) obtained using the elution program defined earlier (see Section 2.2.2.3).

After and confirming that the IS anthranilic acid would not co-elute with the test compound, two calibration curves were traced in order to correlate the **815A** concentration with the ratio between its peak area and the one from the internal standard. For this, several samples with a fixed concentration of IS (5 mM) and concentrations of **815A** ranging from 1.5 to 5 mM were prepared and analyzed. The ratio between the peak areas of **815A** and IS was plotted in function of the concentration of **815A**. Two calibration curves were traced from the chromatograms monitored at 254 nm and 330 nm (Figure 14). For both, the limits of detection (LOD) and quantification (LOQ) were determined according to the Equations 2 and 3.[75]

$$LOD = \frac{3.3 \times Standard\ Deviation}{Slope} \qquad LOQ = \frac{10 \times Standard\ Deviation}{Slope} \qquad \text{Eq. 2 \& 3}$$

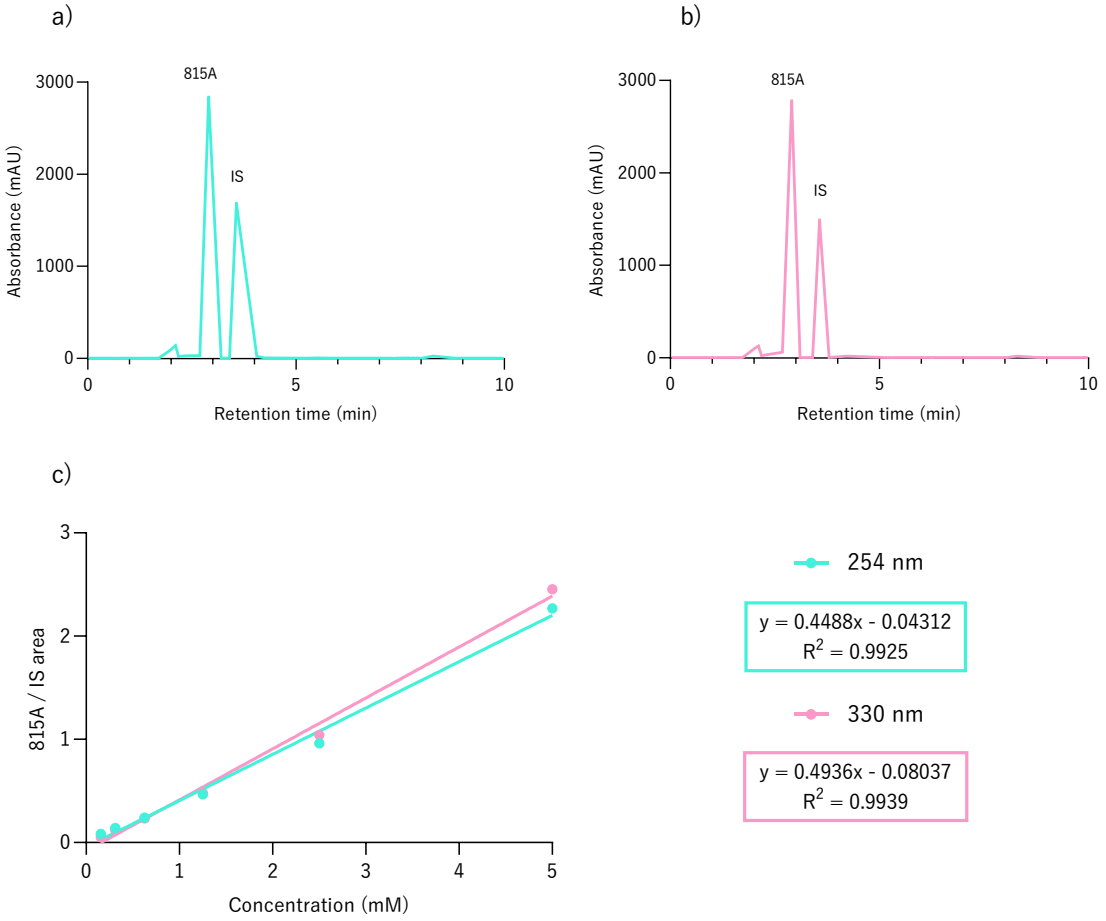

Figure 14: Chromatogram of a 5 mM 815A sample with IS (anthranilic acid, 5 mM) monitored at a) 254 nm and b) 330 nm. c) Calibration curves of 815A traced from chromatograms monitored at 254 and 330 nm using anthranilic acid as internal standard. Assessments conducted using the method described in Section 4.1.2.

No significant differences were observed between the LODs determined for both curves, being these 0.596 mM and 0.537 mM for the curves obtained with 254 and 330 nm, respectively. The major differences were observed in the LOQ, being this value lower (1.6 mM) in the case of the curve traced at 330 nm (LOQ of the 254 nm curve: 1.8 mM). Therefore, and because the monitoring of the chromatogram at 330 nm reduced the interference of the sample's vehicle (DMSO) that could, in some cases, be co-eluted with **815A**, all further calibration curves and sample analyses were conducted at 330 nm.

To further confirm the efficacy of the use of an IS as a mean to mitigate the errors introduced by the HPLC's injection system, several calibration curves traced in different days were analyzed (Figure 15). The analysis of these curved confirmed that the introduction of an internal standard eliminated the reproducibility issues, reducing the inter-assay (inter-day) variability to acceptable values (Table 4).

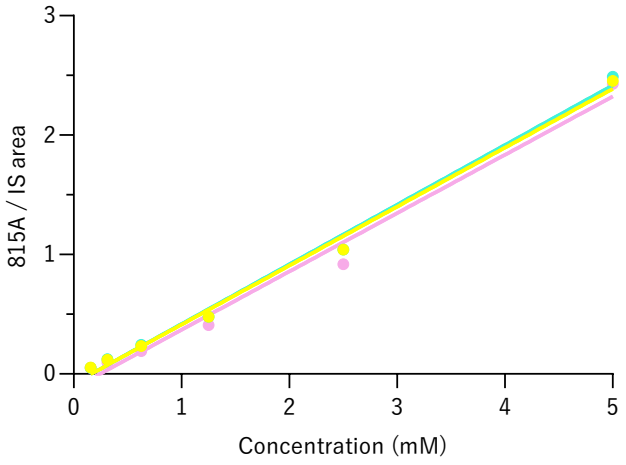

Figure 15: **Calibration curves of 815A plotted using the ratios between the peak areas of 815A and IS (anthranilic acid).** Assessment conducted using a C18 column with a mobile phase composed with 1:1:1 0.1% aqueous formic acid – acetonitrile with 0.1% formic acid – methanol at a flow rate of 1 mL/min flow and chromatogram monitoring at 330 nm.

Table 4: Parameters of the HPLC calibration curve for the quantification of 815A using anthranilic acid as internal standard.

815A concentration (mM)	815A/IS areas ratio			Mean	Standard deviation	%CV
	Green curve	Yellow curve	Pink curve			
0.15	0.05	0.05	0.05	0.05	0	0 %
0.31	0.12	0.12	0.10	0.11	0.01	9.1 %
0.62	0.23	0.24	0.19	0.22	0.02	9.1 %
1.25	0.48	0.48	0.41	0.46	0.03	6.5 %
2.50	1.04	1.04	0.92	1.00	0.06	6.0 %
5.00	2.45	2.49	2.43	2.46	0.03	1.2 %

Mean Calibration Curve

Equation	Standard deviation	R^2	LOD (mM)	LOQ (mM)
y = 0.4949x – 0.0952	0.09	0.99	0.6	1.8

From these results, it was thus possible to develop an optimized HPLC method to quantify the **815A** whilst using a C18 column and the mobile phase previously defined (1:1:1 mixture of 0.1% aqueous formic acid – acetonitrile with 0.1% formic acid – methanol). This method involves the preparation of **815A** samples containing the IS at a concentration of 5 mM in DMSO and further chromatogram monitoring at 330 nm. With this, the lowest concentration of compound **815A** possible to detect was 0.6 mM, whereas the quantification limit was fixed at 1.8 mM.

Despite being selective, this HPLC methodology lacks sensitivity. To overcome this, the introduction of a sample concentrating step will be necessary. This will not only allow the detection of amounts of compound **815A** below 1.8 mM in samples, but will also reduce the possible matrix effects that hamper the unequivocal identification a quantification of the test compound.

2.3. Isolation of compound 815A from biological samples

As mentioned in the previous Section, the lack of a robust HPLC method to simultaneously separate and quantify the **815A** present in biological samples prompted the development of a technique to selectively isolate it from complex matrices. Considering that if pharmacokinetic assays are due to be conducted in the future, this methodology must allow the selective extraction of the compound from biological samples, namely blood plasma. Moreover, in order to perform activity and effect studies of the developed formulations, development of such procedure is crucial. Considering what was observed during the HPLC quantification process optimization, namely how compound **815A** behaved in non-polar conditions, its selective isolation from plasma samples might not be possible to achieve using a simple liquid-liquid extraction. Therefore, considering the high concentration of proteins in plasma, it was decided to start the development of the isolation procedure by reducing the protein content of plasma samples. As mentioned in Section 1.6.3, there are high probabilities that only a small amount of compound will be found in its free form within the systemic circulation due to its probable high affinity for plasma proteins. Therefore, the isolation of **815A** from plasma samples is expected to present some difficulties.

In the literature, the deproteinization of either serum or plasma samples is predominantly conducted using acetonitrile, methanol, trichloroacetic acid, perchloric acid or acetone as precipitating agents. Other processes employ the use of and ultrafiltration devices with specific molecular weight cut offs[85-87], with standard precipitation methodologies being preferred due to the low cost and simple procedures. Precipitating agents, once added to a protein solution, disrupt the interactions that ensure their aqueous solubility, such as ionic interactions with salts, polar interactions with the solvent and also repulsive electrostatic forces with charged molecules which prevent proteins from aggregating.[88,89] Depending on the type of precipitating agent used, the effects exerted on proteins vary. For instance, if organic solvents are used, their molecules progressively displace the water surrounding the proteins, resulting on an enhancement of electrostatic protein-protein interactions, forming aggregates that precipitate. A similar effect happens when proteins are in the presence of high concentrations of salts, which also result in the formation of aggregates and subsequent precipitation.[89]

The pH value has also a major role on the stability of proteins. As mentioned before, the existence of repulsive electrostatic forces between proteins and charged molecules favors their solubility. Its minimum is reached at the protein's isoelectric point (pI), which normally ranges from 4 to 7, where the net charge of the protein is zero.[88]

Bearing all these in mind and considering the test compound's characteristics, several techniques to remove the plasmatic proteins were attempted with the aim of simplifying the sample for further isolation of the compound of interest. Depicted in Figure 16 are all the deproteinization techniques tested in plasma-like samples, namely samples composed by 40% of Bovine Serum Albumin (BSA), mimicking the natural content of albumin in blood plasma of around 55%.[68] All the tests conducted encompassed the removal of plasma proteins, followed by quantification of the test compound through the already defined HPLC method.

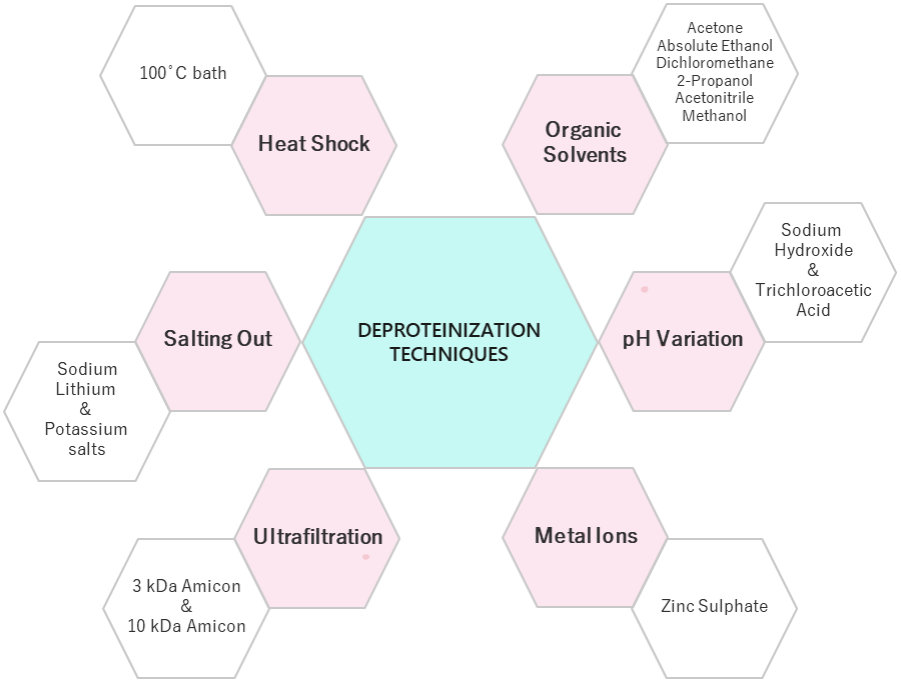

Figure 16: Summary of all the different deproteinization techniques attempted to reduce matrix interferences in the procedures of quantification of compound 815A.

2.3.1. Protein removal by Ultrafiltration

Initially, the possibility of isolating the **815A** from major biomolecules using ultrafiltration tubes with MW cut-offs was assessed. This would enable simultaneously the retention of large molecules and the passage of smaller components, such as the compound of interest. For that, as presented in Figure 16, centrifugal filtration units with MWs cut-offs of 3 and 10 kDa were chosen, considering that compound **815A**, weighing *ca.* 600 Da, would be able to go through the membrane. However, compound **815A** was not detected in the flowthrough. At first, this was thought to be a consequence of its binding to BSA, as predicted before in Section 1.6.3. However, the same results were observed when this test was conducted using protein-free buffer, and the accumulation of a yellow precipitate could be observed in the filter membrane. It was hypothesized that some of the moieties of the test compound, namely its permanent positive charge or the amide or carboxylate groups, could be interacting strongly with the filter materials (polyethersulfone and regenerated cellulose). As a result, the use of this methodology was abandoned.

2.3.2. Protein precipitation

Plasma deproteinization was evaluated using different protein precipitating techniques, as depicted in Figure 16, such as heat shock, inducing pH variations, the addition of organic solvents, metal ions or high concentrations of salts (salting out). In all assays the precipitating agent was tested on its ability to precipitate the plasmatic proteins whilst maintaining the test compound in solution, which was probed through the compound's quantification in the collected supernatant.

In all the tests conducted, except the salting out, only small amounts of **815A** in the supernatants could be detected. In fact, losses higher than 70% of the total compound used in sample spiking were observed. Initially, it was thought that this could be a consequence of the matrix effects hampering the quantification procedure, as previously observed in Section 2.2.2.1. However, there was also the possibility that the **815A** was being precipitated along with the proteins, justifying its low recovery in the supernatant.

Regarding the organic solvent-aided precipitations, that effect was a bit foreseen considering how the compound behaved with both hydrophobic stationary and mobile phases in the HPLC process optimization (Section 2.2.2.1). In addition to this, the compound might be becoming trapped in the plasma proteins. In fact, since the compound gives a yellow tone to the solution, there was a visible tone of that color among the precipitates, giving the idea that it was being precipitated along.

To prove this, an organic solvent was added into a sample constituted by 40% BSA and approximately 0.2 mM of **815A** and other without protein. When cold ethanol was added to the mixtures, only in the BSA-containing sample a precipitate was formed. After HPLC quantification of **815A** in the supernatants, the results showed that the majority of the compound added to the mixture co-precipitated with the protein since it was not detected in the supernatant (Figure 17). In contrast, a loss of just 1% of the compound relatively to the expected mount was observed in the control sample. This confirms the initial prediction that pointed the high plasma protein binding of compound **815A**. It also indicates that an extraction method involving the simple removal of plasma proteins would result in the loss of the test compound, hampering its correct quantification in plasma samples.

To verify if it was possible to recover the compound from the pelleted proteins, the pellet obtained after ethanol precipitation of the spiked BSA sample was treated with proteinase K, a highly efficient protease, as detailed in Section 4.2.1. The goal was to see if the protease activity was enough to enable an easy removal of the test compound from the protein pellet. The data obtained, which is summarized in Figure 17, allowed to confirm that the pellet contains indeed the test compound in it, and also that the protease treatment allows its liberation. However, this strategy was found too laborious to be conducted routinely since only, approximately, 5% of the compound added to the mixture was possible to be recovered from the pellet. Moreover, although apparently effective in recovering the compound of interest, the fact that it involves several steps and extensive sample handling, might increase the quantification error, which, associated with the relatively low sensitivity of the HPLC method, would reduce the overall sensitivity of the quantification procedure. It is important to highlight that prior to this assay, was evaluated if the stability of the compound **815A** was somehow jeopardized with the presence of this enzyme for several days, being concluded that the compound remained stable.

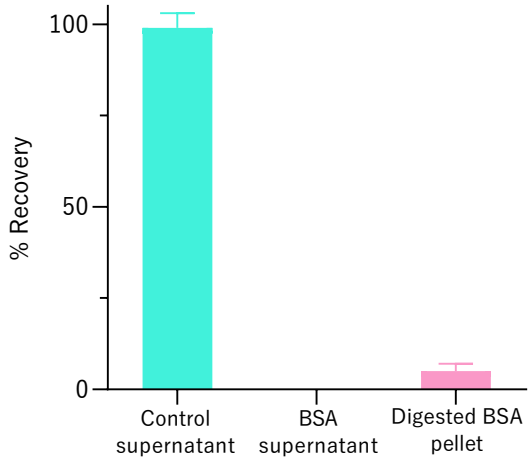

Figure 17: Percentage recovery of compound 815A from samples with and without BSA. Compound **815A** co-precipitates with proteins and it is possible to be, in part, recovered by digesting the pelleted protein. Compound concentrations were determined using the method described in Section 4.1.2. The results are a mean ± SD of three independent experiments.

A final approach to sample deproteinization, based on the addition of high concentrations of salts to the mixture of proteins and test compound, was attempted. As mentioned before, the addition of salts is expected to disrupt the interactions between the proteins and the solvent, causing the first to precipitate. This procedure was expected to result in the co-precipitation of the proteins and the **815A**, as observed with the other methods. However, upon addition of 300 µL of a saturated solution of sodium chloride (NaCl) to 100 µL of the spiked BSA-containing sample, only a small amount of yellow precipitate was observed. UV-Vis analysis of this precipitate confirmed that it was composed almost exclusively by compound **815A**. Such result brought to surface the opportunity of isolating it from protein samples using a simple addition of a salt solution. This process was extensively optimized, as detailed in the next Section.

2.3.3. Isolation process optimization

The serendipitous discovery that compound **815A** could be precipitated using high salt concentrations prompted the development and optimization of such procedure to allow the recovery of the compound from plasma samples. The general procedure, detailed in Section 4.2.1, encompasses the addition of an amount of a salt solution to the plasma or plasma-alike solution spiked with **815A**, followed by incubation and centrifugation steps. The obtained pellet is then resuspended with the same amount of salt solution followed by another centrifugation and washing step, now with water to remove any excess of salt present in the pellet. To fully optimize this procedure, several parameters were considered, namely the proportion of salt solution added to the sample, the inclusion of an incubation period prior to the first centrifugation step, the salt solution concentration and, also, the type of salt used. To evaluate the isolation efficiency of the tested process parameters, UV-Vis was used as an easy and quick methodology to discover the amount of compound precipitated. For that, the final pellet was dissolved in the smallest volume possible of DMSO and then readings at 330 nm were conducted. These

optimization steps were conducted using plasma-surrogate solutions containing by 40% BSA, laced with approximately 0.2 mM **815A**.

Initially, the proportion of salt, its concentration, and the inclusion of an overnight incubation period at 3 ºC were evaluated (Figure 18).

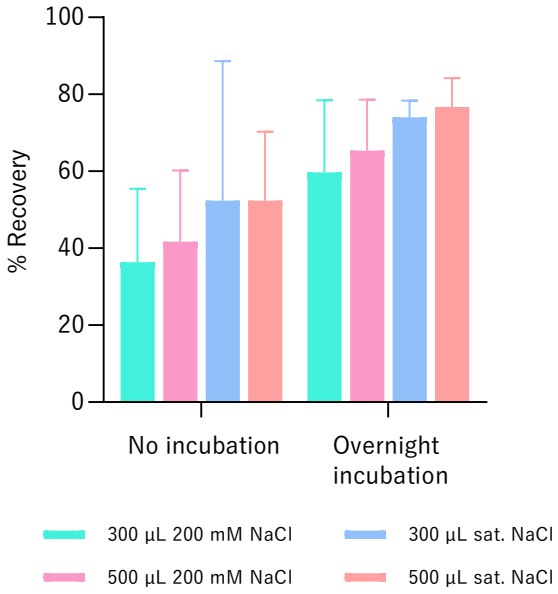

Figure 18: Optimization of the selective precipitation of compound 815A from protein-containing solutions using sodium chloride. More than 70% of **815A** is recovered when five-times the volume of a saturated sodium chloride solution is added to a sample containing 2 mM or the test compound and 40% of BSA, followed by an overnight period of incubation at 3 ºC. Percentage of recovery was assessed using spectrophotometry (330 nm). Results are presented as the mean ± SD of three independent experiments.

The effect of the overnight incubation at 3 ºC in increasing the recovery percentages of **815A** is easily observed. Moreover, the use of higher amounts of salt, in both terms of concentration and proportion of solution added, also increased the recovery of the test compound. This suggests that high concentration salt solutions will provide better results. In addition, there is a clear tendency suggesting that using 5 times the volume of sample improves the recovery percentage. Therefore, the standard procedure was defined as the addition of 5 volumes of saturated salt solution to the sample, followed by an overnight incubation at 3 ºC and subsequent sample processing, as described in detail in Section 4.2.1.

After defining this standard procedure, the effect of salt type was studied. In addition to sodium chloride, other metal halides were used (upon their availability in the laboratory) as selective precipitants of compound **815A**. Their effect in terms of recovery percentage is summarized in Figure 19. Concomitantly, the addition of a proteinase K incubation step before precipitation was explored, in order to increase the recovery percentages. The experiments where the protease was used encompassed the initial addition calcium chloride to a final concentration of 5 mM and 0.5 mg/mL of proteinase K,

followed by a one-hour incubation at 37 ºC, prior to the addition of the salt solutions and subsequent treatment.

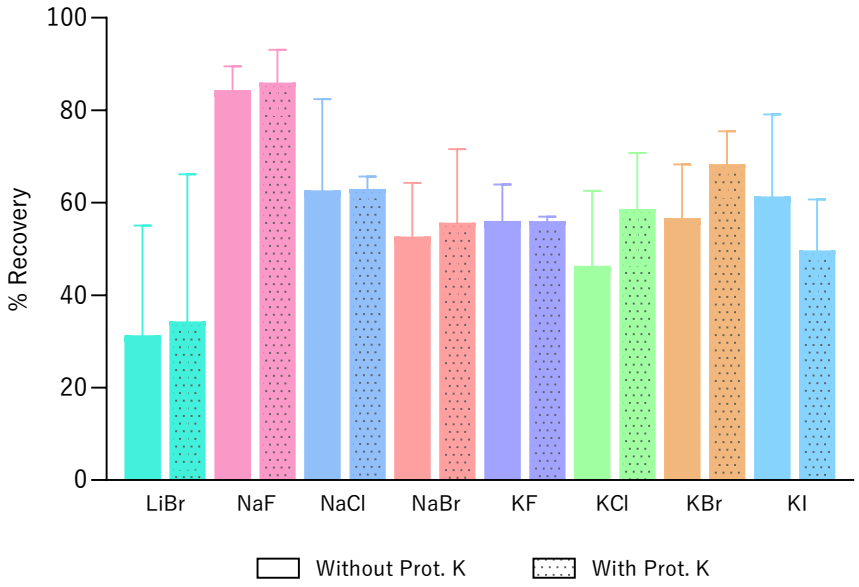

Figure 19: Effect of different salts and of the pre-incubation with proteinase K on the recovery of the test compound from surrogate plasma samples. All assays were performed using saturated solutions of all alkaline metal salts available as precipitating agents. The addition of these salts' solutions to 40% BSA spiked with 0.2 mM **815A** solutions was made with and without the presence of proteinase K (Prot. K). When the enzyme was used, the mixture stayed in incubation at 37 ºC for one hour, and only then the salt solution was added followed by an overnight incubation at 3 ºC. Percentage of recovery assessed using the UV-Vis absorbance at 330 nm. Results are presented as the mean ± SD of three independent experiments.

From the results presented in Figure 19, it seems that the addition of the protease incubation step results only in a minor increment in compound recovery. This suggests that the salt ions are able to release the molecules of **815A** from the proteins and cause their precipitation. However, and although not significant, there are differences in most cases which suggest a beneficial effect of the use of proteinase K in the recovery of the test compound.

The major differences, however, are observed when varying the salt used. While lithium bromide seems to be quite inefficient in promoting the precipitation of compound **815A**, with the use of sodium fluoride a recovery of approximately 85% of the test compound is achieved. The effect of this salt is increased when samples are previously incubated with proteinase K. The effect here observed seems to be caused by the anion and not the cation, as sodium bromide and chloride had almost the same effect. On the other hand, the use of potassium fluoride resulted in lower recovery percentages when compared to the sodium counterpart. The reason behind this observation is unknow. One possible explanation for this difference might lie on the solubility of these two salts, being the sodium fluoride ca. 20 times less soluble than potassium fluoride which may have significant effects on the ionic strength of the mixture and influence the solubility of **815A**.

However, the strikingly effect of sodium fluoride on the selective precipitation of compound **815A** is quite interesting. Fluoride ions, as well as other anions, are able to establish anion-π interactions that

may lead to the formation of stacked structures due to the presence of multiple aromatic rings within the structure of **815A**.[90] For instance, by promoting π-anion-π interactions, in which the π systems are aromatic rings from two different molecules of **815A**, fluoride ions would be contributing to the aggregation of several **815A** molecules causing these to precipitate. In fact, from the four halides tests, fluoride has been found to form the most energetically favorable associations with aromatic systems.[90] Also, the relatively small atomic radius of F, compared to other halides, might contribute to this effect.

Although the effect of fluoride in this system could not be explored, it became evident that the use of saturated solutions of sodium fluoride, in combination with pre-incubation of protein samples with proteinase K, resulted in high recovery percentages of compound **815A**.

The robustness of this method, in combination with the HPLC quantification methodology, was further evaluated using human blood plasma samples spiked with 0.2 mM **815A** (Figure 20). The results show that, overall, this methodology enables a recovery of approximately 80% of compound. When compared to the results obtained previously using the plasma surrogate (Figure 19), the recovery of compound **815A** seems to be slightly lower in a more complex matrix (from *ca*. 86% to an average 76% in plasma samples). This might be due to the higher complexity of the plasma samples that contain components other than proteins that can contribute to maintains the test compound in solution. However, the complexity of the matrix did not influence the selectivity, as the chromatogram of the precipitate shows only the peaks assigned to compound **815A** and the IS.

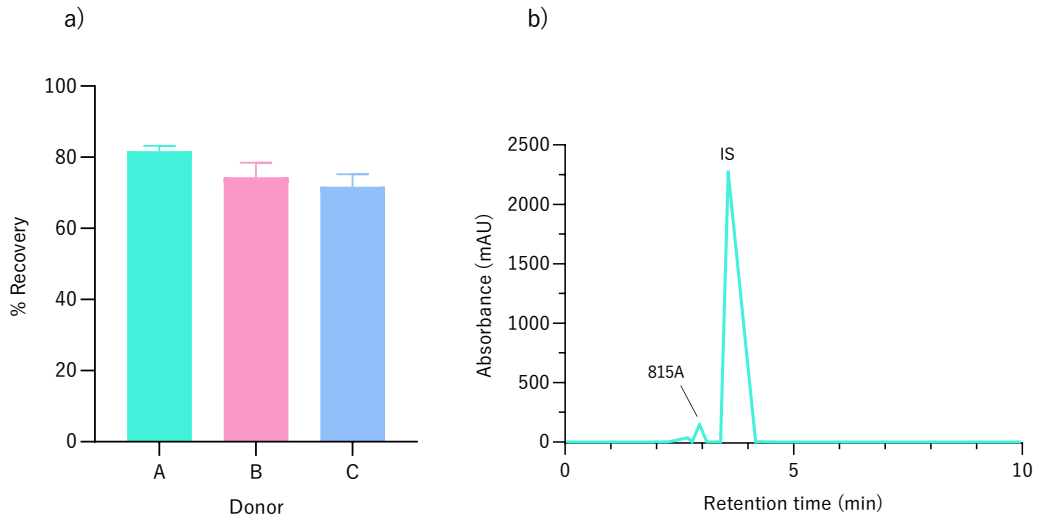

Figure 20: a) Recovery percentages of 815A from spiked plasma from three different donors. Plasma samples from three donors were spiked with 0.2 mM of compound **815A** and treated as described in Section 4.2.1 prior to HPLC analysis using the method described in Section 4.1.2. Results are presented as the mean ± SD of three samples per donor. **b) Representative chromatogram of one of the analyzed samples.**

2.4. Development of an injectable formulation of 815A in free form

At an early stage of development of a NDE, an injectable formulation of the compound is a requisite for the pre-clinical phase, namely for *in vivo* pharmacokinetic screening studies. [91,92]

Parenteral formulations should be isotonic and euhydric, meaning that their osmolarity and pH should be similar to the physiological values, respectively. However, because most NDEs face solubility and stability problems in aqueous physiological conditions, other conditions are often used. When developing these, one must consider that extreme pH and osmolality values can cause damage on the vascular endothelium and throughout the circulation.[93]

During the drug discovery process, ionizable functional groups are usually incorporated into the structures of the API to increase its solubility. However, sometimes this is not enough, and, when trying to increase the API solubility, the first approach is to the adjust the pH of the formulation. In most cases, to be effective, a pH value different enough from the compound's pK_a must be used while respecting the working range of $3.5 \leq pH \leq 9$ to reduce the risk of local irritation and vein damage. If that's not possible, a slow rate infusion must be considered to overcome those risks. This approach is only suitable for electrolytes, and the compounds that do not fit into this category are frequently mixed with cosolvents (water miscible organic solvents), surfactants and/or complexed with, for instance, cyclodextrins. Sometimes a combination of these techniques is required to completely develop a stable and soluble formulation. On the other hand, some APIs may be administrated using dispersion systems, namely emulsions, liposomes, and others. These, due to their complexity and difficult optimization, are usually the last ones to be attempted.[92-94] At preclinical settings, a combination of pH adjustment and the addition of cosolvents/surfactants is often used to quickly develop an injectable formulation of the test compound.[92]

As already mentioned in Section 2.1.1, compound **815A** cannot be directly dissolved in water, being its stock solutions prepared in DMSO. The first logic approach to enhance the compound's solubility would be to adjust the pH of the formulation. Nevertheless, that would require to know all the pK_a values of this compound, in order to buffer the vehicle at the intended pH. However, these could not be determined due to high amount of compound necessary to perform titration experiments. Moreover, this would still require the use of a cosolvent, such as DMSO, to get the compound into aqueous phase and, the effect of different pH values in the compound structure in long term is not known. Therefore, the use of a cosolvent able to increase the **815A**'s solubility was tested.

As mentioned before, DMSO can be used to prepare concentrated stock solutions of compound **815A** and, from those, aqueous solutions can be prepared. DMSO is classified as a class 3 solvent, meaning that its use up to 0.5% (v/v) encompasses low risks to human health and low toxicity, according to the International Council for Harmonization of Technical Requirements for Pharmaceuticals for Human Use (ICH) quality guideline for impurities Q3, namely the Q3C for residual solvents.[95] However, it was decided to avoid the use of this solvent as, in some cases, a yellow precipitate was formed in

buffered solutions containing 50 µM of compound **815A** and 0.5% (v/v) of DMSO stored for some time at 4 ºC.

In previous works, it was found that compound **815A**, although unable to form stable solutions in water or simple buffers (*e.g.*, phosphate buffer), could remain dissolved in culture medium, with and without serum proteins. This suggests that some of the components of the medium may be acting as surfactants, allowing **815A** to remain solubilized. A surfactant aids the wetting of API particles by preventing their aggregation through electrostatic repulsion or steric hindrance, depending on whether they are ionic or polymeric surfactants, respectively.[94] Hence, considering this, the possibility of developing a formulation constituted by water, **815A** and a surfactant was assessed.

2.4.1. Formulation optimization

The firsts surfactants to be tested were polysorbate 20, polyvinyl alcohol, albumin and glucose, which were prepared in accordance with the stablished limits for IV formulations within the Inactive Ingredients Database, approved by the Food and Drug Administration (FDA) (Table 5).

Table 5: Surfactants limits for IV formulations according to the Inactive Ingredients Database.[94]

Surfactant	Maximum potency per unit dose
Polysorbate 20	2% (w/v)
Polyvinyl alcohol	2% (w/v)
Albumin	2% (w/v)
Glucose	5% (w/v)

The formulation preparation encompassed the dilution of a stock solution of **815A** in DMSO in the aqueous surfactant solution at a compound/surfactant ratio of 1:20.[94] After a centrifugation step, a yellow precipitate was found in every mixture, with the exception of those using glucose as surfactant.

Both polysorbate 20 and polyvinyl alcohol are constituted by large hydrocarbonated chains and have multiple hydroxyl groups. The **815A** precipitation with these two is most probably due to the repulsion between the compound and the hydrophobic chains of the surfactants, reducing the interactions between the two and consequently causing precipitation. Regarding albumin, the precipitation of **815A** was not expected considering the known affinity of **815A** for this protein (Section 2.3.2). However, this might be a consequence of the relatively low amount of protein used in comparison to what is found in circulation and in plasma samples. As for the glucose, it is highly probable that hydrogen bonds are

formed with the aqueous medium and with the **815A** leading to its stabilization in solution. In most culture media used in animal cell culture, glucose is added to a final concentration of 1 g/L. It is possible that this relatively high concentration of glucose enabled the stabilization of the compound in solution.

Aiming to achieve a practical way to prepare the injectable formulation, glucose/**815A** mixtures were prepared and dried to remove solvents, including DMSO, as detailed in Section 4.3.1. The intended result would be a loose powder, easily transferable. Instead, a more jellified pellet, easily dissolved in water, was obtained.

Although efficient in solubilizing the test compound and producing a dry formulation easily dissolvable in water, the obtained pellets were difficult to handle and, in some cases, when using larger amounts of mixture, their complete drying was difficult. To try to solve this hurdles, other sugars and sugar alcohols were tested, including mannitol, ribose, fructose, inositol, arabinose and sucrose. Every single one of them allowed **815A**'s solubilization and, overall, all dry formulations were dissolvable in water forming clear solutions. All dry formulations were obtained as jellified pellets, similar to what was observed with glucose, except the formulations using mannitol or inositol (sugar alcohols). These formed free-flowing powders as it was intended, being the one obtained with mannitol the easiest one to dissolve in water.

Considering these results, mannitol was chosen as surfactant for **815A**'s solubilization, and all subsequent assays were conducted using this sugar alcohol.

*2.4.1.1. Variation of **815A**/mannitol proportions*

Further development of the soluble formulation of **815A**/mannitol involved the study of the effect of different amounts of the sugar alcohol in the solubility of the test compound. Mixtures of **815A** with a 5% solution of mannitol, in molar proportions ranging from 1:1 to 1:20 were prepared. In all cases, compound **815A** was fully dissolved and, after drying, the resulting solid dispersions could also be dissolved in water.

However, due to the small amounts of compound used, the assessment of dryness of the samples prepared with 1:1 and 1:2 proportions was difficult. As no methodology for DMSO quantification in these samples (*e.g.* gas chromatography) was available, only visual inspection of the pellets was used to determine if these appeared dry. Therefore, to ensure that the obtained solid dispersions were as close to DMSO-free as possible, the evaporation procedure was carried out for at least 48 hours and the higher proportion of ligand/mannitol (1:20) was used in the final formulation. The use of a high volume of mannitol solution ensured that the proportion water/DMSO was high enough to significantly reduce the boiling point of the mixture[96], reducing drying times and ensuring the complete DMSO removal.

*2.4.1.2. Redissolution and stability of the **815A**/mannitol formulation in water and buffers*

The final dry formulation of compound **815A** in mannitol was subjected to several tests to determine its stability over time and in several experimental conditions. First, samples formulated as described before were stored for one month at 3 ºC prior to its re-solubilization in water to verify if the solid form would remain soluble after some time in storage. All the tested samples are easily dissolved in water affording clear yellow solutions that presented no precipitate. These solutions were kept for an additional week at 3 ºC without any obvious formation of precipitates or changes in color.

It was found that dissolution of the dry formulation into buffers containing salts, including 0.9% (m/v) sodium chloride or phosphate-buffered saline (PBS), was impossible. In all cases, the formation of a yellow precipitate was immediately observed. On the other hand, aqueous solutions obtained by adding pure water to the dry formulation could be easily dispersed into protein-containing moieties, such as blood plasma, without the formation of any visible precipitates.

*2.4.1.3. Extraction of compound **815A** from formulations containing mannitol*

At this point it became necessary to confirm that the previously methods of extraction and quantification of compound **815A** from plasma matrices were still usable when the compound was formulated with mannitol as surfactant.

For that, blood plasma samples spiked with the soluble formulation were subjected to the procedure described in Section 4.2.1. As control, the soluble formulation was treated using the same procedure. After the addition of the NaF saturated solution, the formation of yellow pellets was only observed in plasma-containing samples. It seems to be that the solution high stability conferred by mannitol prevents its precipitation using sodium fluoride, being this only reversed in the presence of plasma proteins. A possible explanation to this might be the compound's high affinity for plasma proteins, which can compete with mannitol for the association with compound **815A**. This would result in the transfer of compound **815A** from the aqueous medium to the protein fraction, and subsequent displacement from the proteins by the effect of sodium fluoride, aggregation, and precipitation. Nuclear magnetic resonance spectroscopy experiments using mixtures of compound **815A** with mannitol were attempted, but it was not possible to determine the type of interactions formed between the two molecules.

To assess the effect of mannitol on the recovery of the test compound from blood plasma, the results previously obtained with samples spiked with DMSO solutions of **815A** (Section 2.3.3) were compared with samples spiked with the **815A**/mannitol formulation (Figure 21). In both cases, the total recovery was approximately 80%, proving that the selective extraction of compound **815A** is equally effective even when the samples are prepared with the soluble formulation.

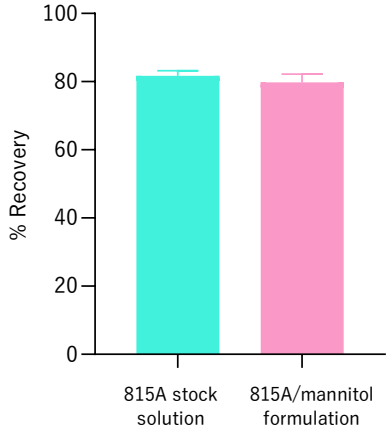

Figure 21: Comparison of compound 815A's recovery efficacy from blood plasma samples spiked with a stock solution in DMSO and the water-soluble formulation. Results are presented as the mean ± SD of the recovery percentages in plasma samples of three donors.

2.5. *In vitro* ADME assays

Prior to any *in vivo* study of a certain compound, several assays can serve as indicators of its ADME fate upon administration. From these, it is possible to adequate certain structural aspects or assess other administration routes or formulations to achieve the desired pharmacokinetic properties. In here, compound **815A**'s *logP* value, plasma stability, membrane permeability and plasma protein binding will be assessed experimentally to confirm some of the data previously estimated and also to correlate with the observations made so far.

2.5.1. *logP* value

The *logP* value is a typical lipophilicity measurement of a compound in which its partition between an aqueous and a non-aqueous phase, generally water and octanol respectively, is determined. The lipophilicity of a new drug candidate will give information about the compound's solubility, membrane permeation, distribution to other tissues and organs, blood-brain barrier permeation, among others.[63,70]

This parameter was calculated in accordance with the work of Schönsee and Bucheli.[97] Briefly, an aqueous solution of 1 mM **815A** in 5% (m/v) mannitol (pH 7) was prepared and 1 mL of it was combined with equal volume of octanol. These mixtures were vigorously vortexed and then left agitating at room temperature for 2.5 hours and the aqueous portion of each sample was collected and the concentration of compound **815A** was determined by spectrophotometry. Control tubes containing only the aqueous mixture were incubated and analyzed in parallel (Table 6).

Table 6: Absorbance values measured at 330 nm in the aqueous fractions of water-octanol mixtures and control samples. Absorbances are pathlength-corrected.

Sample	$Abs_{330\ nm}$	Mean $Abs_{330\ nm}$
Water control	14.80	14.89
	14.89	
	14.98	
Octanol-water mixture	9.433	9.510
	9.593	
	9.506	

From these results the *logP* value is calculated according to Equation 4[97], where $Abs_{control}$ and $Abs_{mixture}$ are, respectively, the absorbance values measured in the control and the aqueous phase collected form the octanol-water mixtures. The application of the formula is simplified by using equal volumes of water and octanol, and the value of *logP* obtained was -0.25 ± 0.03, being this value ten times bigger than the one predicted in Section 1.6.1. However, this has no effect on the predicted properties of the test compound as a negative *logP* value indicates that the compound has a higher affinity for the aqueous medium, as demonstrated by the several tests here described. This also confirms the previous prediction that compound **815A** has a low probability of easily permeate lipidic membranes being, therefore, expected to remain in circulation until clearance, upon IV administration.

$$logP = \log\left(\frac{Abs_{control}}{Abs_{mixture}} - 1\right) \times \left(\frac{V_{water}}{V_{octanol}}\right) \quad \text{Eq. 4}$$

2.5.2. Plasma stability

The stability in plasma of a new drug candidate is essential to ensure the desirable pharmacological effects. Poorly stable compounds tend to have short half-life times and rapid clearances, meaning that adjusts in either the administration route and/or the administrated dose might be required to achieve the optimal response. Certain compounds are more prone to be metabolized by hydrolytic enzymes present in the plasma than others, which is important during drug development since it can lead to strategical alterations within the compound's structure. Usually, candidates containing ester or amide functional groups are more susceptible to plasma enzyme activity. [98,99]

Therefore, knowing the plasma stability of new drug candidates is useful to choose the right candidates for *in vivo* studies and also to acknowledge that, for further pharmacokinetic studies, precautions are required considering that the final results can be misleading due to the compound's continuing degradation after sample collection. Thus, in this study, stability of compound **815A** in plasma was assessed using freshly collected human plasma samples (Section 4.4.1.3). These were

spiked with a stock solution of **815A** in DMSO and incubated at 37 ºC for three consecutive days. Aliquots were collected at different time points throughout the incubation period and submitted to the developed and optimized isolation and quantification processes (Sections 4.1.2 and 4.2.1). Compound **815A**'s plasma stability was then assessed by normalizing the concentrations obtained in all time points relatively to the control as plotted in Figure 22.

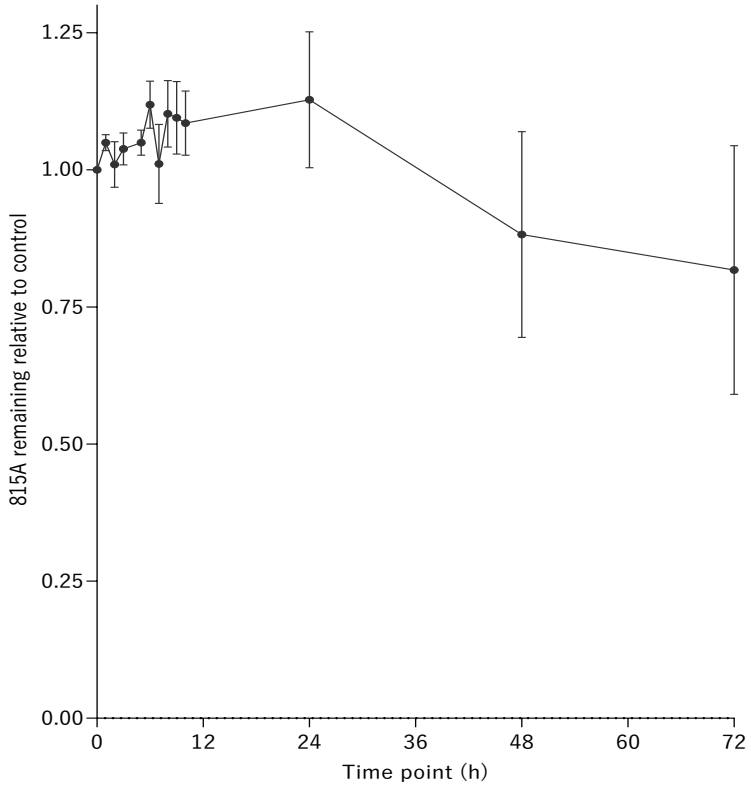

Figure 22: Plasma stability of compound 815A determined by HPLC quantification. Plasma samples were spiked with 2 mM of **815A** in DMSO and incubated at 37 ºC for up to three days. Samples were collected at several timepoints and the concentration of the test compound in each one was determined by HPLC analysis after selective precipitation as already described. Results are presents as the mean ± SD of three. Statistical analysis reports no differences between each point and the control (t = 0).

Although the quantification of compound **815A** presents an apparent reduction of the concentration of test compound through time without, however, statistical significance. Despite this tendency, it appears that compound **815A** is mostly stable to the activity of plasma enzymes, without differences of concentration being observed in the first 24 hours. Considering the predicted high clearance rate (Section 1.6.4) and the determined *logP* value, this suggests that compound **815A** will be probably eliminated without suffering structural changes.

2.5.3. Parallel Artificial Membrane Permeability Assay

A Parallel Artificial Membrane Permeability Assay (PAMPA) allows the prediction of a drug's absorption by mimicking the behavior of the intestinal epithelium, the blood brain barrier or a cellular membrane using a lipid-infused artificial membrane. This assay was first introduced by Kansy in 1998 to evaluate the gastrointestinal absorption of a molecule as a mean to assess its bioavailability.[100-102]

Here it was intended to confirm if the **815A** would stay in the systemic circulation after IV administration, or if it would be able to diffuse through a lipidic membrane. As explained in Section 1.5, the compound was structurally developed to remain in circulation, with low extra-vascular distribution, being expected to have low membrane permeability, as supported by all the parameters already predicted and determined.

The PAMPA assay, as detailed in Section 4.2.4, involves the creation of an artificial lipid membrane by coating of a filter membrane with a mixture of 80:20 dioleoyl phosphatidylcholine: stearic acid. This artificial membrane is mounted between two wells, one containing a solution of the test compound (donor) and the other containing only a liquid moiety (acceptor). In this case, the donor wells were filled with 1 mM **815A** solutions in 5% mannitol and the acceptor wells with the minimum volume possible of 50 mM ammonium bicarbonate (NH_4HCO_3) pH 7.4 that enable the membrane's wetting (Figure 23). The system was incubated for 18 hours at room temperature and the amount of compound **815A** in each well was determined through the developed HPLC method.

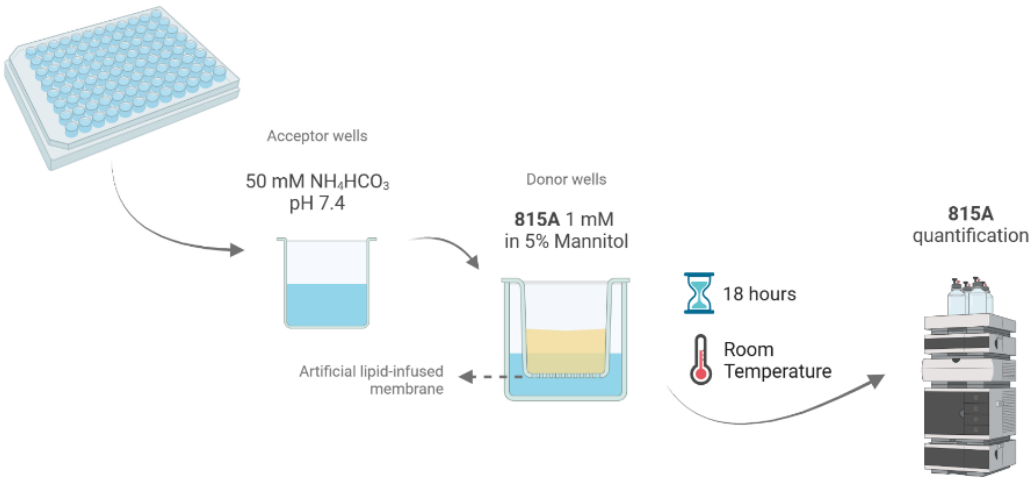

Figure 23: Parallel artificial membrane permeability assay schematics.

No compound **815A** was detected in the acceptor wells and the quantification of **815A** in the donor wells revealed only a small difference relative to the control (Table 7).

Table 7: 815A concentration in the samples from the PAMPA donor wells after incubation of the system at room temperature for 18h. The concentration of compound **815A** was determined by HPLC using the method described in Section 4.1.2. Samples from the donor wells and the initial solution (incubated in a closed tube in parallel) were analyzed. The concentration result for the donor wells are presented as the mean ± SD.

Sample		Peak Areas Ratio	815A mean concentration (mM)
Initial solution		0.3990	0.99
Donor wells	I	0.3949	0.97 ± 0.04
	II	0.3622	
	III	0.3961	

The small difference between the concentration in the initial solution and the donor wells is not significant and is well within the method error. Therefore, PAMPA results suggest that, as expected, compound **815A** is not able to go through the lipidic membranes by passive diffusion. These results are thus in accordance with both the predictions made regarding the compound's lipophilicity and also with the obtained *logP* value. The structural moieties featured in compound **815A** intended to increase its solubility, are, in fact, preventing its diffusion through lipidic membranes, thus restricting its distribution volume to the systemic circulation. Moreover, this confirms the predictions made using the Lipinski's rules that suggested that compound **815A** would be a poorly active API if orally administrated, ratifying the necessity of developing an injectable formulation.

2.5.4. Plasma protein binding

The efficacy of a drug is generally evaluated considering the concentration of $f_{u,p}$ in detriment of the total concentration in plasma, since only the extent unbound will reach the target and exert the desired pharmacological effect. The most widely used and exploited method for PPB is equilibrium dialysis. In this, a dialysis membrane separates two chambers, with one of the chambers containing plasma spiked with the compound in test and the other with a buffer. The dialysis membrane must have a MW cut-off that allows the freely diffusion of unbound drug molecules, while retaining proteins such as albumin. This diffusion of the free compound will proceed up to the moment that a concentration equilibrium is reached. Finally, the $f_{u,p}$ is determined by measuring the concentration of the test compound in each chamber.[103,104]

The determination of the extent of **815A** bound to plasma proteins was performed using a 10 kDa dialysis membrane separating two 5-mL chambers. One chamber was filled with a plasma sample containing compound **815A** at a final concentration of 0.1 mM and the other with 5 mL of a 5% mannitol solution. The dialysis system was left incubating for 3 days at room temperature with constant agitation. The mannitol solution was collected and subjected to the isolation protocol (Section 2.3.3) and then quantified by HPLC. In all replicates, there was no trace of **815A** in the dialyzed samples. This corroborates the predictions made in Section 1.6.3 that pointed the low $f_{u,p}$ of the test compound. It also

confirms the findings described in Section 2.3.2, where compound **815A** was found to precipitate along with the BSA. Therefore, considering all these results, it is safe to say that a large proportion of **815A** will be bond to plasma proteins upon administration.

2.6. Controlled-release formulation development

Controlled-release drug delivery systems are designed to release the API at a predictive rate and for an extended period of time. These are usually developed to ensure maximal drug efficacy, minimal side effects and drug level fluctuations, whilst enhancing the patient's compliance to the therapeutics.[105,106]

Parenteral administrations are mainly characterized by short-term responses due to fast elimination processes. Therefore, for drugs with narrow therapeutic indexes and poor bioavailabilities the use of these types of systems would allow the maintenance of drug levels at an effective concentration for a prolonged period of time, minimizing the number of administrations required within the therapeutical regimen.[105]

The dual immunomodulatory activity of the NKp30 receptor, implies that a specific and narrow therapeutic window will be required to achieve the optimal effect of the **815A**. From what is known, no substantial effects on the NK cells activity will be obtained with **815A** concentrations above 2.5 mM *in vitro* (Section 1.5). Moreover, according to the predictions already conducted in terms of ADME-influencing characteristics, it is most likely that the **815A** will be a short-lived molecule due its high solubility and consequent high rate of elimination. Therefore, the most efficient performance of this compound will be obtained when reached a perfect equilibrium between its bioavailability and elimination. For that, a controlled-release drug delivery system would provide a great solution to avoid big fluctuations on the levels of **815A** in the systemic circulation, ensuring a more prolonged and effective activation of NK cells.

Particulate systems have been widely exploited for parenteral controlled-release systems, specially polymeric systems due to its biocompatibility and biodegradable characteristics.[107] The one polymer that has attracted most attention is poly-lactic-co-glycolic acid (PLGA), which is, in fact, approved by the competent entities for drug delivery systems in humans.[105,107] PLGA's hydrolysis releases the monomers lactic and glycolic acids, easily metabolized by the human body within the Krebs cycle.[108] Besides its biocompatibility, the extensive research conducted on this polymer, allowed the conclusion that PLGA enables the formulation of this kind of systems for several types of drugs (either hydrophobic and hydrophilic), protecting them from being degrading whilst prolonging its release (Figure 24). Moreover, systems with modified-surface particles enabling a targeted release have also been developed.[108] Another aspect highly beneficial from this co-polymer is its variable nature, meaning that the polymer's physicochemical properties depend on the lactic and glycolic acid content. For instance, a higher content of lactic acid, the slower the rate of disintegration of the particle will be.[109]

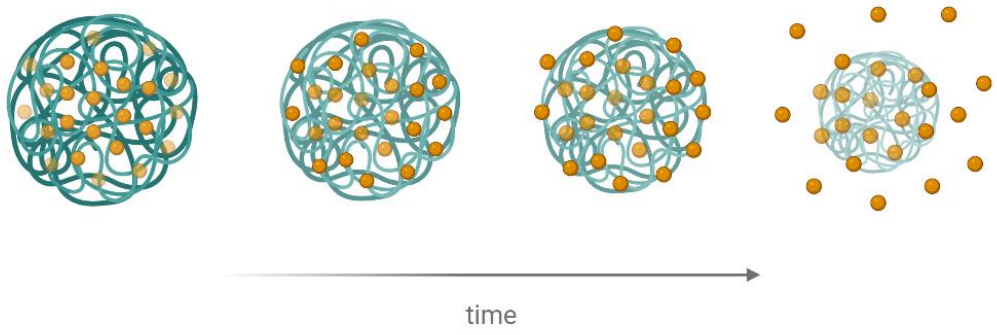

Figure 24: PLGA nanoparticle degradation through time in systemic circulation along with the drug's release.

There are several methods available to produce polymeric nanoparticles. From these, the major and impacting difference will be how the API is "trapped". The final result will consist of a nanosphere if the API is absorbed to the matrix surface, and it will be denominated as a nanocapsule if the API is entrapped inside the particle's core.[107,108] The most standard method to prepare PLGA-nanoparticles (NPs) is the emulsification-solvent evaporation technique, which allows the production of nanospheres. Shortly, this technique entails the formation of an oil-in-water (O/W) emulsion by adding an aqueous solution of a chosen surfactant into a mixture of polymer and API, dissolved in an organic solvent. The NPs are formed through sonication, followed by solvent evaporation, centrifugation and washing steps to collect them.[107,108] This technique can only be used with hydrophobic APIs. For hydrophilic APIs, a double emulsion (W/O/W) is formed. In this, the polymer is still present in the organic phase, the API is dissolved in the aqueous phase and further added into the organic one to form the first emulsion. The secondary emulsion results from the addition of the first emulsion into another aqueous phase, this time with a surfactant present to ease the emulsification process.[108]

Considering the need of developing an **815A** parenteral formulation capable of maintaining the compound's concentration stable for a longer period of time, the development of a nanoparticulate PLGA-based system was attempted. Accounting on the compound's characteristics, the double emulsification technique was used. The used method was based on the works of Haddadi[110] and Alshamsan[111], although adapted for **815A** in specific, as fully described in Section 4.3.2.1.

2.6.1. PLGA-NPs optimization

The NPs production optimization was conducted by giving special attention to the final particles' size. The NPs' size will play an important role in the determination of the particles fate in the body.[94,110,112] Hydrodynamic radii lower than 10 nm are believed to encompass a rapid NPs elimination due to high renal filtration. In contrast, bigger particles (>200 nm) are most likely to be entrapped within the reticuloendothelial system (RES) of several tissues as part of the opsonization process, which can actually lead to faster elimination rates in comparison to the ones of smaller particles.[110,112,113]

For a suitable IV administration with a long-circulation behavior, the best size range of NPs it is believed to be between 10 and 200 nm.[112] Therefore, the NPs' production optimization was conducted by studying the influence of different process parameters in the final size. From the overall parameters, it was decided to study the effects of the amount of PLGA used, the sonication intensity, as well as the introduction or not of a final freeze-drying step.

At an initial stage, two PLGA concentrations were tested (5x and 10x higher than the amount of **815A** used) and the size of the NPs was determined. At the same time, the effect of the sonication parameters, namely the intensity (25% and 50% amplitude), was studied. Size measurements in these experiments were conducted after redispersing the prepared NPs in 1 mL of distilled water, as described in Section 4.3.2.

All tested conditions failed in producing NPs with adequate size (Figure 25).

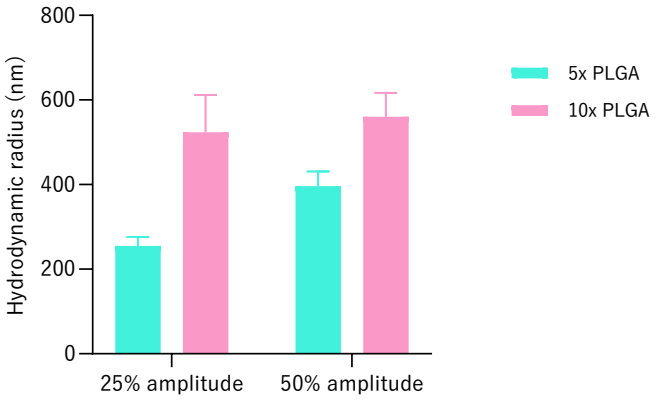

Figure 25: Effects of both PLGA concentration and sonication intensity in the size of nanoparticles. Results are presented as the mean ± SD of three measurements.

NP size seems to increase when larger amounts of polymer are used. This effect of PLGA concentration is more pronounced when considering the experiments using an amplitude of 25%. The size of NPs obtained with the highest concentration of PLGA is more than double of the size of NPs obtained using less PLGA (524 nm vs. 255 nm). However, when using a sonication amplitude of 50%, the amount of PLGA appears to have no effect on the size of NPs. However, the polydispersity index (PdI), which is determined along the particle size distribution, suggests that all conditions resulted in highly heterogeneous dispersions (Table 8). A PdI value closer to 1 describes a high heterogenous sample, while 0 corresponds to a monodisperse system of particles. For polymeric delivery systems, the PdI values should be 0.2 or bellow, being considered as a monodisperse system at values near 0.1.[114]

Table 8: Mean polydispersity index (PdI) values for each experiment.
Results represented as a mean of three measurements per sample.

Assay		Mean PdI
25% Amplitude	5x PLGA	0.875
	10x PLGA	0.895
50% Amplitude	5x PLGA	0.820
	10x PLGA	0.713

In general, the tested conditions resulted in highly heterogenic particle size distributions among the produced NPs. However, by increasing the sonication amplitude in the production of NPs using the higher concentration of PLGA, a tendency towards reducing the PdI value is observed. Considering the administration route to be used, besides aiming to produce NPs within a specific size range, a special attention must be given to the particles size homogeneity to facilitate the understanding of results obtained in assays requiring the circulation of these formulations *in vivo*. As previously mentioned, depending on the size of the particles, speculations can be made for how and when they will be cleared out of circulation. If a low homogeneous system is administrated, any prediction would be misleading and could induce wrong results interpretations. In this way, considering the results presented in Figure 25 and Table 8, in the development of **815A**'s NPs, the use of 25% amplitudes in the sonicator was disregarded.

In the next step of the development, the introducing of a final freeze-drying step into the protocol was evaluated to determine its influence on the NPs size and PdI. For that, a new batch of both 5x and 10x PLGA NPs was produced and submitted to a freeze-drying step once resuspended in a cryoprotectant (1% sucrose solution). The NPs obtained after this were resuspended in an appropriate volume of water and analyzed (Figure 26).

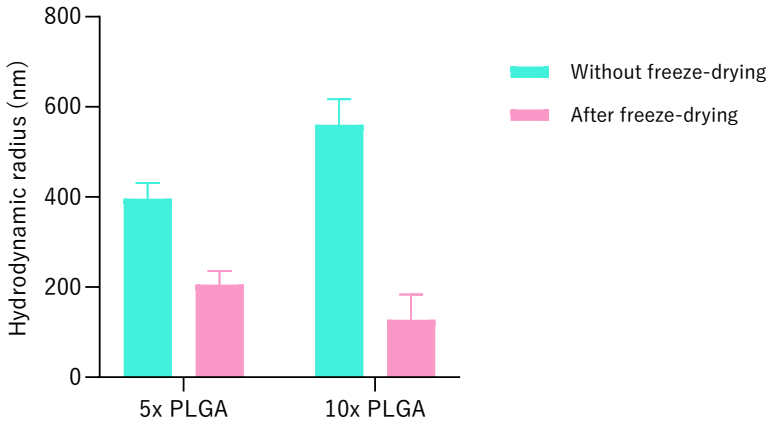

Figure 26: Effects of the addition of a freeze-drying step in the final nanoparticle size. Results are presented as the mean ± SD of three measurements.

Table 9: Polydispersity index differences induced by the introduction of a freeze-drying step in the protocol. Results represented as a mean of three measurements per sample.

NPs	Mean PdI	
	Without freeze-drying	After freeze-drying
5x PLGA	0.820	0.810
10x PLGA	0.713	0.708

Freeze-drying the NPs lead to a substantial decrease of their size. A more notorious effect was obtained in the 10x PLGA NPs, which presented change in the mean hydrodynamic radius from 524 to 128 nm whilst the 5x PLGA NPs had changed from 255 to 205 nm. Despite being expected that bigger concentrations of polymer would consequently produce bigger sized NPs, as previously seen in Figure 25, that tendency was not followed at this point of the optimization. In fact, better results were obtained with the 10x PLGA NPs in terms of both size, which was within the desired range, and in terms of PdI (Table 9).

The use of different PLGA concentrations (5, 10 and 15 mg/mL) was also evaluated. The NPs were produced only varying the polymer concentration, whilst maintaining the sonicator's amplitude at 50% and the final freeze-drying step. In these experiments, however, upon freeze-drying, samples of each condition were dissolved in different volumes prior to size analysis. This was intended to evaluate the possible occurrence of particle aggregation that could result in higher NP sizes but also in high heterogenicity. Therefore, NPs were prepared at different concentrations (0.5, 0.25 and 0.12 mg/mL) and their size distribution immediately assessed (Table 10).

Table 10: The effects of sample preparation prior to PdI and size measurements. Results represented as a mean of three measurements per sample.

NPs	Mean PdI		
	0.5 mg/mL	0.25 mg/mL	0.12 mg/mL
5 mg/mL PLGA	0.844	0.583	0.673
10 mg/mL PLGA	0.843	0.657	0.723
15 mg/mL PLGA	0.580	0.525	0.619
10x PLGA	0.790	0.549	0.503

According to these results, it seems that in fact the formulated hypothesis was correct and there is a high chance that the NPs are forming large aggregates when resuspended, consequently influencing both size and PdI measurements. Corroborating this, are the results obtained within the 10x PLGA NPs. These were obtained by using the same exact batch evaluated before in Table 9 with a PdI of 0.708.

When using higher dilutions, lower PdI values were obtained indicating that some of the aggregation effects can, in fact, be minimized during sample's preparation.

Overall, from all the PLGA concentrations tested, is observed a common tendency of decreasing the PdI values along with the sample's dilution, especially when a dilution from 0.5 to 0.25 mg/mL was used. Therefore, the evaluation of the NP's size was performed using a concentration of 0.25 mg/mL (Figure 27), revealing that only the particles obtained with the 10x PLGA and 15 mg/mL PLGA were within the intended size range, presenting a medium hydrodynamic radius of 118 nm and 163 nm, respectively

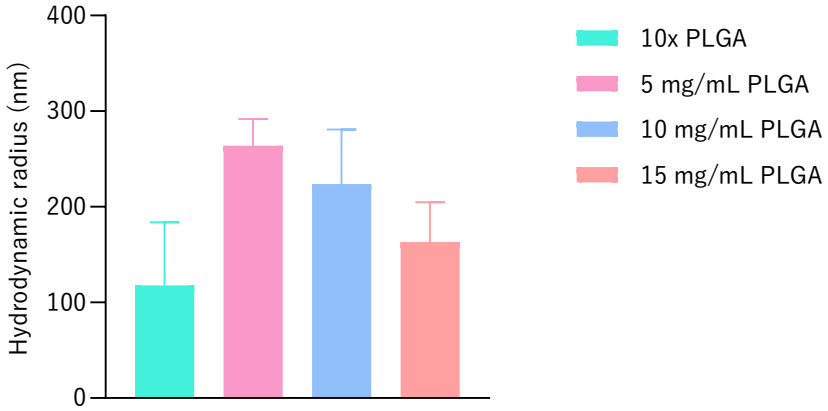

Figure 27: Effect of the PLGA concentration in the final NP size. Results presented of the mean ± SD hydrodynamic radii values with the correspondent standard deviation, of triplicates. NPs samples prepared at a 0.25 mg/mL prior to measurement.

The results from the three new PLGA concentrations did not comply to what was expected. Once more, what is seen is that by increasing the PLGA concentration, the NPs tend to be smaller. This same effect was already observed with the 5x and 10x PLGA conditions, contradicting published studies that the PLGA concentration has direct correlation with the size of NPs.[115,116] Therefore, more studies regarding the effect of the PLGA concentration in the NPs size within the defined protocol will have to be conducted.

Despite not being able to obtain NPs with the desired PdI values, particles produced using the 10x PLGA condition with higher sonication intensities and a freeze-drying step were within the desired size range. Therefore, NPs produced this way were studied for their ability to release compound **815A** in a controlled fashion. Initially, a long-term release assay was setup. This involved the production of large amounts of NPs using the defined method, and their incubation in an adequate medium to assess the release of compound **815A** over time, being the release of test compound monitored by HPLC analysis of the liquid phase (procedure detailed in Section 4.1.2). The dissolution of NPs over time was easily observed when these were pelleted in the tubes each day, without only a few solid residues being observed after 5 days of incubation, in contrast to the large solid pellet observed at t0. Despite that, no compound **815A** could be detected in the samples' supernatants. This was thought to be a direct consequence of the low sensitivity of the developed HPLC method. Nevertheless, because it became obvious that the NPs were being dissolved, and considering that when this happens, their content is

released, an efficacy experiment was designed and conducted to evaluate the usefulness of this system in controlling the activity of NK cells.

2.6.2. PLGA-NPs efficacy

As mentioned before, compound **815A** is efficient in inducing the activation of NK cells within specific concentration intervals. One of the indicators of NK cell activation is the secretion of cytokines, in particular IFN-γ.[46,117] One important aspect is the fact that concentrations of **815A** above the defined range prevent NK cell activity and IFN-γ secretion, as mentioned before (see Section 1.5). Therefore, it is crucial that the amount of **815A** in circulation remains within the defined concentration range to achieve optimal NK cell activity for a prolonged period.

As no information regarding the degradation kinetics of PLGA NPs could be obtained, an indirect approach was attempted. In this, stirred cultures of peripheral blood mononuclear cells (PBMCs) were incubated for 5 days with the free **815A**, **815A**-loaded NPs, or unloaded NPs, produced as described before. Supernatant samples were collected from each condition at regular timepoints and assayed to detect and quantify the levels of IFN-γ (Figure 28).

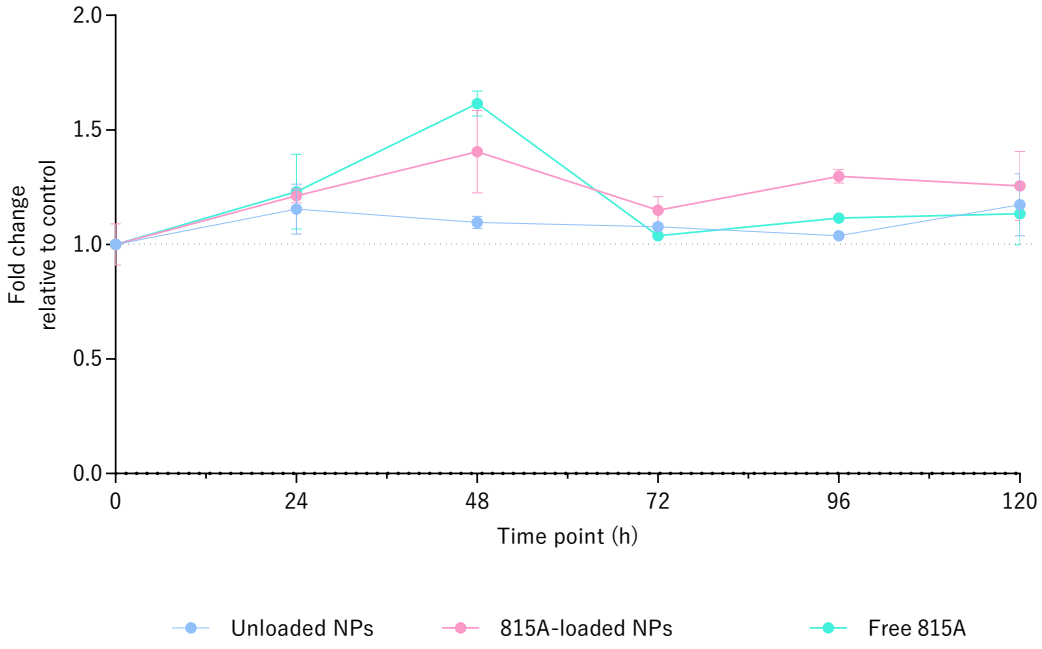

Figure 28: Quantification of IFN-γ in the supernatants of PBMC cultures from donor D, treated with 815A-loaded NPs, unloaded NPs or free 815A, over a 5-day period. The levels of IFN-γ were determined by ELISA in duplicate and normalized to the time point of 0 hours. Values presented are the mean ± SD of two replicates per condition.

In this assay, unloaded NPs were used as control to confirm the biocompatibility of the material and the NPs, as some may be able to induce cytokine release upon contact with immune cells.[118] As observed, the addition of unloaded NPs to the cell culture seems to have increases slightly the production of IFN-γ, but this increase can be due not only to the addition of the NPs but also to the

introduction of cells into an artificial culture system. On the other hand, **815A**-loaded NPs present a much more pronounced effect on the secretion of IFN-γ, reaching quite high levels after 48 hours. Strikingly, the amount of IFN-γ in the supernatant remains mostly constant for the remainder of the experiment. In contrast, the culture treated with the free form of **815A** also presents a peak concentration of the IFN-γ after 48 hours of treatment, but the level of this cytokine falls to basal levels immediately after. The fact that **815A**-loaded NPs seem to be able to maintain the activity of NK cells over an extended period of time suggests that the compound is being released in a controlled fashion. Because, contrarily to what is observed with the free form of **815A**, the levels of IFN-γ are kept steady, one can hypothesize that the **815A**-loaded NPs are releasing the compound at a steady state that allows the maintenance of its concentration neat the therapeutic window. However, a larger set of experiments, donors and conditions is necessary to confirm this.

III. CONCLUSIONS AND PERSPECTIVES

3.1. Conclusions

The major goal of the work here conducted was to develop an IV formulation of the small organic molecule **815A** that induces the cytolytic activity of NK cells. Several properties of this molecule had to be studied before developing the injectable formulation, especially considering that compound **815A** has a poor solubility profile. Despite containing structural features that should allow the easy dissolution of this molecule in aqueous medium, previous work conducted in the research group, concluded that stock solutions of compound **815A** had to be prepared in an organic solvent (DMSO) before dispersion in water. Although efficient to some point, solutions prepared by this method would often present precipitated and only relatively low concentrations of this could be prepared and stored. Moreover, the presence of DMSO in a formulation was undesirable due to its possible toxic effects.

A large set of strategies are available to increase the solubility of APIs for administration via parenteral routes. The simplest encompass adjusting the solution's pH or adding either a co-solvent or a surfactant, whereas the more complex ones evolve the formation of complexes with cyclodextrins or using dispersion systems. Adjusting the solution's pH and using co-solvents were disregarded in this work since the test compound's pKa values were unknown. Thereby, the use of surfactants was exploited being found that sugars and alcohol sugars could easily stabilize and aid the solubilization of the test compound in aqueous media. To try to produce a solid and readily soluble formulation, all **815A**/sugar or sugar alcohol mixtures were dried, removing the co-solvent (DMSO) and resolubilized in water. From all the formulations tested, the mannitol-based ones produced free flowing powders that could be easily dissolved producing clear solutions. Moreover, these were found stable over time, without any visible clouding or precipitation of any of the mixture's components. This is in line with the wide use of mannitol a stabilizer of lyophilizates and biopharmaceutical active substances.[119,120] Fine tuning of the formulation involved varying the proportions of compound **815A** stock solution and the 5% mannitol solution, being concluded that the drying step efficacy and the ease of the following dissolution and handling steps are directly correlated with the amount of aqueous mannitol phase. Therefore, a 1:20 proportion of **815A** stock solution to 5% mannitol was chosen as final free form formulation of the test compound.

The solubility issues of compound **815A** did not only influenced the formulation development but also its separation and quantification methods. Several chromatographic conditions were tested, but none was found efficient in separating compound **815A** from complex matrices. For instance, in a C18 column the non-polar moieties of the compound did not enable its adsorption to the column, eluting along with the sample's vehicle, and effect that was also observed when using a polar stationary phase. Despite being constituted by a large number of hydrophobic moieties, compound **815A** does not seem interact

much with non-polar surfaces. Corroborating this, are the *in vitro* ADME assays conducted to determine its *logP* value and plasmatic membrane's permeability. Both assays indicated that the compound has higher affinities towards aqueous media, surprisingly contrasting with the solubility issues previously mentioned. This dual behavior difficulted the task of finding the right chromatographic conditions to better isolate and quantify the test compound. At this point, the possibility of separating the **815A** counting on its permanent cation through ion exchange chromatography was assessed. The method used involved the modification of a C18 column surface with anionic detergents. However, this approach was also fund unable to retain the test compound, besides being too laborious and poorly reliable.

It was thus understood that none of the assessed chromatographic conditions enabled both its separation and quantification in HPLC in reproductible, efficient and selective way. Therefore, the development of a methodology capable of selectively isolate the test compound from biological samples prior to its quantification had to be developed. This involved the use of a plasma surrogate spiked with test compound. This was submitted to different deproteinization techniques aiming at simplifying the sample and recovering compound **815A**. However, after the protein removal step, no compound, or very low amounts of it, were observed in the supernatant. It was hypothesized that the compound was being removed along with the proteins due to its probably high affinity for them. This was assessed by comparing the data obtained in plasma surrogate samples with the ones obtained using control samples without any protein content. Whereas in the control samples a recovery of 99% of the initial amount of compound **815A** was observed, no compound was detected in the supernatant of protein-containing samples. The tendency of this compound to bond to plasma proteins was confirmed by digesting the protein pellet and confirming the presence of the test compound in it, and afterwards by conducting an equilibrium dialysis assay. In both cases it was concluded that the compound **815A** has a high PPB tendency, as predicted before based on its structural features.

The only deproteinization technique that allowed the isolation the test compound from both plasma surrogates and real plasma samples was the addition of high concentrated salt solutions. Surprisingly, instead of causing protein precipitation, the salt addition resulted in the selective precipitation of the compound **815A**. From all the salts tested, better results were achieved with sodium fluoride. This allowed an 80% recovery of the compound from blood plasma samples. Efficacy that is maintained upon use of the soluble formulation with mannitol. After optimization, this isolation process comprised the addition of a saturated solution of sodium fluoride after the sample's incubation with a potent protease, found to aid on the compound's extraction. Once collected, the final pellet had to be dissolved for further quantification in a C18 column eluted at 1 mL/min with a 1:1:1 mixture of 0.1% aqueous formic acid – acetonitrile with 0.1% formic acid – methanol. There was still a lack of interactions between the compound **815A** and the stationary phase, however these were the only conditions allowing the observation of a well resolved and isolated peak. The method was further refined with the use of an internal standard to reduce the inter-assay variations caused by the injection system..

At this point, all the aims initially traced for this project were completed. A water soluble formulation of compound **815A** had been developed, as well as a protocol that allowed both its isolation and quantification in biological samples. However, considering the known dual immunomodulatory behavior

of the NKp30 receptor, another formulation approach was assessed with the aim of achieving a prolonged and effective activation of NK cells. For that, a controlled-release drug delivery system with biocompatible and biodegradable features was developed. The double emulsification-solvent evaporation technique (W/O/W) was chosen to produce **815A**-loaded polymer (PLGA) nanoparticles. As these NPs were intended to be used in IV formulations, their size would have to be within the range of 10 to 200 nm, with a PdI value below 0.5. Although NPs with hydrodynamic radii averaging 118 nm could be produced by the developed methods, none of the attempts results in samples with PdI below 0.5. Despite this, the effect of encapsulating the test compound in NPs on the activation of NK cells was evaluated using primary cultures of PBMCs. In these, the biocompatibility of PLGA nanoparticles was confirmed, as no increases in the secretion of the cytokine IFN-γ were observed in the culture treated with unloaded-NPs. On the other hand, in the culture treated with **815A**-loaded NPs, an increase in the levels of secreted IFN-γ could be observed after 48 hours. More important, this effect persisted until de end of the experiment (day 5), with the level of IFN-γ in the medium remaining stable. In the control culture, treated with an equivalent amount of **815A** in its free form, the effect dropped immediately after reaching the peak at 48 hours. This suggests that the use of nanoparticles to sustain a controlled and prolonged release of compound **815A** could, in fact, result in a more stable and efficient activation of NK cells, increasing their efficacy in tumor targeting and lysis.

3.2. Critical overview and perspectives

Overall, the results here presented answer some of the questions regarding the behavior of compound **815A** in biological medium. The ADME properties here determined are in accordance with the predicted, especially in terms of *logP*, membrane permeability, plasma stability and plasma protein binding. Regarding the selective extraction and quantification procedures developed herein, some aspects still require further development. The HPLC quantification method presents a low sensibility encompassing high LOD and LOQ values which can highly influence and jeopardize the performance of several assays requiring the use of low concentrations of the test compound. This problem is further enhanced by the necessity of performing the prior isolation of compound **815A** from biological samples, increasing the associated errors. In this work, the use of a C18 column was preferred over the CN column due to the lack of repeatability of analysis performed in the later. However, these were probably caused by matrix effects that could be minimized with the extraction procedure here developed and the use of an internal standard. However, this would still require a great deal of optimization of both the extraction of compound **815A** and of the chromatographic conditions. nevertheless, the low LOQ and LOD values observed with the CN column are quite attractive, and its use should be revisited in the future.

The results obtained in the NK cell stimulation assay using **815A**-load NPs provide valuable insights into the use of a modified release system for the delivery of controlled amounts of the test compound into the blood stream. The fact that, in the assays here performed, NK cell activity seems to be sustained

over a longer period of time, in contrast with what is observed using the free form of **815A**, grants this method great attractiveness.

The work here developed should encourage the further development of a NK cell-based therapy using compound **815A**, promoting the strong and controlled activation of NK cells against cancer.

IV. MATERIALS & METHODS

4.1. General procedures and equipment

4.1.1. Reagents and solvents

All reagents were used without any purification procedures. Compound 815A was obtained from the synthesis line of the Design, synthesis, and toxicology of bioactive molecules (BIOMOL) group of Centro de Química Estrutural (CQE), as a dry powder with a purity greater than 98%, as determined by NMR titration experiments and liquid chromatography – mass spectrometry (LC-MS). All solvents used in the HPLC system were of gradient grade (Thermo Fisher Scientific, Waltham, MA, USA). All other reagents and solvents were of p.a. grade or higher.

4.1.2. High Performance Liquid Chromatography

4.1.2.1. Chromatographic system

HPLC was conducted on an Ultimate 3000 Dionex system consisting of an LPG-3400A quaternary gradient pump and a diode array spectrophotometric detector (Dionex Co., Sunnyvale, CA, USA) and equipped with a Rheodyne model 8125 injector (Rheodyne, Rohnert Park, CA, USA). HPLC analyses were performed with a Luna C18 (2) column (250 mm × 4.6 mm; 5 µm; Phenomenex, Torrance, CA, USA), at a flow rate of 1 $mL.min^{-1}$ using different mobile phases and elution sequences. The optimized conditions consisted of a 10-minute isocratic elution of aqueous 0.1% formic acid – acetonitrile with 0.1% formic acid – methanol, at a proportion of 1:1:1. All samples were prepared in DMSO with or without 10 mM anthranilic acid as internal standard. Each injection admitted 10 µL of sample into the system through the µL-pickup mode using isopropanol/water (9:1) as pickup fluid. Chromatograms were recorded between 220 and 700 nm, using the fixed wavelengths of 254 or 330 nm for monitoring.

4.1.2.2. HPLC columns

The HPLC columns used in this work were:

- Luna C18 (2) column (250 mm × 4.6 mm; 5 µm; Phenomenex)
- Luna C8 (2) column (250 mm × 4.6 mm; 5 µm; Phenomenex)
- Microsorb-MV 100-5 CN (250 mm × 4.6 mm; 5 µm; Varian, Palo Alto, CA, USA)
- XBridge BEH Amide XP 130Å (2.1 mm X 150 mm; 2.5 µm; Waters Corporation, Milford, MA, USA)

All columns were protected with a pre-column (SecurityGuard Cartridge C18 4x3.0 mm; Phenomenex).

4.1.2.3. Column functionalization for cation exchange chromatography

For cation exchange chromatography experiments, a C18 column (Luna C18 (2) column (250 mm × 4.6 mm; 5 µm) was functionalized with either 10 mM of sodium dodecyl sulfate or 2 mM octanoic acid in water, flowing at 0.3 mL/min for 3 hours.[83] Excess surfactant was removed by running the system with water at 0.6 mL/min for 2 hours. The column was recovered by removing all the surfactant running methanol for 24 hours at 0.1 mL/min.

4.1.3. Ultraviolet-visible Spectroscopy

The UV-Vis spectra acquired throughout this work, either for quantitative and/or qualitative purposes, were recorded using a SPECTROstar Nano microplate reader equipped with an *LVis* low-volume measurements plate (BMG Labtech, Ortenberg, Germany).

4.1.4. Zetasizer

The NPs hydrodynamic diameters and polydispersity indexes (PdI) were measured using a Zetasizer (ZEN3600 Nano ZS; Malvern Instruments, Worcestershire, UK). Measures were performed in 1 cm polycarbonate cuvettes, at 25 ºC.

4.1.5. Melting point measurements

The melting point determination was conducted in a Buchï B-545 (Buchï AG, Flawil, Switzerland) using a Ø1.0 mm glass capillaries, without correction. The maximum measurable value was 400 ºC, with an error of 0.8 ºC.

4.2. Study of ADME properties

4.2.1. Isolation of compound 815A from different matrices

The fully optimized isolation protocol encompassed the pre-incubation of the sample with 0.4 mg/mL of proteinase K (Cat# A4392; PanReac Applichem, Darmstadt, Germany) and 5 mM of calcium chloride for one hour at 37 ºC (this step is suppressed or samples without protein), followed by the addition of five times the volume of the initial sample of a saturated solution of sodium fluoride (Cat# A13019; Alfa Aesar, Haverhill, MA, USA), followed by incubation at 3 ºC overnight. Samples were then 16000 x *g* at 4 ºC for 5 minutes. The supernatant was discarded, and the pellet washed with the same volume of saturated sodium fluoride solution and water. The pellet obtained in the end was either dried or dissolved for subsequent analysis.

4.2.2. Plasma stability assays

Freshly isolated human blood plasma samples (obtained as detailed in Section 4.4.1) were spiked with 2 mM of compound **815A** in DMSO. All samples were incubated at 37 ºC for three consecutive days. Aliquots were collected at different time points throughout the incubation period and submitted to the developed and optimized isolation and quantification processes (Sections 4.2.1 and 4.1.2).

4.2.3. *logP* determination

Six tubes containing 1 mL of an aqueous solution of 1 mM of **815A** in 5% mannitol (pH 7) were prepared. To three of these, 1 mL of octanol was added. All tubes were vigorously vortexed for 1 minute and then left agitating at room temperature for 2.5 hours. The aqueous portion of each sample was collected and the concentration of compound **815A** was determined by spectrophotometry (Section 4.1.3).

4.2.4. PAMPA assays

The PAMPA assay (Parallel artificial membrane permeability assay) was conducted using artificial lipidic membranes assembled in filter plates (MultiScreen IP Filter Plate, 0.45 µm; Merck KGaA, Darmstadt, Germany) using a mixture of dipalmitoylphosphatidylcholine:stearic acid (80:20, w/w; Avanti Polar Lipids, Inc., Alabaster, AL, USA). The artificial lipidic membrane was prepared by adding 4 µL of the lipid mixture to each well, being the correct application evidenced by the change in transparency of the membrane. Acceptor wells were filled with 320 µL of 50 mM ammonium bicarbonate buffer pH 7.4, and the donor wells were filled with 150 µL of 1 mM **815A** solutions in 5% mannitol. The plaque was incubated for 18 hours at room temperature. Thed content of both acceptor and donor wells were subjected to analysis to identify and quantify compound **815A**.

4.2.5. Plasma protein binding assays

4.2.5.1. Protein precipitation

Plasma surrogate (40% BSA solution) and water samples were spiked with 0.2 mM of compound **815A**. After being gently mixed, five volumes of absolute ethanol were added to both. All samples were centrifuged at 16000 x *g* for 5 minutes at room temperature and the supernatants were collected and stored. To the resultant pellets, 0.4 mg/mL of proteinase K and 5 mM of calcium chloride were added, and the samples were left incubating for one hour at 37 ºC. All samples, including the supernatants collected before, were vacuum dried before redissolution in DMSO for quantification (Section 4.1.2).

4.2.5.2. Dialysis

The equilibrium dialysis procedure was conducted using a dialysis tubing with a molecular weight cut-off of 10 kDa (D9652; Sigma-Aldrich, St. Louis, MO, USA). The interior of the membrane was filled with 5 mL of blood plasma spiked with 0.1 mM of compound **815A** and submerged in 5 mL of a 5% mannitol solution. The system was left softly stirring for 3 days at room temperature. The mannitol solution was collected and subjected to the isolation protocol (Section 4.2.1) and then quantified by HPLC (Section 4.1.2).

4.3. Intravenous formulations

4.3.1. Free form formulation

The injectable formulation of compound **815A** in its free form was prepared using mannitol as stabilizer. Several stabilizers and proportions were tested following the generic procedure described below.

A sample of compound **815A** dissolved in DMSO was added to twenty times its volume of a 5% mannitol solution. The resultant clear solution was filtered through a 0.22 µm syringe filter into sterile vials and concentrated for 48 hours in a centrifuge concentrator, yielding a white to off-white powder readily soluble in water.

4.3.2. Controlled release system formulation

4.3.2.1. Preparation of nanoparticles

PLGA nanoparticles were prepared routinely using the general procedure described below.

A 10 mg/mL PLGA (poly(lactic-co-glycolide4) 50:50, 5000-10000 Da; Acros Organics, B.V.B.A, Geel, Belgium) solution in ethyl acetate was mixed with a third of its volume of the free form formulation of compound **815A**. The mixture was emulsified using an ultrasonic homogenizer coupled with a MS 72 probe (Bandelin Sonoplus, Berlin, Germany) with a 50% amplitude defined, for 3 minutes. Thereafter, the primary emulsion (W/O) was added to another tube containing an equal volume of 5% mannitol and, once more, was well mixed and sonicated. This secondary emulsion (W/O/W) was added drop wise into three times its volume of stirring 5% mannitol and, subsequently, left overnight at 400 rpm at constant temperature (30 ºC) to evaporate all the solvent (HLC Heating-ThermoMixer MHR 2;, Ditabis AG, Pforzheim, Germany). The suspended NPs were collected after consecutive centrifugation/washing steps with deionized water at 4000 x *g* for 20 minutes. Lastly, the NPs were resuspended in 2-3 mL of 1% Sucrose and freeze-dried (Alpha 1-2 LDplus; Christ, Osterode am Harz, Germany).

4.4. Biological assays

4.4.1. NK cell activation assays

The presented protocol follows all recommendations of the Institutional Ethics Committee (process 15/2021 CE-IST). All participants provided a written informed consent and personal data protection was safeguarded in all instances.

4.4.1.1. Blood collection

Peripheral blood was obtained by venipuncture of the median cubital vein of four volunteers (Table 11) using a closed S-Monovette® system (Sarstedt, AG & Co. KG, Nümbrecht, Germany). Blood was collected into tubes containing EDTA or clot activator, for cell and serum isolation, respectively.

Table 11: Blood donors' characteristics.

Donor	Gender	Age (years)	Weight (kg)
A	Male	25	68
B		40	72
C		33	85
D	Female	23	74

4.4.1.2. Blood serum isolation

To isolate blood serum, blood collected into clot activator tubes was left at room temperature for 30/45 minutes before centrifugation at 1500 x *g* for 10 minutes. The serum layer was carefully separated from the clot and stored at -20 ºC.

4.4.1.3. Blood plasma and PBMCs isolation

Blood collected into EDTA tubes was layered onto an equal volume of Ficoll Histopaque®-1077 (Cat# 10771; Sigma-Aldrich) in 50 mL conical sterile tubes. After a 30-minute centrifugation at 400 x *g*, the upper layer of plasma was transferred into a sterile tube, filtered through a 0.22 µm syringe filter and immediately frozen. The interphase containing the PBMCs were transferred into a 50-mL tube and immediately diluted with sterile PBS. Cell suspensions were centrifuged at 300 x *g* for 10 minutes and the pellets washed with 40-45 mL of sterile PBS at least two times to remove Ficoll and platelets.

4.4.1.4. PBMC cultures

PBMCs isolated as described before were resuspended to a density of $1x10^6$ cells/mL in culture medium comprised of a 1:1 mixture of DMEM (Cat# D5523; Sigma-Aldrich) and Ham's nutrient mixture F12 (Cat# N3520; Sigma-Aldrich) base media, supplemented with 5% autologous serum (isolated as described in Section 4.4.1.2), 15 µM HEPES (4-(2-hydroxyethyl)-1-piperazineethanesulfonic acid; Cat# A1069; PanReac Applichem), 100 U/mL penicillin and 100 µg/mL streptomycin (Cat# P4333; Sigma-Aldrich), 24 µM β-mercaptoethanol (Cat# M3148; Sigma-Aldrich), 20 mg/L *L*-ascorbic acid (Cat# A4544; Sigma-Aldrich), 5 µg/L sodium selenite (Cat# S5261, Sigma-Aldrich), 0.25 µg/mL Amphotericin B (Cat# 17-836E; Lonza, Basel, Switzerland), and 250 U/mL of rhIL-2 (Cat#200-02; Peprotech, London, UK).

The cell suspension was equally divided in three sterile Erlenmeyer flasks (approx. 30 mL per flask) equipped with cotton plugs. To each, either unloaded NPs, **815A**-loaded NPs or **815A** in DMSO stock solution, were added. The amounts of **815A**-loaded NPs and **815A** stock solution were adjusted to yield a final maximum concentration of test compound of 5 µM. The controlled flask (unloaded-NPs) received the same amount of NPs as the **815A**-loaded NPs' flask. All systems were incubated at 37 ºC in an orbital stirring platform (100 rpm). Samples of each flask (1 mL each) were collected every 24 hours and stored at -20 ºC after a first centrifugation at 200 x *g* and the second at 10000 x *g* both for 10 minutes at room temperature.

4.4.1.5. ELISA assays

IFN-γ quantifications were performed using a commercial ELISA kit (Human IFN-gamma DuoSet ELISA, Cat# DY285B; R&D Systems, Minneapolis, MN, USA) according to the manufacturer's instructions. Colour development was achieved using the Substrate Reagent Pack (Cat# DY999; R&D Systems) and measured at 450 nm with correction at 570 nm in a plate reader (Section 4.1.3).

V. REFERENCES

1 ECIS-European Cancer Information System. https://ecis.jrc.ec.europa.eu/. Accessed 19-10-2021.

2 Causas de morte – 2017, Instituto Nacional de Estatística, I.P. 2017, Lisboa.

3 Sung, H. *et al.* Global Cancer Statistics 2020: GLOBOCAN Estimates of Incidence and Mortality Worldwide for 36 Cancers in 185 Countries. *CA: A Cancer Journal for Clinicians* **71**, 209-249 (2021).

4 You, W. & Henneberg, M. Cancer incidence increasing globally: The role of relaxed natural selection. *Evolutionary Applications* **11**, 140-152 (2018).

5 Hofmarcher T, B. G., Svedman C, Lindgren P, Jönsson B and Wilking N. Comparator Report on Cancer in Europe 2019 – Disease Burden, Costs and Access to Medicines. *The Swedish Institute for Health Economics* (2020).

6 Abudu, R. *et al.* Trends in International Cancer Research Investment 2006-2018. *JCO Global Oncology*, 602-610 (2021).

7 Global Oncology Trends 2019. *Therapeutics, Clinical Development and Health System Implications Institute Report* (2019).

8 Oiseth, S. J. & Aziz, M. S. Cancer immunotherapy: a brief review of the history, possibilities, and challenges ahead. *Journal of Cancer Metastasis and Treatment* **3**, 250 (2017).

9 Rosenberg S. A., Lotze, M. T. *et al.* Observations on the systemic administration of autologous lymphokine-activated killer cells and recombinant interleukin-2 to patients with metastatic cancer. *New England Journal of Medicine* **313**, 23, 1485-1492 (1985).

10 Block, K. I., Boyd, D. B., Gonzalez, N. & Vojdani, A. The Immune System in Cancer. *Integrative Cancer Therapies* **1**, 3, 294-316 (2002).

11 Morgan D. F, Ruscetti, F. W. & Gallo, R. Selective in vitro growth of T lymphocytes from normal human bone marrows. *Science* **193**, 4257, 1007-1008 (1976).

12 Kim, R., Emi, M. & Tanabe, K. Cancer immunoediting from immune surveillance to immune escape. *Immunology* **121**, 1, 1-14 (2007).

13 Swann, J. B. & Smyth, M. J. Immune surveillance of tumors. *Journal of Clinical Investigation* **117**, 5, 1137-1146 (2007).

14 Rohaan, M. W., van den Berg, J. H., Kvistborg, P. & Haanen, J. B. A. G. Adoptive transfer of tumor-infiltrating lymphocytes in melanoma: a viable treatment option. *J Immunother Cancer* **6**, 1, 102 (2018).

15 Buell, J. F., Gross, T. G. &Woodle, E. S. Malignancy after transplantation. *Transplantation*, **80**, 2, S254-264 (2005)

16 Rama, I. & Grinyó, J. M. Malignancy after renal transplantation: the role of immunosuppression. *Nature Reviews Nephrology* **6**, 9, 511-519 (2010).

17 Schuster, M., Nechansky, A. & Kircheis, R. Cancer immunotherapy. *Biotechnology Journal* **1**, 2, 138-147 (2006).

18 Kokate, R. A Systematic Overview of Cancer Immunotherapy: An Emerging Therapy. *Pharmacy & Pharmacology International Journal* **5**, 2, 31-35 (2017).

19 Capitini, C. M., Fry, T. J. & Mackall, C. L. Cytokines as Adjuvants for Vaccine and Cellular Therapies for Cancer. *Am J Immunol* **5**, 3, 65-83 (2009).

20 Berraondo, P. *et al.* Cytokines in clinical cancer immunotherapy. *British Journal of Cancer* **120**, 6-15 (2019).

21 Marelli, G., Howells, A., Lemoine, N. R. & Wang, Y. Oncolytic Viral Therapy and the Immune System: A Double-Edged Sword Against Cancer. *Frontiers in immunology* **9**, 866-866 (2018).

22 Zhang, Y. & Zhang, Z. The history and advances in cancer immunotherapy: understanding the characteristics of tumor-infiltrating immune cells and their therapeutic implications. *Cellular & Molecular Immunology* **17**, 8, 807-821 (2020).

23 Esfahani, K. *et al.* A review of cancer immunotherapy: from the past, to the present, to the future. *Curr Oncol* **27**, 2, S87-S97 (2020).

24 Galluzzi, L. *et al.* Classification of current anticancer immunotherapies. *Oncotarget* **5**, 24, 12472-12508 (2014).

25 Gill, S., Maus, M. V. & Porter, D. L. Chimeric antigen receptor T cell therapy: 25years in the making. *Blood Reviews* **30**, 3 157-167 (2016).

26 Garrido, F. & Aptsiauri, N. Cancer immune escape: MHCexpression in primary tumours versus metastases. *Immunology* **158**, 4, 255-266 (2019).

27 Garcia-Lora, A., Algarra, I. & Garrido, F. MHC class I antigens, immune surveillance, and tumor immune escape. *Journal of Cellular Physiology* **195**, 3, 346-355 (2003).

28 Papaioannou, N. E., Beniata, O. V., Vitsos, P., Tsitsilonis, O. & Samara, P. Harnessing the immune system to improve cancer therapy. *Annals of Translational Medicine* **4**, 14, 261-261 (2016).

29 Cheung, T. C. & Ware, C. F. in *Encyclopedia of Biological Chemistry (Second Edition)* (eds William J. Lennarz & M. Daniel Lane), 454-459 (Academic Press, 2013).

30 Nagasawa, D. T. *et al.* Passive immunotherapeutic strategies for the treatment of malignant gliomas. *Neurosurg Clin N Am* **23**, 3, 481-495 (2012).

31 Divgi, C. R. & Larson, S. M. Radiolabeled monoclonal antibodies in the diagnosis and treatment of malignant melanoma. *Seminars in Nuclear Medicine* **19**, 4, 252-261 (1989).

32 Ventola, C. L. Cancer Immunotherapy, Part 3: Challenges and Future Trends. *P&T* **42**, 8, 514-521 (2017).

33 Chiriva-Internati, M. & Bot, A. A new era in cancer immunotherapy: discovering novel targets and reprogramming the immune system. *International Reviews of Immunology* **34**, 2, 101-103 (2015).

34 Fellner, C. Ipilimumab (yervoy) prolongs survival in advanced melanoma: serious side effects and a hefty price tag may limit its use. *P&T* **37**, 9, 503-511 (2012).

35 Hay, A. E. & Cheung, M. C. CAR T-cells: costs, comparisons, and commentary. *Journal of Medical Economics* **22**, 7, 613-615 (2019).

36 Lorenzo-Herrero, S. *et al.* NK Cell-Based Immunotherapy in Cancer Metastasis. **Cancers** 11, 1, 29 (2018).

37 Souza-Fonseca-Guimaraes, F., Cursons, J. & Huntington, N. D. The Emergence of Natural Killer Cells as a Major Target in Cancer Immunotherapy. *Trends in immunology* **40**, 2, 142-158 (2019).

38 Kiessling, R., Klein, E. & Wigzell, H. "Natural" killer cells in the mouse. I. Cytotoxic cells with specificity for mouse Moloney leukemia cells. Specificity and distribution according to genotype. *European Journal of Immunology* **5**, 2, 112-117 (1975).

39 Ribatti, D. Historical overview on the morphological characterization of large granular lymphocytes/natural killer cells. *Immunology Letters* **190**, 58-63 (2017).

40 Cao, Y. *et al.* Immune checkpoint molecules in natural killer cells as potential targets for cancer immunotherapy. *Signal Transduction and Targeted Therapy* **5**, 250 (2020).

41 Minetto, P. *et al.* Harnessing NK Cells for Cancer Treatment. *Frontiers in immunology* **6**, 10, 2836 (2019).

42 Pinheiro, P. F., Justino, G. C. & Marques, M. M. NKp30 - A prospective target for new cancer immunotherapy strategies. *British Journal of Pharmacology* **177**, 20, 4563-4580 (2020).

43 Ljunggren, H. G. & Kärre, K. In search of the 'missing self': MHC molecules and NK cell recognition. *Immunology Today* **11**, 7, 237-244 (1990).

44 Caligiuri, M. A. Human natural killer cells. *Blood* **112**, 3, 461-469 (2008).

45 Vivier, E., Ugolini, S., Blaise, D., Chabannon, C. & Brossay, L. Targeting natural killer cells and natural killer T cells in cancer. *Nature Reviews Immunology* **12**, 4, 239-252 (2012).

46 Paul, S. & Lal, G. The Molecular Mechanism of Natural Killer Cells Function and Its Importance in Cancer Immunotherapy. *Frontiers in Immunology* **8**, 1124 (2017)

47 Boivin, W. A., Cooper, D. M., Hiebert, P. R. & Granville, D. J. Intracellular versus extracellular granzyme B in immunity and disease: challenging the dogma. *Laboratory Investigation* **89**, 11, 1195-1220 (2009).

48 Ni, L. & Lu, J. Interferon gamma in cancer immunotherapy. *Cancer Medicine* **7**, 9, 4509-4516 (2018).

49 Josephs, S. F. *et al.* Unleashing endogenous TNF-alpha as a cancer immunotherapeutic. *Journal of Translational Medicine* **16**, 242 (2018).

50 Barrow, A. D., Martin, C. J. & Colonna, M. The Natural Cytotoxicity Receptors in Health and Disease. *Frontiers in immunology* **10**, 909 (2019).

51 Pende, D. *et al.* Identification and molecular characterization of NKp30, a novel triggering receptor involved in natural cytotoxicity mediated by human natural killer cells. *The Journal of Experimental Medicine* **190**, 10, 1505-1516 (1999).

52 Joyce, M. G., Tran, P., Zhuravleva, M. A., Jaw, J., Colonna, M., Sun, P. D. Crystal structure of human natural cytotoxicity receptor NKp30 and identification of its ligand binding site. *Proceedings of the National Academy of Sciences* **108**, 15, 6223-6228 (2011).

53 Li, Y., Wang, Q. & Mariuzza, R. A. Structure of the human activating natural cytotoxicity receptor NKp30 bound to its tumor cell ligand B7-H6. *J Exp Med* **208**, 4, 703-714 (2011).

54 Hsieh, C. L., Nagasaki, K., Martinez, O. M. & Krams, S. M. NKp30 is a functional activation receptor on a subset of rat natural killer cells. *Eur J Immunol* **36**, 8, 2170-2180 (2006).

55 Memmer, S. *et al.* The Stalk Domain of NKp30 Contributes to Ligand Binding and Signaling of a Preassembled NKp30-CD3ζ Complex. *Journal of Biological Chemistry* **291**, 49, 25427-25438 (2016).

56 Pogge Von Strandmann, E. *et al.* Human Leukocyte Antigen-B-Associated Transcript 3 Is Released from Tumor Cells and Engages the NKp30 Receptor on Natural Killer Cells. *Immunity* **27**, 6, 965-974 (2007).

57 Banu, N. *et al.* B7-H6, an immunoligand for the natural killer cell activating receptor NKp30, reveals inhibitory effects on cell proliferation and migration, but not apoptosis, in cervical cancer derived-cell lines. *BMC Cancer* **20**, 1, 1083 (2020).

58 Pinheiro, P. B. P. F. *Triggering a specific immune response against cancer. Activation of natural killer cells with small organic molecules* PhD Degree in Chemistry thesis, Instituto Superior Técnico da Universidade de Lisboa, (2020).

59 Mittal, S. K., Cho, K.-J., Ishido, S. & Roche, P. A. Interleukin 10 (IL-10)-mediated Immunosuppression. *Journal of Biological Chemistry* **290**, 45, 27158-27167 (2015).

60 Winiwarter, S., Ridderström, M., Ungell, A. L., Andersson, T. B. & Zamora, I. *Use of Molecular Descriptors for Absorption, Distribution, Metabolism, and Excretion Predictions i*n *Comprehensive Medicinal Chemistry II*, Triggle, D. & Taylor, J. (2). Elsevier Science, Amsterdam, 2007.

61 Lipinski, C. A., Lombardo F Fau - Dominy, B. W. & Feeney, P. J. Experimental and computational approaches to estimate solubility and permeability in drug discovery and development settings. *Advanced drug delivery reviews* **46**, 1, 3-26 (2001).

62 Moriguchi, I., Hirono, S., Liu, Q., Nakagome, I. & Matsushita, Y. Simple Method of Calculating Octanol/Water Partition Coefficient. *Chemical and Pharmaceutical Bulletin* **40**, 1, 127-130 (1992).

63 Tozer, T. N. & Rowland, M. *Essentials of pharmacokinetics and pharmacodynamics*. (2). Wolters Kluwer, China (2016).

64 Coimbra, J. T. S., Feghali, R., Ribeiro, R. P., Ramos, M. J. & Fernandes, P. A. The importance of intramolecular hydrogen bonds on the translocation of the small drug piracetam through a lipid bilayer. *RSC Advances* **11**, 2, 899-908 (2021).

65 Di, L. & Kerns, E. H. *Solubility* in *Drug-Like Properties*, Di, L. & Kerns, E. H. (2). Elsevier Science, Amsterdam (2016).

66 Bergström, C. A. S. & Larsson, P. Computational prediction of drug solubility in water-based systems: Qualitative and quantitative approaches used in the current drug discovery and development setting. *Int J Pharm* **540**, 1-2, 185-193 (2018).

67 Drug Metabolism and pharmacokinetics Analysis Platform. https://drumap.nibiohn.go.jp/. *Acessed 19-10-21*.

68 VanPutte, C. L. & Seeley, R. R. *Cardiovascular System: Blood* in in *Seeley's Anatomy & Physiology*, Regan, J., Russo, A., VanPutte, C. L. & Seeley, R. R. (12) McGraw-Hill Higher Education, New York (2014).

69 Lalatsa, A., Schätzlein, A. G. & Uchegbu, I. F. *Drug Delivery Across the Blood–Brain Barrier* in *Comprehensive Biotechnology*, Moo-Young, M. (2) Elsevier Science, Amsterdam (2011).

70 *Applied biopharmaceutics & pharmacokinetics*, Shargel, L. & Yu, A. B. C. (7) McGraw Hill, New York (2016).

71 Watanabe, R. *et al.* Development of an in silico prediction system of human renal excretion and clearance from chemical structure information incorporating fraction unbound in plasma as a descriptor. *Scientific Reports* **9**, 18782 (2019).

72 *European pharmacopoeia,* Council Of Europe : European Directorate for the Quality of Medicines and Healthcare (10) Council of Europe, E.D.Q.M., Strasbourg (2019)

73 *Técnicas e Operações Unitárias em Química Laboratorial*, Pombeiro, A. J. L. O. (4) Fundação Calouste Gulbenkian, Lisbon (2003).

74 *Principles of instrumental analysis*, Skoog, D. A., Crouch, S. R. & Holler, F. J. (6) Thomson Brooks/Cole, Belmont (2007).

75 *Fundamentals of Analytical Chemistry*, Skoog, D. A., West, D. M., Crouch, S. R. & Holler, F. J. (9) Thomson Brooks/Cole, Belmont (2013).

76 *Modern analytical chemistry*, Harvey, D. (1) McGraw Hill, New York (1999).

77 Carsten Paul, F. S., Michael W. Dong. HPLC Autosamplers: Perspectives, Principles, and Practices. *LCGC North America* **37**, 37, 514-529 (2019).

78 Swartz, M. HPLC DETECTORS: A BRIEF REVIEW. *Journal of Liquid Chromatography & Related Technologies* **33**, 9-12, 1130-1150 (2010).

79 Žuvela, P. *et al.* Column Characterization and Selection Systems in Reversed-Phase High-Performance Liquid Chromatography. *Chemical Reviews* **119**, 6, 3674-3729 (2019).

80 Rambla-Alegre, M., Carda-Broch, S. & Esteve-Romero, J. Column Classification and Selection for the Determination of Antibiotics by Micellar Liquid Chromatography. *Journal of Liquid Chromatography & Related Technologies* **32**, 8, 1127-1140 (2009).

81 Okusa, K., Tanaka, H. & Ohira, M. Development of a new cyano-bonded column for high-performance liquid chromatography. *Journal of Chromatography A* **869**, 1-2, 143-149 (2000).

82 Glenn, K. M. & Lucy, C. A. Stability of surfactant coated columns for ion chromatography. *The Analyst* **133**, 11, 1581-1586 (2008).

83 Fasciano, J. M., Mansour, F. R. & Danielson, N. D. Ion-Exclusion High-Performance Liquid Chromatography of Aliphatic Organic Acids Using a Surfactant-Modified C18 Column. *Journal of Chromatographic Science* **54**, 6, 958-970 (2016).

84 Ohtaka, R. *et al.* Precision of Internal Standard Method in HPLC Analysis. *Yakugaku Zasshi* **123**, 5, 349-355 (2003).

85 Ralston, P. B. & Strein, T. G. A Study of Deproteinization Methods for Subsequent Serum Analysis with Capillary Electrophoresis. *Microchemical Journal* **55**, 270-283 (1997).

86 Daykin, C. A., Foxall, P. J. D., Connor, S. C., Lindon, J. C. & Nicholson, J. K. The Comparison of Plasma Deproteinization Methods for the Detection of Low-Molecular-Weight Metabolites by 1H Nuclear Magnetic Resonance Spectroscopy. *Analytical Biochemistry* **304**, 2, 220-230 (2002).

87 Hunter, G. A method for deproteinization of blood and other body fluids. *J Clin Pathol* **10**, 2, 161-164 (1957).

88 Polson, C., Sarkar, P., Incledon, B., Raguvaran, V. & Grant, R. Optimization of protein precipitation based upon effectiveness of protein removal and ionization effect in liquid chromatography–tandem mass spectrometry. *Journal of Chromatography B* **785**, 2, 263-275 (2003).

89 Novák, P. & Havlíček, V. *Protein Extraction and Precipitation* in *Proteomic Profiling and Analytical Chemistry,* Ciborowski, P. & Silberring, J.(2) Elsevier Science, Amsterdam (2016).

90 Rather, I. A., Wagay, S. A. & Ali, R. Emergence of anion-π interactions: The land of opportunity in supramolecular chemistry and beyond. *Coordination Chemistry Reviews* **415**, 213327 (2020).

91 Lee, Y.-C., Zocharski, P. D. & Samas, B. An intravenous formulation decision tree for discovery compound formulation development. *International Journal of Pharmaceutics* **253**, 1-2, 111-119 (2003).

92 Strickley, R. G. Solubilizing excipients in oral and injectable formulations. *Pharmaceutical research* **21**, 2, 201-230 (2004).

93 Roethlisberger, D., Mahler, H. C., Altenburger, U. & Pappenberger, A. If Euhydric and Isotonic Do Not Work, What Are Acceptable pH and Osmolality for Parenteral Drug Dosage Forms? *Journal of Pharmaceutical Sciences* **106**, 2, 446-456 (2017).

94 Patel, D., Zode, S. S. & Bansal, A. K. Formulation aspects of intravenous nanosuspensions. *International Journal of Pharmaceutics* **586**, 119555 (2020).

95 Connelly, J. *ICH Q3C Impurities* in *ICH Quality Guidelines: An Implementation Guide*, Teasdale, A., Elder, D. & Nims, R. W. (1) Wiley, Hoboken (2017).

96 Cho, J. & Kim, D. M. Comparison of distillation arrangement for the recovery process of dimethyl sulfoxide. *Korean Journal of Chemical Engineering* **24**, 3, 438-444 (2007).

97 Schönsee, C. D. & Bucheli, T. D. Experimental Determination of Octanol–Water Partition Coefficients of Selected Natural Toxins. *Journal of Chemical & Engineering Data* **65**, 4, 1946-1953 (2020).

98 Di, L., Kerns, E. H., Hong, Y. & Chen, H. Development and application of high throughput plasma stability assay for drug discovery. *International Journal of Pharmaceutics* **297**, 1-2, 110-119 (2005).

99 Di, L. & Kerns, E. H. *In Vivo Environments Affect Drug Exposure* in *Drug-Like Properties*, Di, L. & Kerns, E. H. (2). Elsevier Science, Amsterdam (2016).

100 Kansy, M., Senner, F. & Gubernator, K. Physicochemical High Throughput Screening: Parallel Artificial Membrane Permeation Assay in the Description of Passive Absorption Processes. *Journal of Medicinal Chemistry* **41**, 7, 1007-1010 (1998).

101 Berben, P. *et al.* Drug permeability profiling using cell-free permeation tools: Overview and applications. *European journal of pharmaceutical sciences : official journal of the European Federation for Pharmaceutical Sciences* **119**, 219-233 (2018).

102 He, S., Zhiti, A., Barba-Bon, A., Hennig, A. & Nau, W. M. Real-Time Parallel Artificial Membrane Permeability Assay Based on Supramolecular Fluorescent Artificial Receptors. *Frontiers in Chemistry* **8**, 597927 (2020).

103 Barton, P., Austin, R. P. & Fessey, R. E. *In Vitro Models for Plasma Binding and Tissue Storage in Comprehensive Medicinal Chemistry II*, Triggle, D. & Taylor, J. (2). Elsevier Science, Amsterdam, 2007.

104 Di, L. & Kerns, E. H. *Plasma Protein Binding Methods* in *Drug-Like Properties*, Di, L. & Kerns, E. H. (2). Elsevier Science, Amsterdam (2016).

105 Heng, P. W. S. Controlled release drug delivery systems. *Pharmaceutical Development and Technology* **23**, 9, 833 (2018).

106 Indurkhya, A. *et al. Influence of Drug Properties and Routes of Drug Administration on the Design of Controlled Release System* in *Dosage Form Design Considerations*, Tekade, R. K. (1) Academic Press, Cambridge (2018).

107 Zielińska, A. *et al.* Polymeric Nanoparticles: Production, Characterization, Toxicology and Ecotoxicology. *Molecules* **25**, 16, 3731 (2020).

108 Danhier, F., Ansorena, E., Silva, J. M., Coco, R., Breton, A. L. & Préat, V. PLGA-based nanoparticles: an overview of biomedical applications. *Journal of controlled release: official journal of the Controlled Release Society* **161**, 2, 505-522 (2012).

109 Kapoor, D. N., Bhatia, A., Kaur, R., Scharma, R., Kaur, G. & Dhawan, S. PLGA: a unique polymer for drug delivery. *Therapeutic Delivery* **6**, 1, 41-58 (2015).

110 Rafiei, P. & Haddadi, A. Docetaxel-loaded PLGA and PLGA-PEG nanoparticles for intravenous application: pharmacokinetics and biodistribution profile. *International Journal of Nanomedicine* **12**, 935-947 (2017).

111 Alshamsan, A. Nanoprecipitation is more efficient than emulsion solvent evaporation method to encapsulate cucurbitacin I in PLGA nanoparticles. *Saudi Pharmaceutical Journal* **22**, 3, 219-222 (2014).

112 Moghimi, S. M., Hunter, A. C. & Andresen, T. L. Factors Controlling Nanoparticle Pharmacokinetics: An Integrated Analysis and Perspective. *Annual Review of Pharmacology and Toxicology* **52**, 481-503 (2012).

113 Owensiii, D. & Peppas, N. Opsonization, biodistribution, and pharmacokinetics of polymeric nanoparticles. *International Journal of Pharmaceutics* **307**, 1, 93-102 (2006).

114 Danaei, M. *et al.* Impact of Particle Size and Polydispersity Index on the Clinical Applications of Lipidic Nanocarrier Systems. *Pharmaceutics* **10**, 2, 57 (2018).

115 Huang, W. & Zhang, C. Tuning the Size of Poly(lactic-co-glycolic Acid) (PLGA) Nanoparticles Fabricated by Nanoprecipitation. *Biotechnology journal* **13**, 1 (2018).

116 Sahin, A. *et al.* A small variation in average particle size of PLGA nanoparticles prepared by nanoprecipitation leads to considerable change in nanoparticles' characteristics and efficacy of intracellular delivery. *Artificial Cells, Nanomedicine, and Biotechnology* **45**, 8, 1657-1664 (2017).

117 Marshall, J. D., Heeke, D. S., Abbate, C., Yee, P. & Van Nest, G. Induction of interferon-gamma from natural killer cells by immunostimulatory CpG DNA is mediated through plasmacytoid-dendritic-cell-produced interferon-alpha and tumour necrosis factor-alpha. *Immunology* **117**, 1, 38-46 (2006).

118 David, C. A. W., Barrow, M., Murray, P., Rosseinsky, M. J., Owen, A. & Liptrott, N. J. In Vitro Determination of the Immunogenic Impact of Nanomaterials on Primary Peripheral Blood Mononuclear Cells. *Int J Mol Sci* **21**, 16, 5610 (2020).

119 Cleland, J. L., Lam, X., Kendrick, B., Yang, J., Yang, T. H., Overcashier, D., Brooks, D., Hsu, C. & Carpenter, J. F. A specific molar ratio of stabilizer to protein is required for storage stability of a lyophilized monoclonal antibody. *Journal of Pharmaceutical Sciences* **90**, 3, 310-321 (2001).

120 Kaialy, W., Khan, U. & Mawlud, S. Influence of mannitol concentration on the physicochemical, mechanical and pharmaceutical properties of lyophilised mannitol. *Int J Pharm* **510**, 1, 73-85 (2016).

VI. APPENDIX

6.1. *logP* value calculation

The logP value was calculated according to the Moriguchi's method, which accounts on the effect of different structural characteristics and moieties according to Equation A1.[62] The attributed values at each factor for 815A are presented in Table A1.

$$logP = 1.244(CX)^{0.6} - 1.017(NO)^{0.9} + 0.406(PRX) - 0.145(UB)^{0.6} + 0.511(HB) + 0.268(POL) - 2.212(AMP) + 0.912(ALK) - 0.392(RND) + 3.684(QN) + 0.474(NO_2) + 1.581NCS + 0.773BLM - 1.041 \quad \text{Eq. A1}$$

Table A1: Parameters required for the calculation of *logP* according to Equation A1.[62]

Parameter	Description	Final Value
CX	Number of carbon and halogen atoms	29
NO	Number of nitrogen and oxygen atoms	15
PRX	Proximity effect of nitrogen/oxygen Direct bond: 2 ; Indirect bond: 1	13
UB	Unsaturated bonds (Except NO_2)	13
HB	Intramolecular hydrogen bond	1
POL	Aromatic substituents	7
AMP	Amphoteric property	1
ALK	Alkane, alkene	0
RND	Ring structures except for condensed rings	2
QN	Quaternary nitrogen	1
NO_2	Nitro groups	2
NCS	Isothiocyanate	0
BLM	β-lactam	0

Considering **815A** chemical formula ($C_{29}H_{26}N_7O_8^+$), both the CX and NO parameters are easily determined, having a total score of 29 and 15 respectively. The PRX parameter describes the proximity interactions between nitrogen and oxygen atoms, being scored with 2 for each direct bond between these atoms and 1 when the bonds are intercalated with either a carbon, a sulfur or a phosphorous. Hence, each nitro group represents a total score of 4 due to the two direct bonds present, and, in contrast, a carboxylic acid is scored 2 due to the intercalated interaction with a carbon in between the two atoms. Other functional groups, such as amides and the quinazolinone ring were scored 1 each,[62] thus, leaving the PRX parameter scoring 13 proximity interactions. A total of 13 unsaturated bonds (UB parameter) are present within this molecule.

There is one intramolecular hydrogen bond (HB) formed between the amide proton and the adjacent carboxylic acid. This information was already collected by the research group by nuclear magnetic resonance analysis of the molecule. The group concluded that the bond formation was highly probable whenever the carboxylic acid was in its charged state (carboxylate), specially, due to the presence of a

near base (DABCO moiety) and also at neutral pH considering the pK_a value of this functional group (approximately 4.4).[58]

The POL parameter accounts for the presence of heteroatoms linked either directly or intercalated with a carbon atom to the aromatic rings. In **815A** seven moieties falling into this category can be found. Regarding the AMP parameter, the presence of both a carboxylic acid and amines suggest that the molecule has amphoteric properties, being able to behave like a base or an acid depending on the pH.

The remaining parameters are easily extracted from the molecule's structure. There are no alkanes or alkenes, isothiocyanates and β-lactams, hence being given a 0 score to the ALK, NCS and BLM parameters. Finally, the RND, QN, NO_2 and parameters have a total score of 2, 1 and 2, respectively, considering the number of ring structures (without the condensed ones), quaternary nitrogen and nitro groups. Based on these parameters, the predicted *logP* value of the test compound is -2.49.

6.2. HPLC-UV-Vis experiments: CN column

Table A2: Different elution conditions tested using a Microsorb-MV 100-5 CN (250 mm x Ø4.6 mm). Samples (10 uL) of compound **815A** at the concentration of 1mM in DMSO were analyzed using the system described in Section 4.1.2. Chromatograms were monitored at 254 nm.

Elution program	Rt (min)	Peak width (min)	Observations
1 ml/min; 30 min Isocratic: 40% acetonitrile	15.55	1.46	Wide peak; reproductible results.
1 ml/min; 30 min Isocratic: 35% acetonitrile	15.02	1.44	Was intended to decrease the peak's width by decreasing the amount of acetonitrile, however the effect was almost none.
1 ml/min; 30 min Isocratic: 25% acetonitrile	16.61	2.72	Instead of decreasing, the peak's width increased.
1 ml/min; 30 min Isocratic: 50% acetonitrile	19.1 - 21	1.4 – 1.06	The peak narrowed with the increase of acetonitrile.
2 ml/min; 30 min Isocratic: 50% acetonitrile	9.1 – 10.02	0.97 – 0.64	By doubling the flow, it was possible to narrow the peak.
1 ml/min; 30 min Isocratic: 65% acetonitrile	2.75	0.42	The majority of the injected sample eluted only during the next sample's analysis.
1 ml/min; 30 min Isocratic: 75% acetonitrile	2.76	0.28	